Comparison between measured and simulated activity using Gafchromic™ film with radionuclides.

---

by

Maria Magdalena Joubert

UNIVERSITY OF THE FREE STATE
UNIVERSITEIT VAN DIE VRYSTAAT
YUNIVESITHI YA FREISTATA

A dissertation submitted in fulfilment of the requirements for the degree of

Magister of Medical Science in Medical Physics

In the Department of Medical Physics in the Faculty of Health Sciences at the University of the Free State

---

Supervisor: Dr. F.C.P. du Plessis

Co-Supervisor: Dr. J.A. van Staden

Submission date: 7 August 2020

DECLARATION

Author: Maria Magdalena Joubert

Degree: M.Med.Sc in Medical Physics

Title: Comparison between measured and simulated activity using Gafchromic™ film with radionuclides.

Date of submission: 7 August 2020

I, Maria Magdalena Joubert, declare that this masters research dissertation or, interrelated, publishable manuscripts/published articles, that I herewith submit for the degree of Magister of Medical Science in Medical Physics at the University of the Free State is my independent work and that I have not previously submitted it for a qualification at another institution or higher education.

I hereby declare that I am aware that the copyright is vested in the University of the Free State. All royalties regarding intellectual property that was developed during the course of and/or in connection with the study at the University of the Free State will accrue to the University.

This research was approved by the Health Sciences Research Ethics Committee; ethics clearance number: UFS-HSD2019/1505/0110. The study did not contain any human or animal subjects.

Signature: M. M. Joubert

ABSTRACT

In this study, Gafchromic™ film XR-QA2 and RT-QA2 were used to characterise the film energy response against various radionuclides. The film response was investigated with respect to different backscatter materials. The sensitivity of the two types of films was compared, and a film stack method was tested to allow the user to obtain sequential, cumulative doses at different time points. Monte Carlo (MC) simulations were used to link optical density (OD) values from measurements to the absorbed dose in the film. This was achieved by using conversion factors obtained by BEAMDP, BEAMnrc and DOSXYZnrc simulations to get the absorbed dose in the film. A neutron depletion theoretical model was introduced that can describe film response as a function of cumulated activity and absorbed dose.

Background: Gafchromic™ film has been used for quality assurance in various studies but not in nuclear medicine applications. Once the OD has been determined after film exposure to a radionuclide, it can be linked to the absorbed dose using the air kerma rate constant at distances that approximates point sources and the dose in water can be linked to the dose in film using MC simulations to get conversion factors. MC simulations are known as a gold standard to get the absorbed dose in materials.

Materials and Methods: XR-QA2 and RT-QA2 Gafchromic™ film were irradiated with the following radionuclides: Am-241, Cs-137, Tc-99m and I-131. The OD was calculated, and a function describing the relationship between the OD and the time-activity was derived based on the neutron depletion model. Different backscatter materials such as Corrugated fibreboard carton (CFC) or air equivalent material, polystyrene, Polymethyl Methacrylate (PMMA or perspex) and lead were used to investigate the effect it has on film response. The sensitivity of each film was investigated and compared. BEAMDP, BEAMnrc and DOSXYZnrc simulations were used to link the film response, OD, to the absorbed dose. The MC simulations were done replicating the exact geometry as with the physical measurements to get the absorbed dose in the film.

Results: The new neutron depletion model fitted the OD vs cumulative activity accurately as well as the OD vs absorbed dose. The XR-QA2 Gafchromic™ film has shown to be the most sensitive film when using air equivalent material with radionuclides, especially with low energy

radionuclides such as Am-241. When using more than one layer, the OD sensitivity of the film can be increased as well. The film stack method investigated also showed to be less time consuming when relating stacked film data to single film data. The fluence obtained from BEAMDP confirmed that the radionuclide containers have an effect on the radionuclide spectra's. Lead was also the backscatter material which showed higher OD change but lower absorbed dose values.

Conclusions: The neutron depletion theoretical model is more accurate than higher-order polynomial fits because it contains less free parameters. The XR-QA2 Gafchromic™ is better to use in nuclear medicine because of its sensitivity at low energies and because the sensitivity can be increased by using multiple layers of film. Film stack methods can be used to decrease experiment times. BEAMnrc can be used to accurately model radionuclides within their containers to evaluate the container effects. Lead showed a higher induced OD with lower absorbed dose, and the air equivalent material showed the lower OD change but higher absorbed dose.

Keywords: Gafchromic™ film; XR-QA2; RT-QA2; Radionuclides, Monte Carlo, DOSXYZnrc, BEAMnrc, Simulations, Optical density, Cumulated Activity.

DEDICATION

I dedicate this work to my

Amazing Mother

who always supports me, loves me and believes in me. Being a role model for me, showing me everything is possible when you put your mind to it, never giving up.

ACKNOWLEDGEMENTS

My sincere appreciation and thankfulness go to:

- My supervisor

  Dr. FCP du Plessis for his support, guidance, mentorship, patience, encouragement and for giving me the opportunity to be part of this research community and to further my career as a Medical Physicist. It was without a doubt that his determination for results and vision for this study contributed immensely toward the studies completion and success.

- My co-supervisor

  Dr. JA van Staden for his support, guidance, encouragement and enthusiasm throughout the research project. A knock on the door was all that was required for regular assistance.

- My co-author

  Dr. D van Eeden for her support throughout and all her contribution to this work. For all her words of wisdom and encouragement, keeping my spirits high throughout the study and lastly for all her patience to teach me new programming skills.

- HPC administrator

  A van Eck for all his assistance with the cluster. Assisting any time and still always being friendly.

- My mother M. Muller and my best friend J. Viljoen and my family

  For their continuous love and support. Keeping me calm and encouraged, giving me the strength to push through and always reminding me of the bigger picture.

- The South African Medical Research Council (MRC)

  This work was supported by the Medical Research Council of South Africa in terms of the MRC's Flagships Awards Project [grant number SAMRC-RFA-UFSP-01-2012/HARD]

- **Father Almighty**, above all, for giving me the patience, mental strength and encouragement needed to complete this project. For all his blessings and mercy, He has bestowed upon me, carrying me through and keeping me safe throughout this project.

  "I can do all things through Christ who gives me strength"- Philippians 4:13

- I would also like to thank all the new people I had met on this journey, giving me sound advice, emotional support or even just a laugh when it was needed. I am very grateful for all of the contributions that helped me reach my goal.

TABLE OF CONTENTS

ABBREVIATIONS AND ACRONYMS

ALARA	As Low As Reasonably Achievable
Am-241	Americium-241
BEAMDP	BEAM Data Processor
Bi_2O_3	Bismuth Oxide
CFC	Corrugated fibreboard carton
cGy	centi Gray
CsBr	Caesium Bromide
Cs-137	Caesium-137
CM	Component module
dpi	Dots per inch
EADL	Evaluated Atomic Data Library
ECUT	Electron cut-off energy
EGS	Electron Gamma Shower
EGSnrc	Electron Gamma Shower National Research Council of Canada
GBq	Giga Becquerel
Gy	Gray
I-131	Iodine-131
ICRU	International Commission on Radiation Units and Measurements
ISP	International Speciality Products Technologies
ISQR	Inverse square
keV	kilo electron Volt
KM	Koch and Motz
MBq	Mega Becquerel
MBq-h	Mega Becquerel hour
MC	Monte Carlo
MeV	Mega electron Volt
mGy	milli Gray
NCBI	National Center for Biotechnology Information
NIST	National Institute of Standards and Technology

NRC	Nuclear Regulatory Commission
OD	Optical Density
ρ	Physical density
PCUT	Photon cut-off energy
PEGS4	Pre-processor for Electron Gamma Shower v4.0
PMMA	Polymethyl Methacrylate
PRESTA	Parameter Reduced Electron-Step Transport Algorithm
PSF	Phase space file
QA	Quality assurance
RCF	Radiochromic film
RGB	Red Green Blue
ROI	Region of interest
Tc-99m	Technetium-99m
TIFF	Tagged image file format
TLD's	Thermoluminescent dosimeters
Z	Atomic number
Z_{eff}	Effective atomic number
Γ	Air kerma rate constant
Φ	Fluence

Chapter 1: Introduction

TABLE OF CONTENTS

1.1. Overview

In this chapter, the background of Radiochromic film (RCF) and Monte Carlo (MC) simulations is given. The type of radionuclides and films used in this study, as well as MC simulations, are discussed. The aim of the study is given, and the structure of the document is set out.

1.2. Radiochromic film (RCF) background

In 1826 Joseph Niepce projected a view onto a pewter plate coated with a light-sensitive solution which formed an image after 8h which resulted in one of the earliest radiochromic processes documented (1).

In 1895 it was noticed that fluorescent light could cause a platinobarium screen to glow by Wilhelm Conrad Roentgen which led to the discovery of X-rays (2). One of his experiments included a photographic plate of his wife Bertha's hand, showing the wedding ring on her finger (2).

In 1910-1920 Dr. Hampson's Roentgen Radiometer, which consisted of a colour wheel, made out of 25 colours, was used to quantify absorbed dose with the use of barium platinocyanide pastille discs (3).

Since 1965 media that changes colour when irradiated by ionizing radiation were used as colouration detectors (1). Human skin was used as a colouration detector as well to define the erythema dose required to turn the skin of the hand or arm red (3).

At present, there are various kinds of detectors, but they each have their own disadvantages. These include ionization chambers and semiconductors that do not have sufficient spatial resolution and thermoluminescent dosimeters (TLD's) which are labour intensive taking up time to get the readings from glow curves (4). Film-based detectors with photographic silver halide emulsions have large sensitivity differences to photon energies in the 10-200 keV region and require wet chemical processing (4).

RCF is self-developing as it changes colour to indicate exposure to radiation through a polymerization process, and the colour of the film can be related to the radiation dose (5). This makes the film easy to be analyzed with common computer desktop scanners (6). These films are not light sensitive which makes them easy to handle and have a low spectra sensitivity variation with a very high spatial resolution and is near tissue-equivalent (4,7). More advantages of RCFs include that they are easy to use, cost-effective, portable, non-invasive and tissue equivalent (5).

RCF is a broadly used dosimetry medium in radiotherapy and medical imaging in diagnostic radiology for over 20 years (5,6,8). RCFs have evolved very rapidly over the past few years, which resulted in a variety of RCFs with different chemical compositions that can be uniquely used for different purposes (4). In 1986 RCF which are sensitive to low doses were developed by the International Speciality Products Incorporate (ISP) and are known as Gafchromic™ film (1,5). The RCF is mostly used for dose assessment and quality checks which include checking for damage to electronic devices and beam diagnostics (5).

As there are no comprehensive guidelines on the use and calibration of RCFs (4), this study also includes a neutron depletion calibration curve formulation which is fully derived in Chapter 2.

The storage used for Gafchromic™ film needs to have extra precaution measures to avoid long exposures to ambient light. This is a disadvantage because long exposures to ambient light can affect the colouration of the film and cause it to darken.

1.2.1. XR-QA2- and RT-QA2 Gafchromic™ film

Two types of RCFs are used in this study which are referred to as XR-QA2- and RT-QA2 Gafchromic™ film from Ashland suppliers.

The Gafchromic™ XR-QA2 film was designed for general diagnostic radiology quality assurance (QA) with a low absorbed dose range from 0.1 cGy to 20 cGy and the Gafchromic™ RT-QA2 film routinely used in radiation therapy was specifically designed for QA procedures with an absorbed dose range between 0.02 Gy and 8 Gy (9).

Both these films are designed with an opaque white backing material and a yellow coloured transparent front polyester cover. This enhances the visual colour change caused by incident radiation (10).

Various investigations have been done for the XR-QA2 Gafchromic™ film, including energy dependence (11–13). It was found that the film has a pronounced energy dependent response for energy ranges used for x-ray diagnostic imaging (13). However, when investigating the dose absorption in low-cost materials (jeltrate, chicken bone, cow bone and chalk), it was found that the XR-QA2 Gafchromic™ film was energy independent (14). According to specifications, the XR-QA2 Gafchromic™ film is sensitive in the dose range 1-200 mGy. Still, it was shown that the XR-QA2 Gafchromic™ film sensitivity increases in the energy range 18-39 keV and decreases at 38-46.5 keV (15). For accuracy, the film has to be close to the source (14).

The RT-QA2 Gafchromic™ film energy dependence has not been studied yet as far as we know, but investigations showed that the film can be used as an alternative to EBT2 film and that the film depends on incident photon energies and the depth of measurement (16).

The manufacturer of the Gafchromic™ films (Ashland Inc, Wayne, N) made films, used at low energies, more sensitive by adding high Z components to the sensitive layer of the film (13). This was done for the XR-QA2 Gafchromic™ film making it more sensitive as the higher atomic number increased the photoelectric absorption of incident photons as shown in figure 1.1 (17,18)

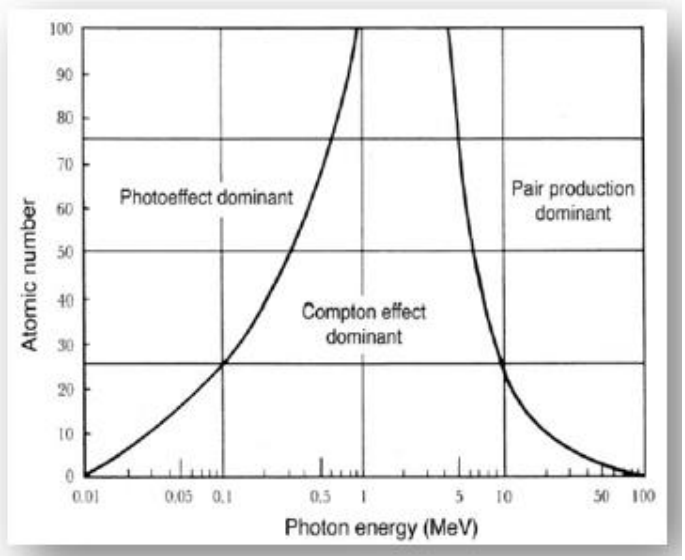

Figure 1.1: Radiation interaction processes dominating at certain photon energies (MeV) and atomic numbers (Z)(19).

The photoelectric effect occurs when the energy of an incident photon is fully absorbed by an atom. The absorbed energy is then used to eject an orbital electron from the atom which leads to the emission of characteristic x-rays (or Auger electrons). As seen in figure 1.1, the photoelectric effect is dominant for high atomic number absorbers at diagnostic energies, while Compton interactions are dominant for low atomic absorbers (20).

1.3. Radionuclides

Radionuclides are commonly known as radioactive isotopes, and these are elements with unstable nuclei. These elements emit radiation spontaneously by means of radioactive decays such as alpha, beta and/or gamma decay. These radionuclides can occur naturally or be man-made by using nuclear reactors, cyclotrons or generators.

In this study, four common radionuclides were used. They are, Am-241, Tc-99m, I-131 and Cs-137. Table 1.1 shows some properties of the radionuclides as well as how they are produced.

Table 1.1: Properties and production modes of radionuclides used in this study (21–24)

Radionuclide	Particle emitted	Half-life	Mode of Production
Am-241	Alpha particles and gamma rays	432.2 years	Nuclear reactor
Tc-99m	Gamma rays	6.02 hours	Generator
I-131	Beta particles and gamma rays	8.02 days	Nuclear reactor
Cs-137	Beta particles and gamma rays	30.07 years	Nuclear reactor

The inverse square law is the decrease in fluence that is inversely proportional to the square of the distance from the source. This law can only be applied when the distance between the radionuclide (source) and film is such that the source can be considered a point source. Close exposures to film would result in a higher OD change than when the film is further away and will also reach saturation faster. If the detector is in contact with the source, this law can not be used.

Backscatter materials used when working with radionuclides and the film sensitivity are of importance as they can affect the results obtained due to backscatter and absorption effects which differ with materials. The materials investigated in this study are CFC which is an air equivalent material, polystyrene, PMMA (perspex) and lead. The effective atomic number (Z_{eff}) of each material will determine which effect in figure 1.1 is more dominant, and the thickness of each material will affect the results.

1.4. Monte Carlo studies background

Monte Carlo (MC) calculations are designed to use statistical processes to model the interactions of photons and charged particles as they interact with matter (25).

The Electron Gamma Shower (EGS) code was developed first in 1994 and led to the EGS3, EGS4, EGS4/PRESTA and then to EGSnrc code which remains the most widely used radiation package in medical physics (26).

The BEAM code was developed by NRC for electron beam radiotherapy and was first released in 1995 and is in continuous development still (26). In 2001 DOSXYZnrc was created by porting the DOSXYZ code to the EGSnrc system and in 2004 DOSXYZnrc was able to run on Windows-based systems and not just on Linux platforms (27).

The MC method is primarily used to model linear accelerators in medical physics (28). It has shown to be the most accurate method to determine the absorbed dose in a medium in radiotherapy (29,30). The use of MC simulations and analysis has become the gold standard in radiotherapy (31).

The MC method starts from first principles and includes secondary particle transport as it tracks individual particle histories (28). The clinical application of the MC method requires detailed and accurate information regarding the beam characteristics such as energy, angular and spatial distributions of the particles in the beam which can be obtained from a phase space file (PSF) scored in BEAMnrc using the BEAM code (29). By using this information, the MC method can be seen as a convenient and accurate method to simulate the dose distributions for patient treatment or in a rectilinear voxel phantom by using DOSXYZnrc (27,28). The BEAMnrc and DOSXYZnrc is an EGSnrc-based MC simulation (27).

BEAMDP can use the PSF obtained in BEAMnrc to investigate the energy spectrum and fluence from the source. The EGS_Windows V4.0 can be used to make sure the geometry setup is correct, and MCSHOW helps to see the isodose curves.

The MC method has a drawback regarding time as it needs a long computing time to get accurate, absorbed dose values with reasonable statistical accuracy, especially when using photon beams (28,30). In recent advances, computer processing speeds have increased since faster processors are more available and by using parallel processing, which makes the MC method acceptable for

radiotherapy clinics (28,31). Another disadvantage is that a large amount of storage space is required to store the PSFs especially when a high amount of histories are required for accuracy and that the PSFs need to be recreated every time that the geometry changes (32).

1.4.1. BEAMnrc and DOSXYZnrc simulations

This study uses MC methods such as BEAMnrc and DOSXYZnrc, to model radionuclides in containers to get the absorbed dose in the film. This has not been attempted according to the existing literature thus far. The BEAMnrc method is used to simulate an accelerator, but in this study, it will be used to simulate the radionuclide under consideration in its container by using component modules (CMs) to create the source in the container. In this approach, a full MC simulation of the radiation transport through the radionuclide container will be performed to generate a PSF. The PSF contains the necessary data such as position, momentum and energy for each particle travelling through the container on to the phase space scoring plane which is perpendicular to the radionuclide source just below the container (28,30). This PSF is then used directly in the DOSXYZnrc MC simulation as a source model (28).

1.4.1.1. BEAMnrc simulations

Figure 1.2 shows the schematic of the steps to follow when using BEAMnrc, and each step is explained to better understand the whole process of the BEAMnrc simulations used.

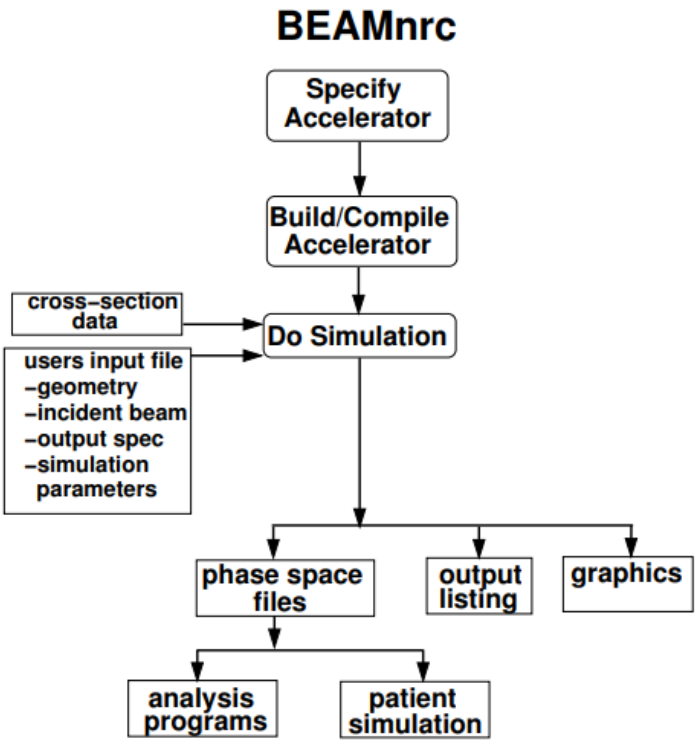

Figure 1.2: Steps to follow in BEAMnrc (33)

First, the CMs used had to be chosen to build and compile the accelerator. The FLATFILT and SLABS CMs were used to model the radionuclides with their containers. After the containers have been simulated, a PEGS4 file has to be selected, which includes all the material compositions used during the simulations. This includes the Gafchromic™ film compositions, the container materials and the backscatter materials used. Lastly, an input file has to be created to set all the parameters and include accurate measurements of the physical containers to be used to ensure the simulation geometries will be the same as the physical geometries. The source file has to be selected in the input file, which was spectra files created with the appropriate data. In the input file, one can also select that a PSF should be obtained and decide after which CM it should be collected. The simulation is then started, and a PSF is obtained. This PSF is then used in DOSXYZnrc as a source file.

1.4.1.2. DOSXYZnrc simulations

In DOSXYZnrc the same PEGS4 file is used as in BEAMnrc, and an input file is created. The input file contains the voxel dimensions for the phantom and the layer of materials used. The source file is the full PSF obtained in BEAMnrc. The output file is a *.3ddose file which was converted to a text file by using a Fortran code.

1.5. Research aim

The aim of this study is to convert the film density measured to absorbed dose and compare the measured results with the simulated results. This will consist of the following two objectives:

a) Characterize Gafchromic^{TM} film response against radionuclide activity.

b) Perform Monte Carlo simulations to relate film response to absorbed dose in water and to convert it into absorbed dose in film.

1.6. Structure of the document

This document consists of four Chapters. These chapters entail the background, theory and research conducted in this study. The outcomes of the investigations and results are described in the chapters. A brief discussion of the chapters follows to accustom the reader of what the study is about.

Chapter 1 gives an overview of the Gafchromic^{TM} film, radionuclides and simulation programmes used during this study. Background of each is given and explained why it is used in this study emphasising their advantages.

Chapter 2 is the first article "Characterization of Gafchromic^{TM} film response against radionuclide activity." This chapter gives the methods that were used and the results that were obtained by using the two different films. Optical density was obtained, and a theoretical neutron depletion model is described and used.

Chapter 3 follows on chapter 2 and is the second article "The relation between XR-QA2 and RT-QA2 Gafchromic™ film optical density and absorbed dose in water produced by radionuclides" and the influence of backscattering materials. This chapter gives the methods used to get the dose values in films by doing MC simulations and by using the specific air kerma rate factor for each radionuclide. The absorbed dose values were linked to the OD values from chapter 2 by using the neutron depletion model.

Chapter 4 gives a recap of all the chapters results and gives a main conclusion regarding the study. Possibility of improvements and future work is discussed in this chapter as well. At the end of the chapter is an appendix section.

References

1. Williams MJ, Metcalfe PE. Radiochromic film dosimetry and its applications in radiotherapy [Internet]. 2011 [cited 2020 Jul 28]. Available from: http://ro.uow.edu.au/engpapers/4075
2. Glasser O. W. C. Roentgen and the discovery of the Roentgen rays. Am J Roentgenol [Internet]. 1995 Nov 1;165(5):1033–40. Available from: https://doi.org/10.2214/ajr.165.5.7572472
3. Glasser O. The Evolution of Dosimeters in Roentgen Ray Therapy. Radiology. 1941 Aug 1;37(2):221–7.
4. Niroomand-Rad A, Blackwell CR, Coursey BM, Gall KP, Galvin JM, McLaughlin WL, et al. Radiochromic film dosimetry: recommendations of AAPM Radiation Therapy Committee Task Group 55. American Association of Physicists in Medicine. Med Phys. 1998;25:2093–115.
5. Casolaro P, Campajola L, Breglio G, Buontempo S, Consales M, Cusano A, et al. Real-time dosimetry with radiochromic films. Sci Rep [Internet]. 2019 [cited 2019 Nov 14];9(1):1–11. Available from: https://doi.org/10.1038/s41598-019-41705-0
6. Butson E, Alnawaf H, Yu PKN, Butson M. Scanner uniformity improvements for

radiochromic film analysis with matt reflectance backing. Australas Phys Eng Sci Med. 2011;34:401–7.

7. Menegotti L, Delana A, Martignano A. Radiochromic film dosimetry with flatbed scanners: A fast and accurate method for dose calibration and uniformity correction with single film exposure. Med Phys. 2008;35(7):3078–85.

8. Giaddui T, Cui Y, Galvin J, Chen W, Yu Y, Xiao Y. Characteristics of Gafchromic XRQA2 films for kV image dose measurement. Med Phys. 2012;39(2):842–50.

9. Ashland. Gafchromic™ RTQA2 film [Internet]. [cited 2019 Oct 30]. Available from: http://www.gafchromic.com/documents/PC-11804_Gafchromic_RTQA2.pdf

10. Butson MJ, Cheung T, Yu PKN. Measuring energy response for RTQA radiochromic film to improve quality assurance procedures. Australas Phys Eng Sci Med. 2008;31(3):203–6.

11. Chiu-Tsao S-T, Ho Y, Shankar R, Wang L, Harrison LB. Energy dependence of response of new high sensitivity radiochromic films for megavoltage and kilovoltage radiation energies. Med Phys [Internet]. 2005 Oct 18 [cited 2020 Jul 2];32(11):3350–4. Available from: http://doi.wiley.com/10.1118/1.2065467

12. Lindsay P, Rink A, Ruschin M, Jaffray D. Investigation of energy dependence of EBT and EBT-2 Gafchromic film. Med Phys [Internet]. 2010 Jan 13 [cited 2020 Jul 2];37(2):571–6. Available from: http://doi.wiley.com/10.1118/1.3291622

13. Tomic N, Quintero C, Whiting BR, Aldelaijan S, Bekerat H, Liang L, et al. Characterization of calibration curves and energy dependence GafChromic ™ XR-QA2 model based radiochromic film dosimetry system. Med Phys [Internet]. 2014 May 29 [cited 2020 Jul 2];41(6Part1):062105. Available from: http://doi.wiley.com/10.1118/1.4876295

14. Alsadig AA, Abbas S, Kandaiya S, Ashikin NARNN, Qaeed MA. Differential dose absorptions for various biological tissue equivalent materials using Gafchromic XR-QA2 film in diagnostic radiology. Appl Radiat Isot. 2017 Nov 1;129:130–4.

15. Di Lillo F, Mettivier G, Sarno A, Tromba G, Tomic N, Devic S, et al. Energy dependent calibration of XR-QA2 radiochromic film with monochromatic and polychromatic x-ray

beams. Med Phys [Internet]. 2016 Jan 6 [cited 2020 Jul 25];43(1):583–8. Available from: http://doi.wiley.com/10.1118/1.4939063

16. Jagtap AS, Mora G. Investigation of absorbed-dose energy dependence of RTQA2 film over EBT2 film using Monte Carlo simulation [Internet]. 2019 [cited 2020 Jul 2]. p. 1. Available from: https://www.postersessiononline.eu/173580348_eu/congresos/ICCR-MCMA2019/aula/-P_119_ICCR-MCMA2019.pdf

17. Aldelaijan S, Tomic N, Papaconstadopoulos P, Schneider J, Seuntjens J, Shih S, et al. Technical Note: Response time evolution of XR-QA2 GafChromic™ film models. Med Phys. 2018;45(1):488–92.

18. Cheung T, Butson MJ, Yu PKN. Experimental energy response verification of XR type T radiochromic film. Phys Med Biol. 2004;49(21):N371–N376.

19. Podgorsak EB, editor. Radiation Oncology Physics: A Handbook for Teachers and Students. Vienna: International Atomic Energy Agency; 2005. 1–657 p.

20. Alsadig AA, Abbas S, Kandaiya S, Ashikin NARNN, Qaeed MA. Differential dose absorptions for various biological tissue equivalent materials using Gafchromic XR-QA2 film in diagnostic radiology. Appl Radiat Isot. 2017;129:130–4.

21. Bushberg JT, Seibert JA, Leidholdt Jr EM, Boone JM. The Essential Physics of Medical Imaging. 2nd ed. Mitchell CW, editor. Philadelphia: LIPPINCOTT WILLIAMS & WILKINS, a WOLTERS KLUWER business; 2002. 1–933 p.

22. International Atomic Energy Agency. Manual for reactor produced radioisotopes. IAEA-TECDOC-1340 [Internet]. Vienna; 2003 Jan [cited 2020 Nov 3]. Available from: https://www-pub.iaea.org/MTCD/publications/PDF/te_1340_web.pdf

23. Winberg MR, Garcia RS. National Low-Level Waste Management Program Radionuclide Report Series [Internet]. Idaho; 1995 Sep [cited 2020 Oct 21]. Available from: https://inis.iaea.org/collection/NCLCollectionStore/_Public/27/032/27032341.pdf?r=1&r=1

24. United States Environmental Protection Agency. EPA Facts About Cesium-137 [Internet].

2002 Jul [cited 2020 Nov 3]. Available from: http://www.epa.gov/superfund/resources/radiation

25. Annabell NW. The Use of Gold Nanoparticles for Tumour Dose Enhancement from Microbeam Radiotherapy [Internet]. 2013 [cited 2020 Jul 29]. Available from: https://pdfs.semanticscholar.org/ea53/b395ba70c73ad332a5bab49bf6a79093db4f.pdf

26. Bielajew AF, Hirayama H, Nelson WR, Rogers DWO. History, overwiew and recent improvements of EGS4. Technical Report PIRS-0436 [Internet]. Ottawa; 1994 [cited 2020 Jul 29]. Available from: https://www.slac.stanford.edu/cgi-bin/getdoc/slac-pub-6499.pdf

27. Walters B, Kawrakow I, Rogers DWO. DOSXYZnrc Users Manual. National Research Council of Canada Report PIRS-794 revB [Internet]. 2020 [cited 2020 May 20]. Available from: https://nrc-cnrc.github.io/EGSnrc/doc/pirs794-dosxyznrc.pdf

28. Fix MK, Keall PJ, Dawson K, Siebers J V. Monte Carlo source model for photon beam radiotherapy: photon source characteristics. Med Phys [Internet]. 2004 Oct 28 [cited 2020 Jun 7];31(11):3106–21. Available from: http://doi.wiley.com/10.1118/1.1803431

29. Deng J, Jiang BJ, Kapur A, Li J, Pawlicki T, Ma C-M. Photon beam characterization and modelling for Monte Carlo treatment planning. Phys Med Biol. 2000;45(2):411–27.

30. Fix MK, Keller H, Rüegsegger P, Born EJ. Simple beam models for Monte Carlo photon beam dose calculations in radiotherapy. Med Phys [Internet]. 2000 Dec 1 [cited 2020 Jun 7];27(12):2739–47. Available from: http://doi.wiley.com/10.1118/1.1318220

31. Chetty I, DeMarco JJ, Solberg TD. A virtual source model for Monte Carlo modeling of arbitrary intensity distributions. Med Phys [Internet]. 2000 Jan 1 [cited 2020 Jun 7];27(1):166–72. Available from: http://doi.wiley.com/10.1118/1.598881

32. Kawrakow I, Walters BRB. Efficient photon beam dose calculations using DOSXYZnrc with BEAMnrc. Med Phys [Internet]. 2006 Jul 28 [cited 2020 Jan 7];33(8):3046–56. Available from: http://doi.wiley.com/10.1118/1.2219778

33. Rogers DWO, Faddegon BA, Ding GX, Ma C-M, We J, Mackie TR. BEAM: A Monte Carlo code to simulate radiotherapy treatment units. Med Phys [Internet]. 1995 May 1 [cited

2020 Jul 29];22(5):503–24. Available from: http://doi.wiley.com/10.1118/1.597552

Chapter 2: Characterization of Gafchromic™ film response against radionuclide activity

Maria. M. Joubert, Johan. A. van Staden, Freek. C. P. du Plessis
Department of Medical Physics, University of the Free State, Bloemfontein 9301

TABLE OF CONTENTS

ABSTRACT

Purpose: In this study, we used Gafchromic™ film XR-QA2 and RT-QA2 to characterize the film energy response against various radionuclides. We introduced a neutron depletion theoretical model that can describe film response as a function of cumulated activity. The film response was investigated with respect to different backscatter media such as polystyrene, perspex, lead and corrugated fibreboard carton (CFC). The sensitivity of the two types of film to different energies was also studied. Lastly, a film stack method was tested to allow the user to obtain sequential, cumulative doses at different time points.

Methods: Pieces of Gafchromic™ film XR-QA2 and RT-QA2 were exposed to Am-241, Cs-137, Tc-99m, and I-131 to obtain various cumulative activities. After 24h each film piece was digitized by scanning it with an Epson Perfection V330 flatbed scanner to obtain 48-bit RGB TIFF images. Afterwards, each image was processed with the Image J software package. The film response was fitted to a theoretically derived function based on the neutron depletion model and the Beer-Lambert Law and compared with an existing fitting function. Layers of the film were also placed together and irradiated with the above-mentioned radionuclides to investigate the possibility of increasing the sensitivity of the film as a dosimeter. The energy response of the two types of film was investigated by irradiating pieces of film with different photon energies.

Results: The theoretical response model fits *OD* vs cumulative activity accurately. XR-QA2 Gafchromic™ film shows good energy film response by using CFC as a backscatter material when using radionuclides. From the results, it is also evident that XR-QA2 Gafchromic™ film is more sensitive to low energy gamma rays than RT-QA2 Gafchromic™ film. Its *OD* sensitivity can be increased by 2 ± 0.2 when using a double layer film and by 2.8 ± 0.3 when using a triple-layer film. By using a film stack, the experimental time can be decreased by using the second-order polynomial relationship obtained to relate the stacked film data to the single film data.

Conclusions: The neutron depletion theoretical model is accurate and contains less free parameters than higher-order polynomial fits. The Gafchromic™ XR-QA2 film is also better to use in nuclear medicine because of its higher sensitivity. The sensitivity of the film as a dosimeter can

also be increased by using multiple layers of film. Experiment times can also be decreased by using the film stack method.

Keywords: Gafchromic™ film; XR-QA2; RT-QA2; radionuclides.

2.1. INTRODUCTION

Gafchromic™ film is widely used for radiation dosimetry in conventional radiotherapy and diagnostic radiology because of it being self-developing, not being light sensitive (thus it can be handled in room light) and it provides high spatial resolution (1–4). To our knowledge, these films have not been used in nuclear medicine for radionuclide dosimetry. Gafchromic™ film has the potential for usage as dosimeters in the domain of radionuclide dosimetry.

Oliveira et al. showed the response of Gafchromic™ film XR-QA2 with Tc-99m (5). They concluded that Gafchromic™ film could partially substitute the individual calibration of activity dose calibrators, a practice that is always troublesome for nuclear medicine centres due to transferring of sources and cost implication there-of (5).

With recent advances in theranostics in the field of nuclear medicine, it will be useful to know the energy response and sensitivity for certain types of Gafchromic™ films. Theranostics is a field in medicine where the diagnostic test is used to optimise the specific targeted therapy in order to customize the activity dose administered to the patient individually and not use a one dose fits all concept (6,7). Radioiodine theranostics is an example that has been used extensively for thyroid cancer (6,8).

Gafchromic™ XR-QA2 film is the latest version of the XR-QA film. The original XR-QA film had two sensitive layers consisting of caesium bromide (CsBr), a second version was designed, XR-QA (Version 2), where the two layers were combined as one (9). The use of CsBr was problematic due to the instability the film showed when exposed to high temperatures and humidity for extended periods (9). The CsBr was replaced with bismuth oxide (Bi_2O_3) for the creation of the XR-QA2 film. XR-QA2 eliminated the instability of the XR-QA (Version 2) and also increased the photoelectric absorption of incident photons (9,10).

Gafchromic™ RT-QA2 film is most commonly used for light field alignments, radiation field alignments and other geometric tests and is more economical than the Gafchromic™ EBT films. The RT-QA and Gafchromic™ RT-QA2 film composition are the same; the only difference is that the RT-QA was manufactured by International Speciality Products inc (ISP) and the Gafchromic™ RT-QA2 film was manufactured by Ashland Inc.. It is essential to know that Ashland Inc. aquisitioned ISP in 2011.

Gafchromic™ XR-QA2 film was designed for general diagnostic radiology quality assurance with a much lower dose range from 0.1 cGy to 20 cGy (11,12). The Gafchromic™ RT-QA2 film routinely used in radiation therapy was specifically designed for quality assurance (QA) procedures with an absorbed dose range between 0.02 Gy and 8 Gy.

This study aims to characterize the energy response of the Gafchromic™ film XR-QA2 and RT-QA2 against the radionuclides Am-241, Cs-137, Tc-99m, and I-131. We also introduce a neutron depletion theoretical model that can describe film response as a function of cumulated activity. We investigated the film response with respect to different backscatter media, namely polystyrene, perspex, lead and corrugated fibreboard carton (CFC). Lastly, a method that can enhance the sensitivity measurements for dosimetry with film, as well as a film stack method for obtaining cumulative activities at different time points, was evaluated.

2.1.2. Theory

Deriving film response as a function of exposure using a saturation model.

The active layer in Gafchromic™ film is a dye that undergoes polymerization when activated by radiation. If we assume that a finite amount of interactions will lead to complete saturation of the film, then we can argue that after a sufficient amount of radiation, no further increase in optical density (*OD*) will occur.

Assume the total amount of interaction points, leading to polymerization, is N_{Po} at time $t = 0$.

When the film is irradiated with an activity $A(t)$, then the amount of interaction points will deplete with time.

The probability (α) for an interaction point to be activated per unit time is given by:

$$\alpha = \sigma A \tag{2.1}$$

where σ is the probability of activation of a point and A is the disintegration rate of the gamma radiation.

Thus;

$$N_P(t) = N_{Po}e^{-\propto t} \tag{2.2}$$

$N_P(t)$ is the amount of points not activated by gamma radiation at a given time.

If it's assumed that the rate of formation of the activated points $N_D(t)$ is proportional to the amount of interaction points available at time t then:

$$\frac{dN_D}{dt} = \alpha N_P(t) \tag{2.3}$$

Inserting Eq. 2.2 into Eq. 2.3 yields:

$$\frac{dN_D}{dt} = \alpha N_{Po}e^{-\propto t} \tag{2.4}$$

A solution of Eq. 2.4 give the activated points at time t as:

$$N_D(t) = N_{Po}(1 - e^{-\alpha t}) \tag{2.5}$$

This formulation relies on a constant activity $A(t)$ during irradiation, thus ignoring decay of activity.

For Gafchromic™ film, the pixel values from an irradiated film can be normalized by dividing by its density value when unirradiated. If we take the log of the normalised pixel values, we get the absorbance. This is, dependent on the concentration C of the activated points on the film.

$$C = \frac{N_D}{V} \tag{2.6}$$

Through the division of the volume of the film being irradiated (V) in Eq. 2.5, and substitution of C in Eq. 2.6 we can re-write it as:

$$C(t) = C_{sat}(1 - e^{-\alpha t}) \tag{2.7}$$

Where, $C_{sat} = \frac{N_{Po}}{V}$, the assumption is at saturation all activation points are now activated and equals the original amount of activation points, N_{Po}.

The Beer-Lambert law gives the relationship between the polymer concentration and the absorbance, which is shown in Eq. 2.8 below (13).

$$Absorbance = Log\frac{I_0}{I} = \varepsilon bC \tag{2.8}$$

with ε the absorption coefficient, b is the thickness of the sample through which the light (radiation) travels and C is the concentration of activation points in the film.

The transmission (T) of light (radiation) is defined as $\frac{1}{Absorbance}$. Therefore, $Log\frac{1}{T} = \varepsilon bC$ is also equivalent to the *OD*.

In tagged image file format (TIFF) images, the maximum grayscale represents 0 % and the minimum grayscale 100% transmission. The number of grayscale levels depends on the bit depth of the image. A 16-bit image has a depth of 65535 grayscale levels. The pixel value (P) on the image is directly proportional to the transmission of the light in the film. The transmission can be calculated as:

$$T = \frac{P}{65535} \tag{2.9}$$

Therefore, the substitution of Eq. 2.9 into Eq. 2.8 yields:

$$Log\frac{65535}{P} = \varepsilon bC \tag{2.10}$$

Combining Eq. 2.7 and Eq. 2.10 result in the optical density values OD :

$$OD = Log\frac{65535}{P} = \varepsilon bC_{sat}(1 - e^{-\alpha t}) \tag{2.11}$$

In order to account for the film background (γ) which is present irrespective of irradiating the film, the equation for OD is adjusted to:

$$OD = \varepsilon b C_{sat}(1 - e^{-\alpha t}) + \gamma \quad (2.12)$$

Eq. 2.12 can now be simplified by accepting $\varepsilon b C_{sat} = \beta$, therefore:

$$OD = \beta(1 - e^{-\alpha t}) + \gamma \quad (2.13)$$

If films are irradiated with a specific radionuclide for different time periods, curve fitting of *OD* vs irradiation time will yield the constants α and β.

2.2. MATERIALS AND METHODS

Gafchromic™ XR-QA2 (batch no. lot # 01251801) and RT-QA2 (batch no. lot # 03141801) film with a white backing material and a yellow coloured transparent polyester cover on the front were used in this study. Both films have four layers, as shown in figure 2.1. The films change colour upon irradiation, which can be seen on the yellow polyester layer (14). As these films show a colour change during irradiation, analysis can be done by using a document scanner (15). The active layer's atomic composition of each film is shown in table 2.1. Due to the inclusion of high atomic number (Z) elements in the Gafchromic™ XR-QA2 film, the photoelectric cross-section increases (4,16). To reduce variance between film batches, a single film batch was used in this study.

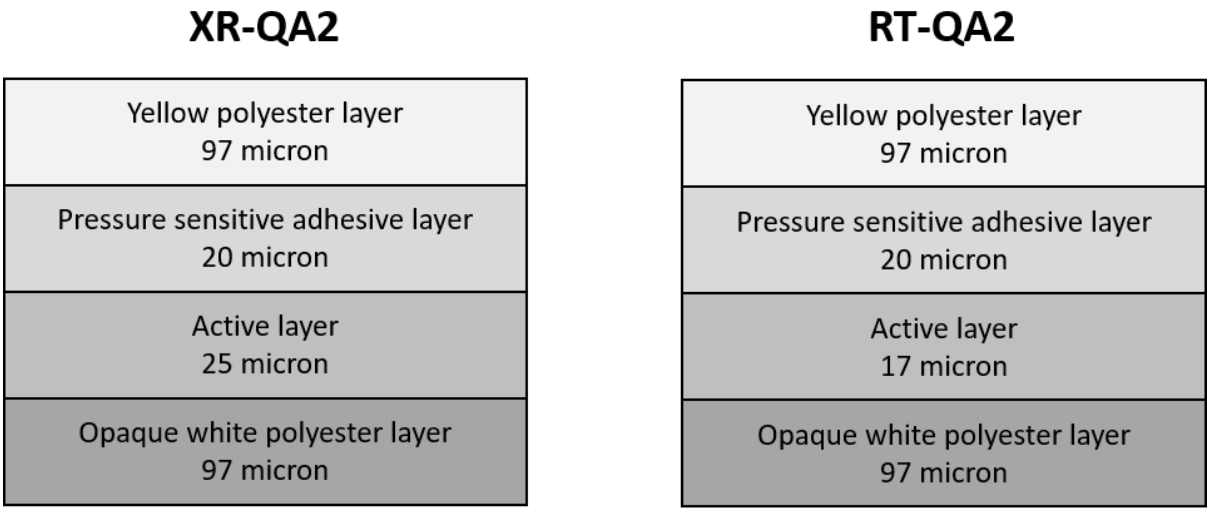

Figure 2.1: The structure of the Gafchromic™ film XR-QA2 and RT-QA2 (11,12)

Table 2.1: Atomic composition of the Gafchromic™ film active layer showing the effective atomic number (Z_{eff}) in the active layer (17) for each film model (RT-QA2 and XR-QA2).

Composition by element and atom (%)										
Film Model	H	Li	C	N	O	Al	S	Ba	Bi	Z_{eff}
XR-QA2	40.6	0.1	39.8	0.2	18.1	0.0	0.5	0.5	0.2	29.98
RTQA2	42.1	0.0	38.2	0.0	18.5	0.1	0.5	0.5	0.0	22.71

The experimental setup is shown in figure 2.2. The energy dependence of the two types of film was evaluated by using radionuclides with different gamma-ray energies, as shown in table 2.2. The Am-241 source was in a plastic vial since it does not decay with beta particles, and the energy of the gamma rays is fairly low (59.5 and 13.95 keV). The Cs-137 source was in a lead container with a 1mm perspex plate over the opening. The Tc-99m and the I-131 sources were in a glass vial.

The different backscatter materials used in the study are shown in figure 2.3. Each Gafchromic™ film sheet was cut into small film pieces (2.5 cm x 2 cm). The film pieces were placed at a fixed position on the backscattering medium and irradiated by placing the radionuclides showed in table 2.2 on the films. The film exposure times measured were: 7, 10, 20, 30, 40, 50, 60, 70, 80, 90 minutes for all radionuclides except for Tc-99m where the 80- and 90-min exposure times were excluded due to its relative short half-life (6.02 hours).

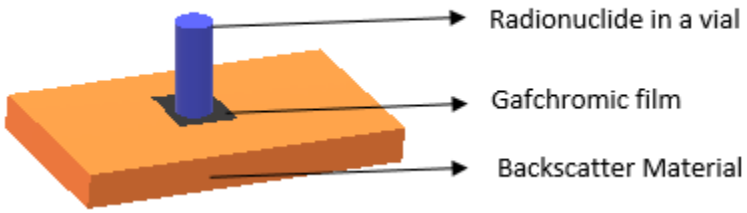

Figure 2.2: The irradiation schematic for the experimental setup.

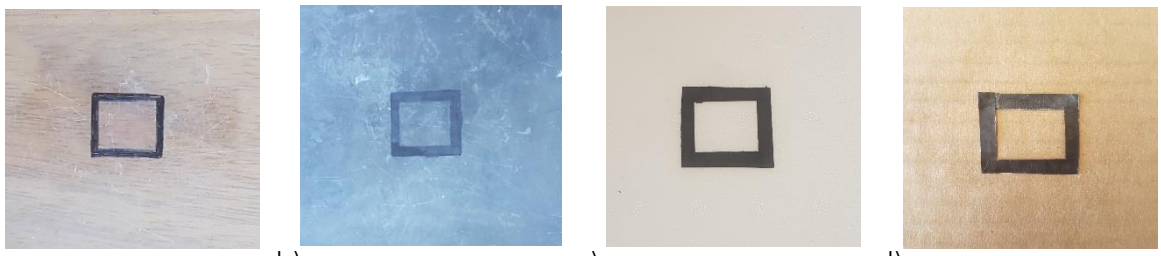

a) b) c) d)

Figure 2.3: Backscattering materials of a) Perspex, b) lead, c) polystyrene and d) CFC used for the experimental exposures.

Table 2.2: Properties of radionuclides used in this study (18–20).

Radionuclide	Gamma energies (keV)	Beta Energies (keV)	Beta range	Half-life
Am-241	59.5 (35.9%) 26.3(2.4%) 13.95 (9.6%)	N/A	N/A	432.2 years
Cs-137	283.53 (0.00058 %) 661.657 (85.1 %)	513.97 (94.4 %) 892.22 (0.00058 %) 1175.63 (5.6%)	2.1 mm in glass 3.8 mm in plastic	30.07 years
Tc-99m	140.51 (89%) 18.37 (4.1%) 18.25 (2.15%)	N/A	N/A	6.02 hours
I-131	364.49 (81.7%) 636.99 (7.17%) 284.31 (6.14%) 80.185 (2.62%) 722.91 (1.773%) 29.78 (2.59%)	606.31 (89%) 333.81 (7.27%)	0.9 mm in glass 1.6 mm in plastic	8.02 days

To reduce systematic errors due to ambient light, the films were stored in a light-protecting envelope and only removed during irradiation. Each film was scanned before irradiation to subtract the background values from the irradiation values to limit the inaccuracies in scan measurements. The irradiated films were scanned after 24h to allow for full polymerization to occur. An Epson Perfection V330 Photo flatbed scanner was used to scan the films in the reflective mode since a document scanner will not add to the colouration of the film (21). By using a template, the films were placed in the same central location on the scanner to avoid common scanning artefacts such as positional scan dependence with the yellow side face down on the scanner (1,16). The software package "EPSON SCAN" was used to set the scanning parameters. The professional mode was used where all the image adjustment options were turned off. A resolution of 50dpi was used. Images were scanned as 48-bit RGB colour images in reflective mode (4). The images were saved as TIFF image files. To minimize the errors and uncertainties, each film was scanned five times, and the average maximum pixel value was then used in the graphs.

Image J version 1.52i software (National Institutes of Health, Bethesda, MD) (22) was then used to analyse the TIFF images. Only the red channel was used as it is the most sensitive in the low range doses (14,23). This resulted in a 16-bit image with pixel values ranging from 0 to 65535. A circular region of interest (ROI) with a diameter of 1cm was used to get the average maximum pixel value from five scans, which was used for calculations. The ROI was positioned centrally on the film to exclude mechanical damage on the edges caused by cutting the film. Percentage error bars are shown for all results obtained.

The cumulated activity was calculated as,

$$\tilde{\mathrm{A}} = \int_0^t A(t)dt \tag{2.14}$$

$$\tilde{A} = \frac{A(t)}{\lambda} \times \left(1 - e^{-\lambda t_{exposure}}\right) \tag{2.15}$$

$A(t)$ is the activity of the radionuclide when exposure started, corrected for decay. $\lambda = \frac{ln2}{T_{1/2}}$, where, $T_{1/2}$ is the half-life of the radionuclide under consideration, $t_{exposure}$ is the time that the film was exposed to the radionuclide.

2.2.1. Film energy response and calibration curves

Film energy response data points were measured for Gafchromic™ XR-QA2 film. CFC was used as the backscattering media to limit the amount of backscatter. The data points were fitted with the neutron depletion theoretical model (Eq. 2.13) and an exponential model from Oliveira et al. (5):

$$netOD(\tilde{A}) = \alpha_1\left(1 - e^{\frac{ln2}{\beta_1}\tilde{A}}\right)\alpha_2\left(1 - e^{\frac{ln2}{\beta_2}\tilde{A}}\right)\alpha_3\left(1 - e^{\frac{ln2}{\beta_3}\tilde{A}}\right) \quad (2.16)$$

, where $\tilde{A}$ is the same as in Eq. 2.14.

The parameters $\alpha_1,\ \alpha_2,\ \alpha_3,\ \beta_1,\ \beta_2$ and β_3 were adjusted to fit the experimental points by a non-linear least-squares model (5).

2.2.2. Film response with respect to different backscatter media

Film energy response curves for Gafchromic™ XR-QA2 and RT-QA2 were compared to each other using polystyrene, perspex, lead and CFC as a backscattering medium, respectively, to determine its effect on film sensitivity.

2.2.3. Sensitivity enhancement

Cheung, T et al. have shown that the sensitivity of the films can be increased if the number of films used per measurement is increased (24). OD obtained with single layer films were compared with OD of layers of two and three films stacked together to investigate the effect on sensitivity. The films were stuck together with tape covering about 1mm of the film's edges as not to influence the ROI (24). The films had to be tightly bounded to ensure that there were no air gaps and to reduce the effect of reflected light within the film stack (24).

The principle used is described by the Beer-Lambert law, which states that the light absorbed by a medium varies exponentially with the path length of the light in the medium (25). This leads to higher absorbance by using more than one film at a time (24).

2.2.4. Film stack evaluation

By using film stacks, we can identify a method that can be used to decrease the irradiation time without a loss in net sensitivity. Film stacks can also be used to obtain the cumulative dose at different time points. Ten pieces of film were stacked on top of a Cs-137 source, and the top film of the stack was removed after a predetermined time has passed until only a single film remained and is illustrated in figure 2.4. The *OD* of the individual film pieces was measured after 24h. The upper film was removed to avoid the rest of the films being moved from the radiated position. The films were not stuck together with tape as in section 2.2.3 to be able to remove them one by one. By taping them together, the irradiation position of the film stack can change, giving rise to possible errors in the measurement. After processing, the data from the film stack was then compared to data collected from section 2.2.1, which was done by exposing the films sequentially. This was done to see if there is a relationship that can be obtained and used as a correction factor to relate the stacked film data to the single film data.

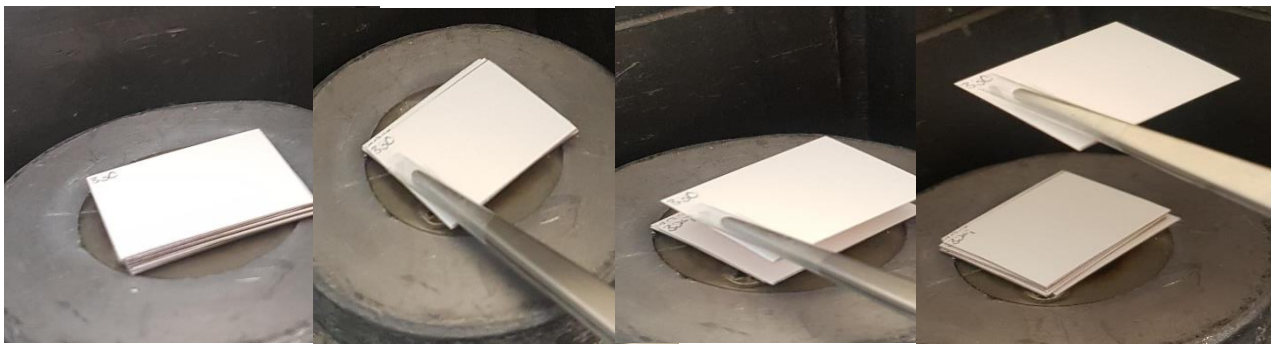

Figure 2.4: The film stack process showing the removal of the upper film.

2.2.5. Energy dependency

There are different amounts of high atomic number dopants in the Gafchromic^{TM} products (table 2.1). This results in different sensitivities to different radiation qualities (gamma-ray energies) emitted by radionuclides listed in table 2.2.

Various radiation energies of unknown photon energy composition (primary and scattered photons) from emitted gamma rays of the radionuclides may limit the application of Gafchromic^{TM}

film for dosimetry in Nuclear Medicine. Radionuclides with different primary photon energies were used to evaluate the energy dependence of the Gafchromic™ XR-QA2 and RT-QA2 films.

By comparing the OD response of the two types of film for the different radionuclide photon energies with each other, it could be determined if the two types of film were energy-dependent and which film is more sensitive and better to use for dosimetry in Nuclear Medicine. The Gafchromic™ XR-QA2 and RT-QA2 sheets of films were cut into multiple squares as explained before, and the film pieces were placed in a fixed position on a polystyrene block (29.5cm × 29.5cm × 19.5cm). The film pieces were irradiated one at a time for different exposure times with the radionuclides showed in table 2.2. After irradiation, the films were stored for 24 h before the films were scanned and processed as explained before. The *OD* values were plotted against the cumulated activity values for each radionuclide.

Only gamma energies were considered to perform the energy dependence test. By using appropriate shielding, the beta particles could be eliminated without compromising the gamma emissions. The beta energy range information in table 2.2 was used for this.

Am-241 and Tc-99m emit no beta particle. A 5mm perspex layer was placed between the Cs-137 source and the film since it emits a beta particle with a maximum energy of 513.97 keV (94.4% abundance) and has a beta range of about 3.8 mm in plastic. I-131 was placed in a glass vial with a thickness of 1mm, thus attenuating the beta particle (max energy 606.31 keV) because of the 0.9 mm beta range in glass.

2.3. RESULTS

2.3.1. Film response and fitted calibration curve

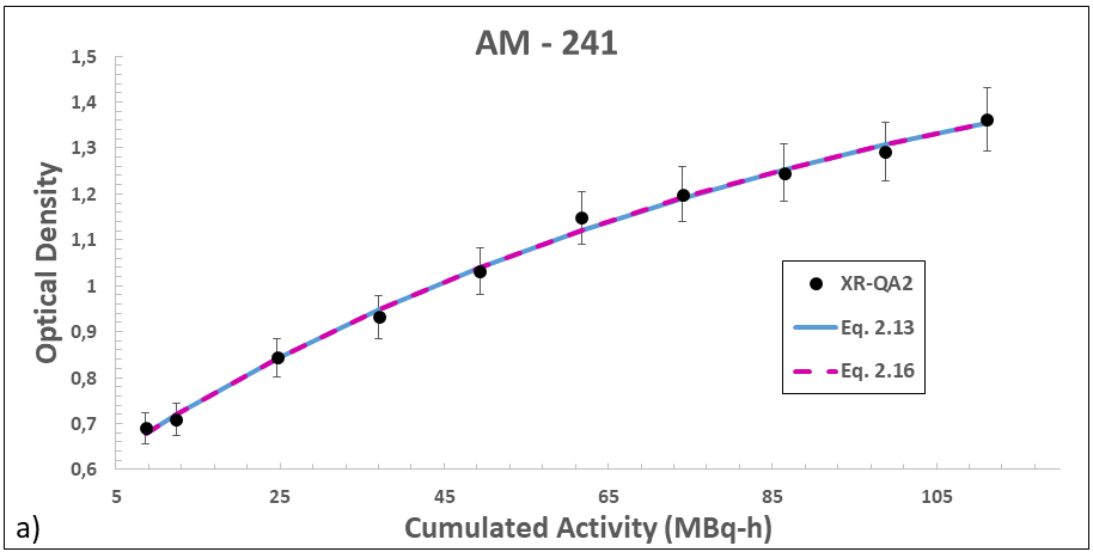

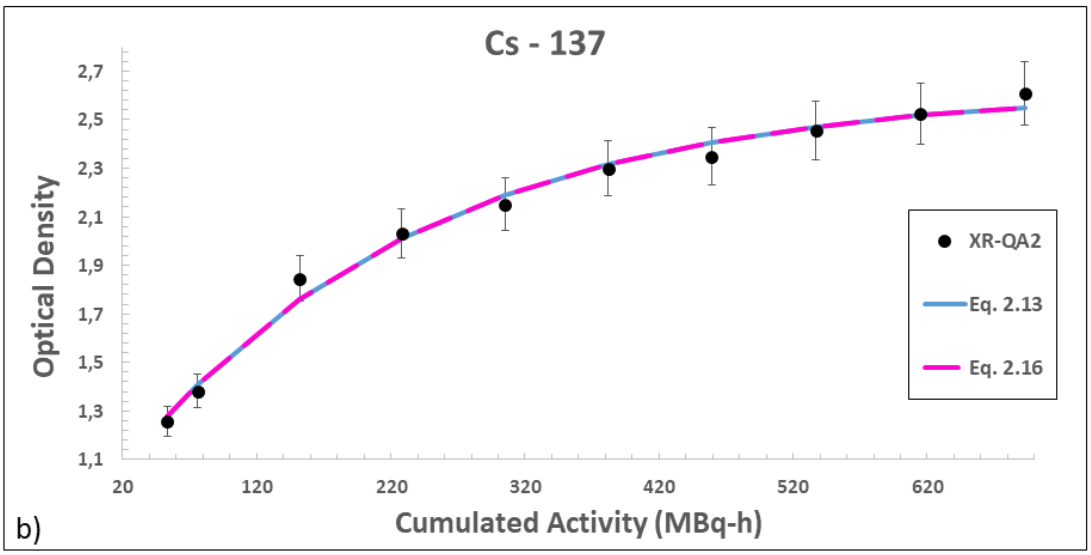

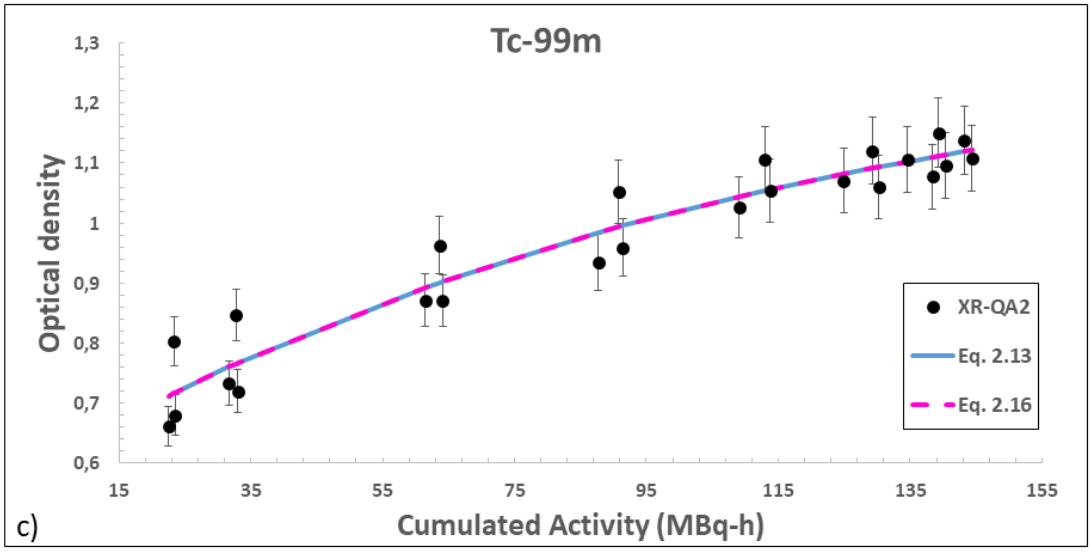

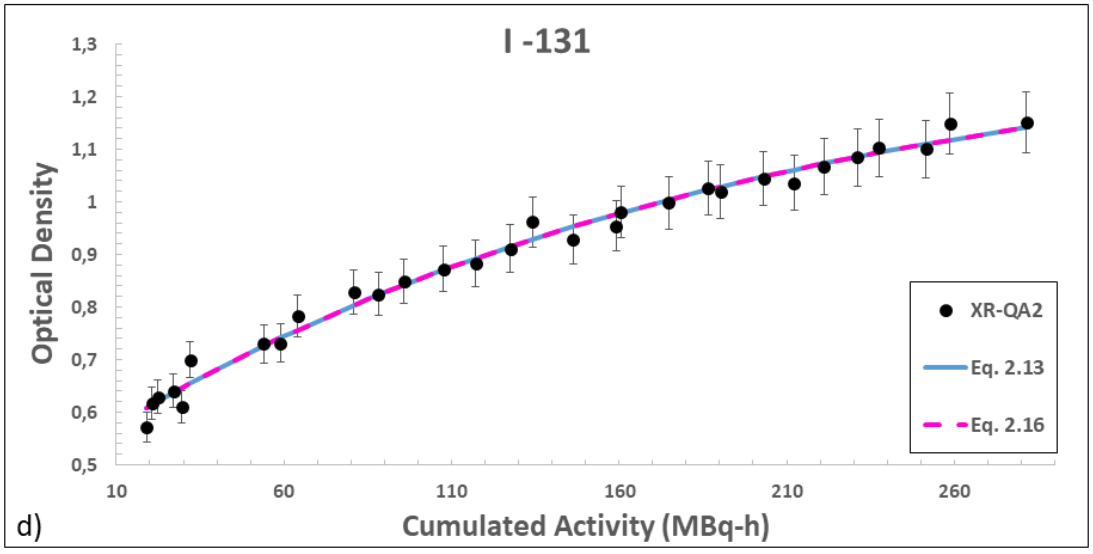

Figure 2.5: Film energy response and calibration curves for (a) Am-241, (b) Cs-137, (c) Tc- and (d) I-131 with XR-QA2 Gafchromic™ film.

OD as a function of cumulative activity is shown in figure 2.5: (a)-(d). From these graphs, it can be seen that both the calibration curves from the theoretical (Eq. 2.13) and exponential (Eq. 2.16) models fit the measured data points accurately. It should be noted that the exponential model uses six variables, whereas the neutron depletion theoretical model only uses three variables which were derived from first principles as shown from the theory section.

2.3.2. Film response with respect to different backscatter media

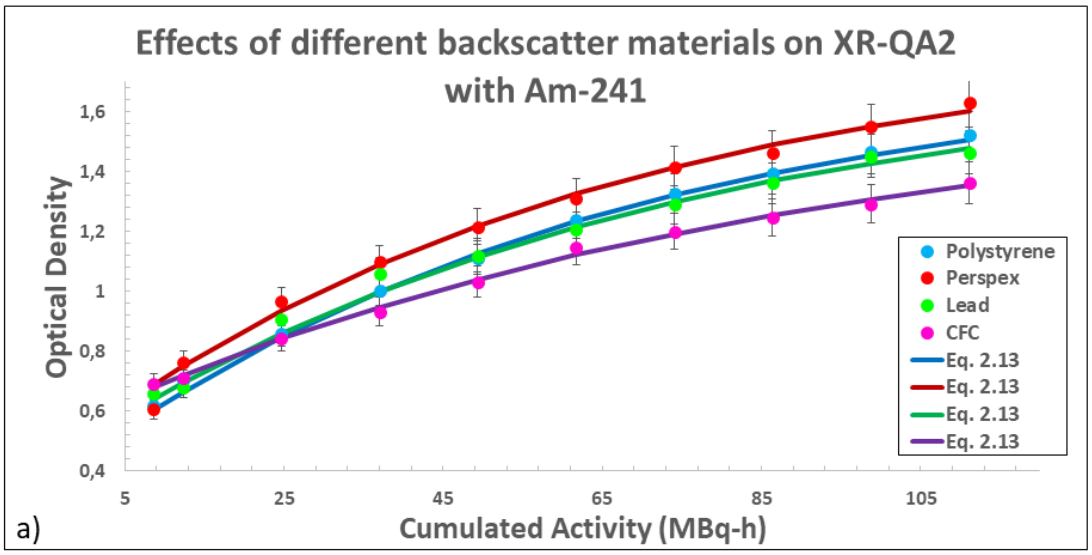

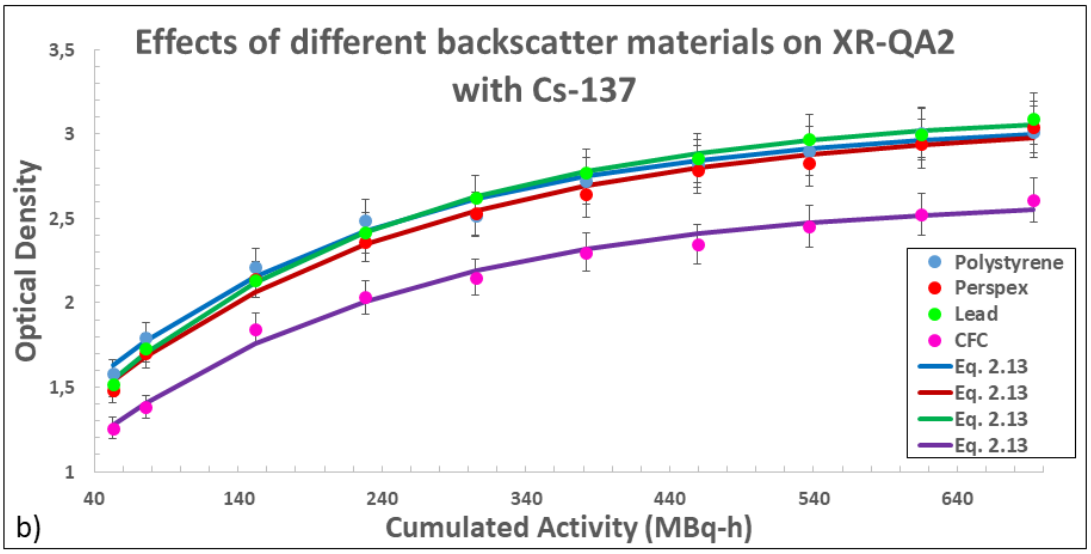

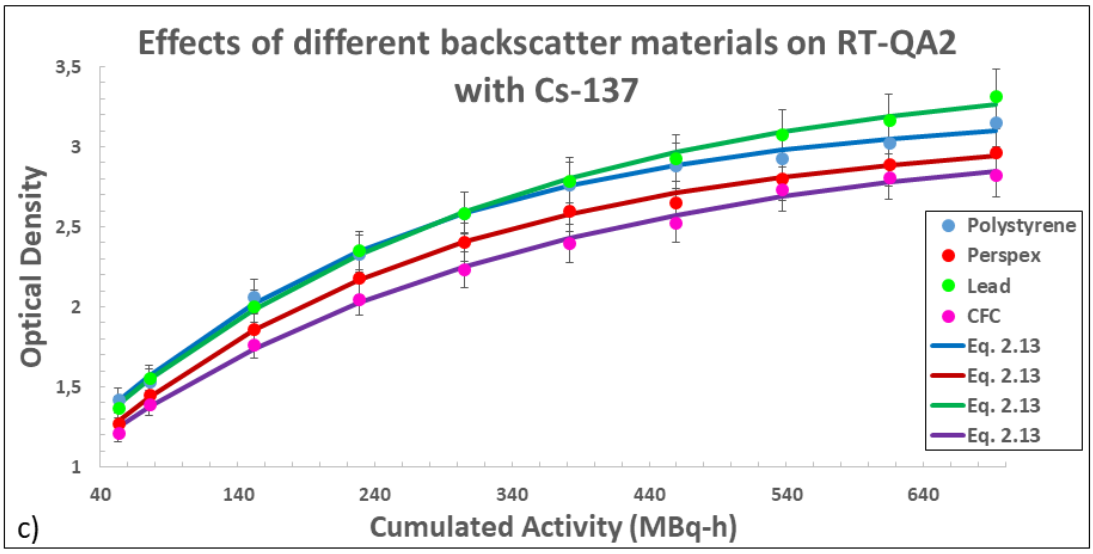
Effects of different backscatter materials on RT-QA2 with Cs-137
Optical Density
Cumulated Activity (MBq-h)
3,5
3
2,5
2
1,5
1
40
140
240
340
440
540
640
Polystyrene
Perspex
Lead
CFC
Eq. 2.13
Eq. 2.13
Eq. 2.13
Eq. 2.13

c)

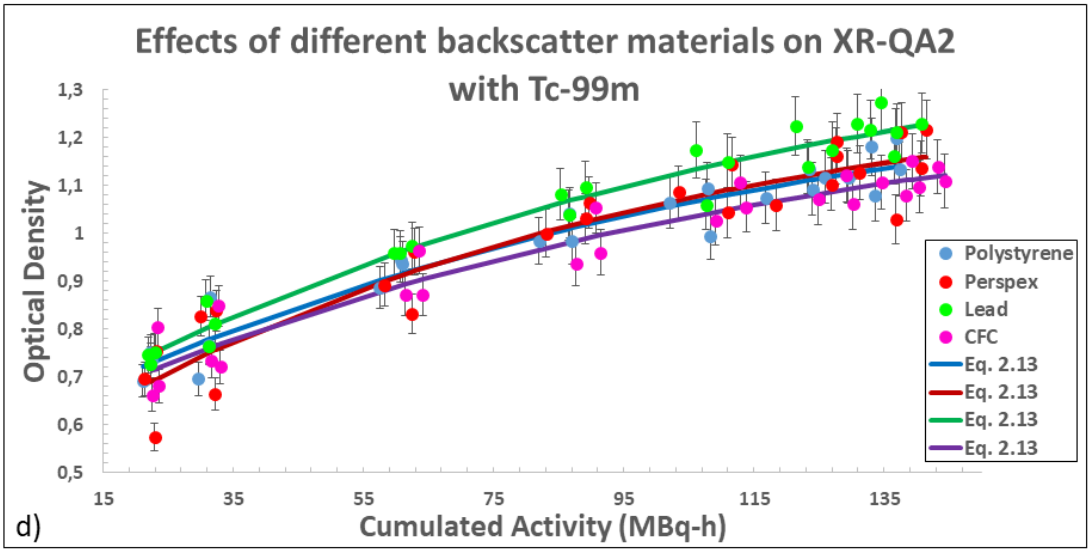
Effects of different backscatter materials on XR-QA2 with Tc-99m
Optical Density
Cumulated Activity (MBq-h)
1,3
1,2
1,1
1
0,9
0,8
0,7
0,6
0,5
15
35
55
75
95
115
135
Polystyrene
Perspex
Lead
CFC
Eq. 2.13
Eq. 2.13
Eq. 2.13
Eq. 2.13

d)

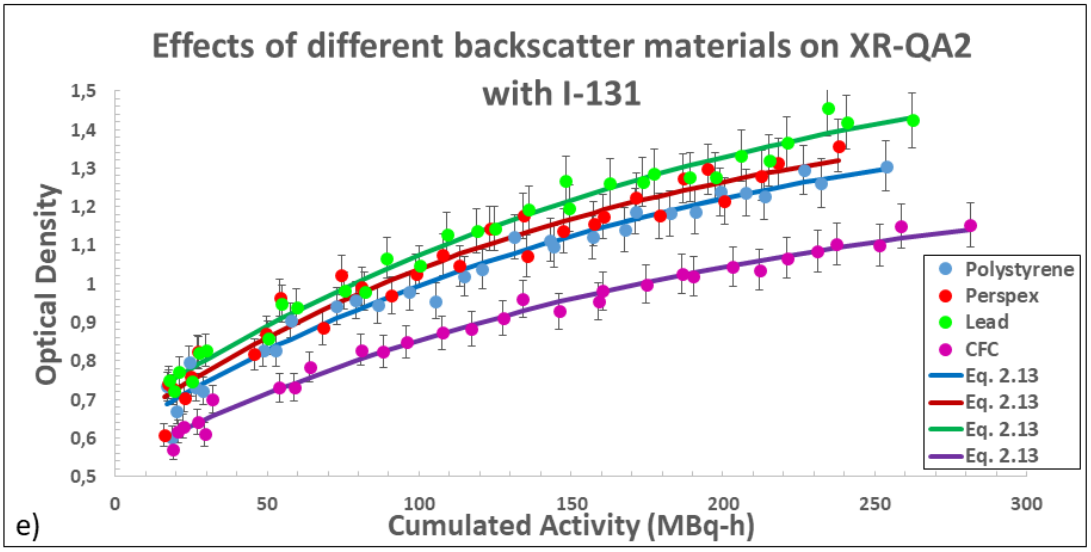

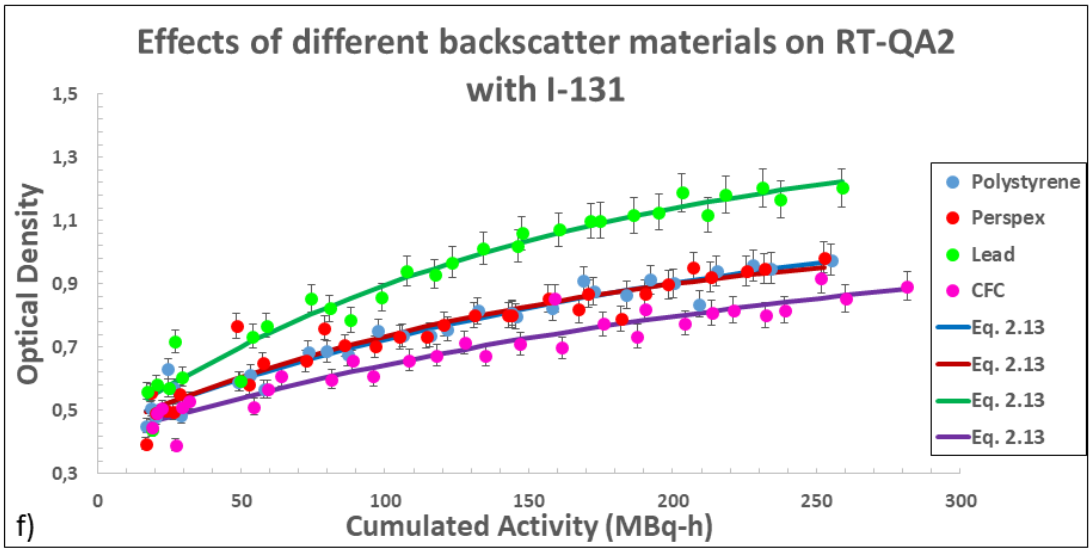

Figure 2.6: Film response curves by plotting OD versus cumulative activity for different backscatter media (a) Am-241 with XR-QA2 film, (b) Cs-137 with XR-QA2 film, (c) Cs-137 with RT-QA2, (d) Tc-99m with XR-QA2 (e) I-131 with XR-QA2 and (f) I-131 with RT-QA2.

It is shown that for very low activities such as the Am-241 used, which is 74MBq, the perspex material has more backscatter for the XR-QA2 Gafchromic™ film. In the case of Cs-137, the effect of backscatter material is shadowed by the experimental uncertainties for the same film. I-131 shows profound differences with RT-QA2 Gafchromic™ film; in other cases, studied this effect is

not pronounced. It can also be seen that the neutron depletion theoretical model (Eq. 2.13) fits the experimental data well.

Film response curves of OD versus cumulative activity for Am-241 and Tc-99m with the RT-QA2 Gafchromic™ film is not showed since the graphs gave erratic results because there was no change in optical density on the film.

2.3.3. Sensitivity enhancement

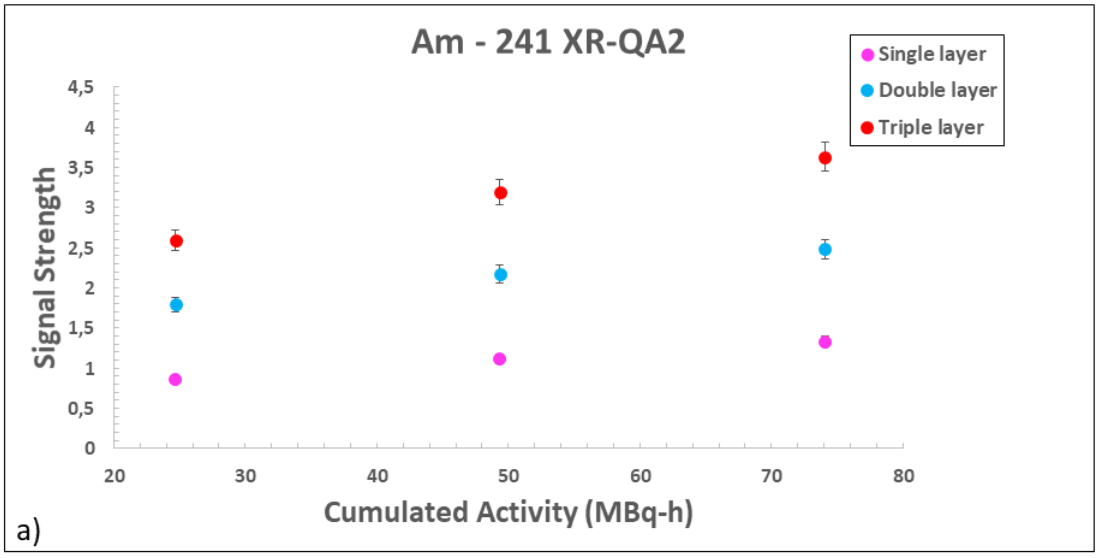

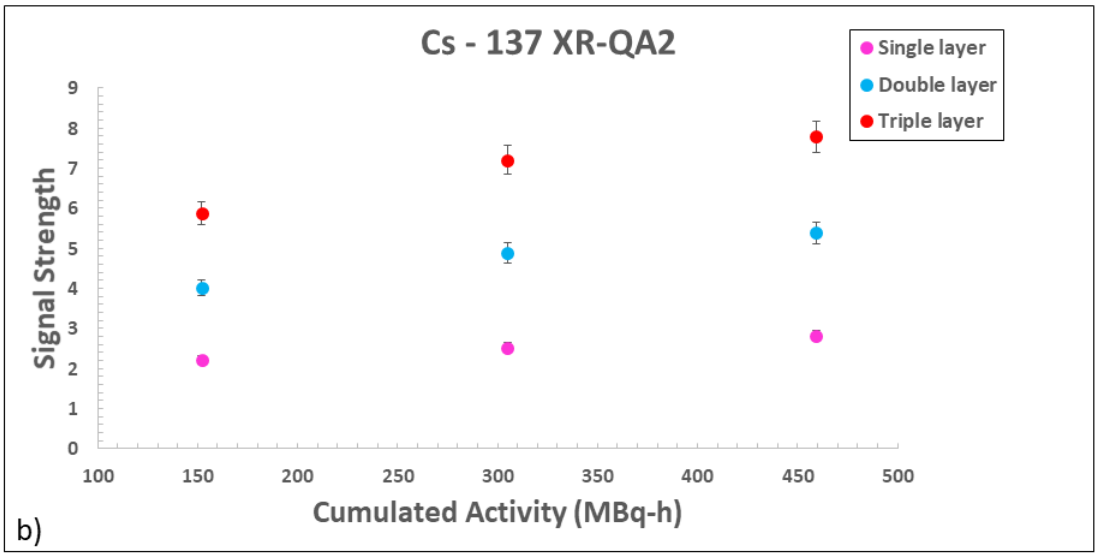

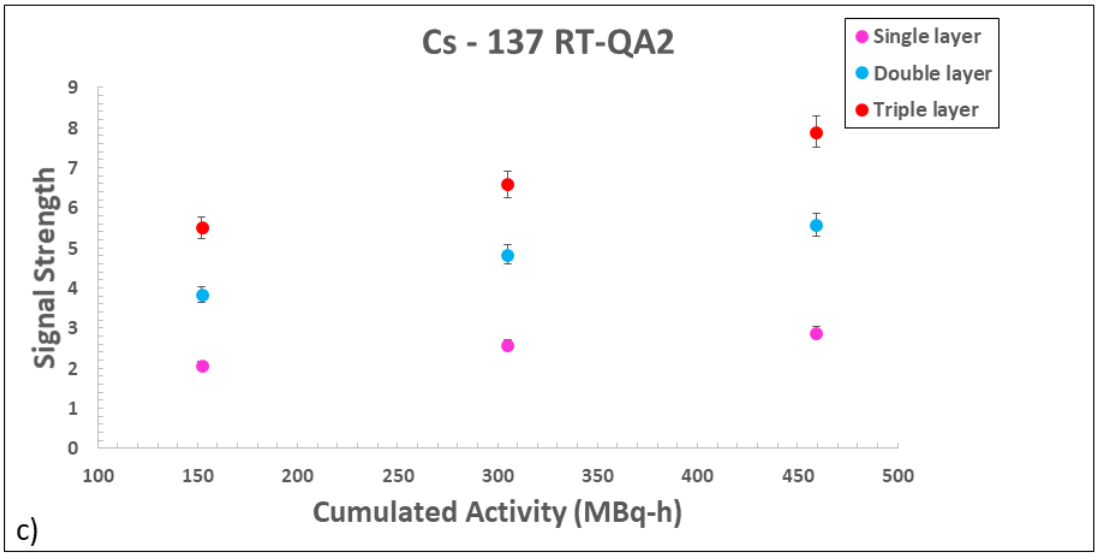
Cs - 137 RT-QA2
Single layer
Double layer
Triple layer
Signal Strength
0
1
2
3
4
5
6
7
8
9
100
150
200
250
300
350
400
450
500
Cumulated Activity (MBq-h)
c)

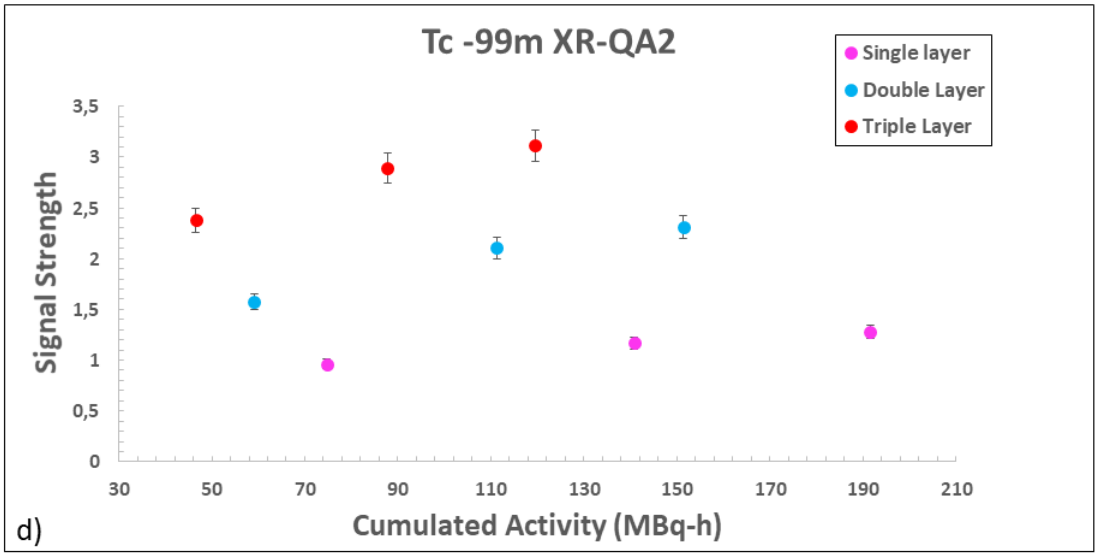
Tc -99m XR-QA2
Single layer
Double Layer
Triple Layer
Signal Strength
0
0,5
1
1,5
2
2,5
3
3,5
30
50
70
90
110
130
150
170
190
210
Cumulated Activity (MBq-h)
d)

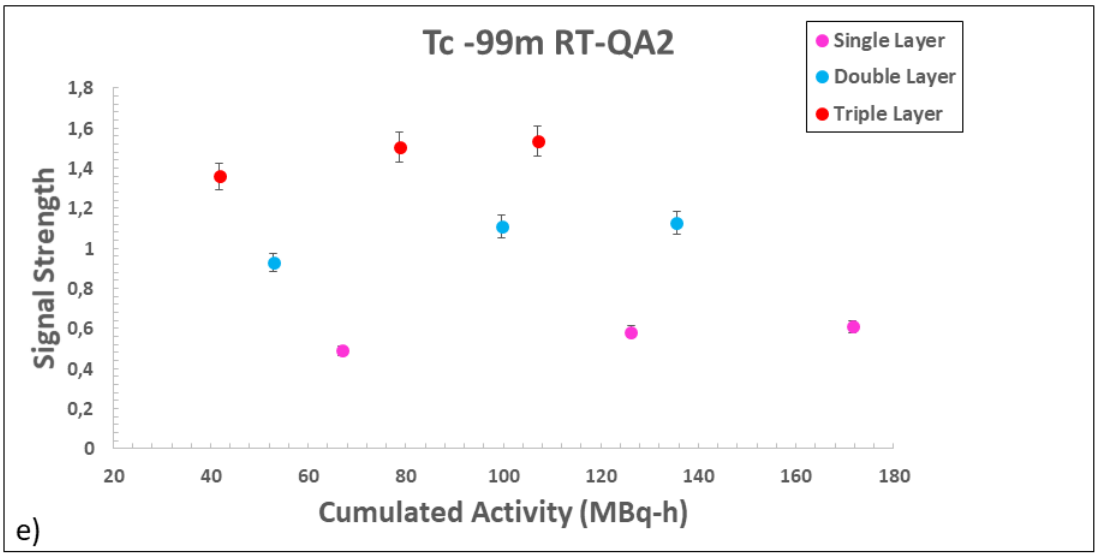
Tc -99m RT-QA2
Single Layer
Double Layer
Triple Layer
Signal Strength
1,8
1,6
1,4
1,2
1
0,8
0,6
0,4
0,2
0
20
40
60
80
100
120
140
160
180
Cumulated Activity (MBq-h)
e)

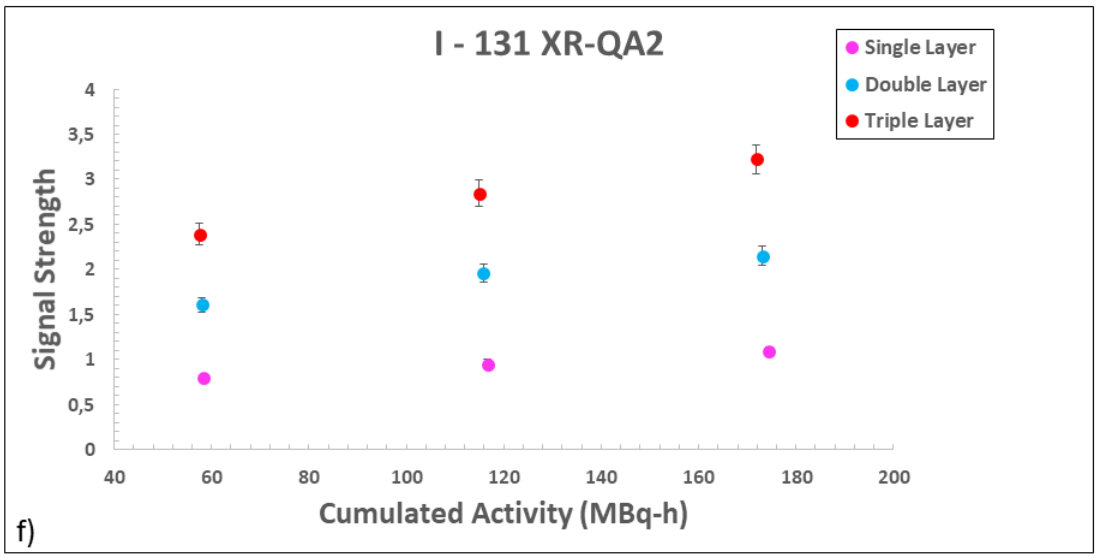
I - 131 XR-QA2
Single Layer
Double Layer
Triple Layer
Signal Strength
4
3,5
3
2,5
2
1,5
1
0,5
0
40
60
80
100
120
140
160
180
200
Cumulated Activity (MBq-h)
f)

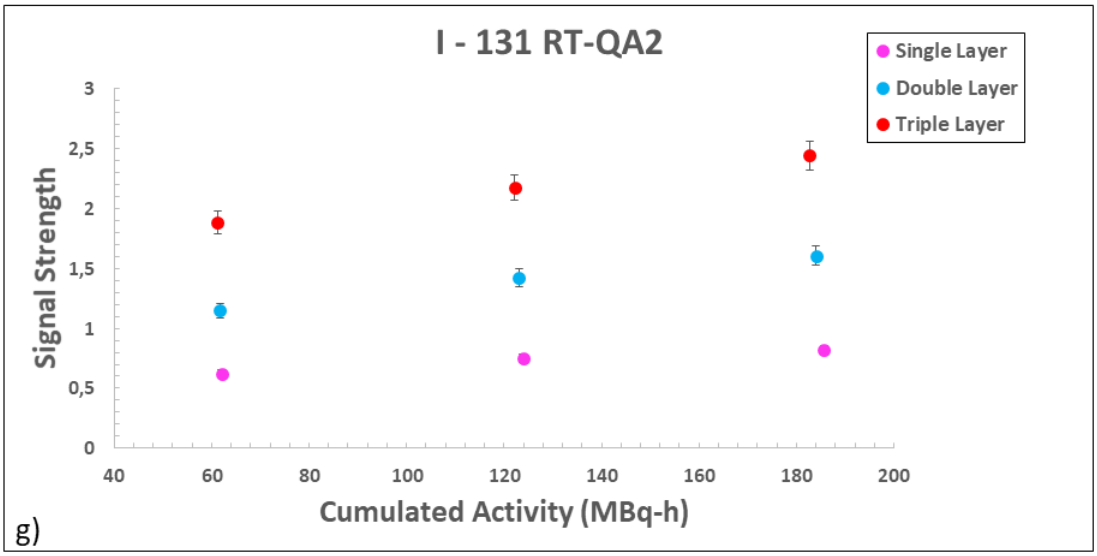

Figure 2.7: Sensitivity comparison with single, double and triple layer of films for (a) Am-241 with XR-QA2 film, (b) Cs-137 with XR-QA2 film, (c) Cs-137 with RT-QA2, (d) Tc-99m with XR-QA2, (e) Tc-99m with RT-QA2, (f) I-131 with XR-QA and (g) I-131 with RT-QA2.

Figure 2.7: (a)-(g) show the increase in signal strength for single, double and triple layer films for cumulated activities for up to 459.27 MBq-h. For the two and three film layer measurements, the sum of the OD values was used as a sensitivity enhancement rule; thus, the reference to signal strength and not OD values in the graphs atop.

These results show an increase in sensitivity of approximately 2.8 ± 0.3 times for the triple layer film compared to the single layer film. This emphasize an increase in sensitivity with the use of multiple layers of film. As the pathlength of the gamma-ray increases due to multiple film layers, more photons will be absorbed in the film layers for a certain cumulated activity value. This will result in larger *OD* values, thus enhancing the signal strength or sensitivity of the film. From figure 2.7: (a)-(g), it is evident that the signal strength can be increased by using multiple film layers.

It should be noted that although the sensitivity is increased due to the longer absorption path, it is also increased due to more scattering and possibly more build up as well.

2.3.4. Film stack evaluation

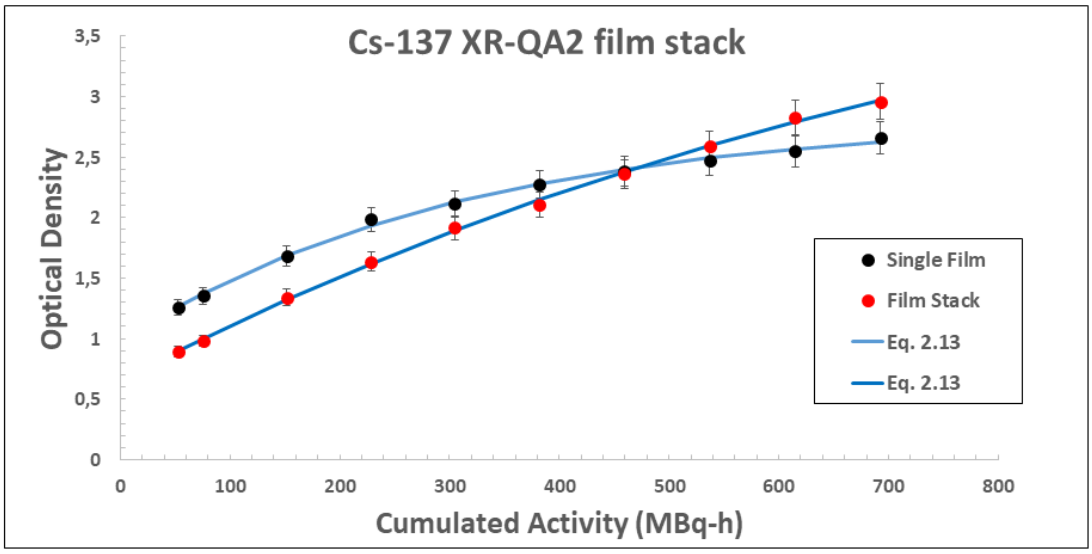

Figure 2.8: ODs of single film and film stack with Gafchromic™ XR-QA2 film as a function of cumulative activities of Cs-137.

OD values of Gafchromic™ XR-QA2 films for a single film and a single film on top of a stack of films exposed to a Cs-137 source are presented in figure 2.8. For the film stack, the individual films are removed from the top of the stack, and the OD is measured after 24 h. From figure 2.8, it can be seen that the first data point is lower for the stack compared to the single film for the same exposure time since the stack itself attenuates some of the Cs-137 gamma rays. Removal of the films from the stack converge to the single film data point, but interestingly enough, it crosses the single film data set around 459 MBq-h. The stack enhances the dose given to the film closer to the source and is ascribed to backscattering of the film stack itself that increases the dose to the last layers of film, that is not present for the single film measurements. Thus, stacked films have both attenuation effects from the bottom film layers and backscattering effects from the top layers to consider if OD values are measured.

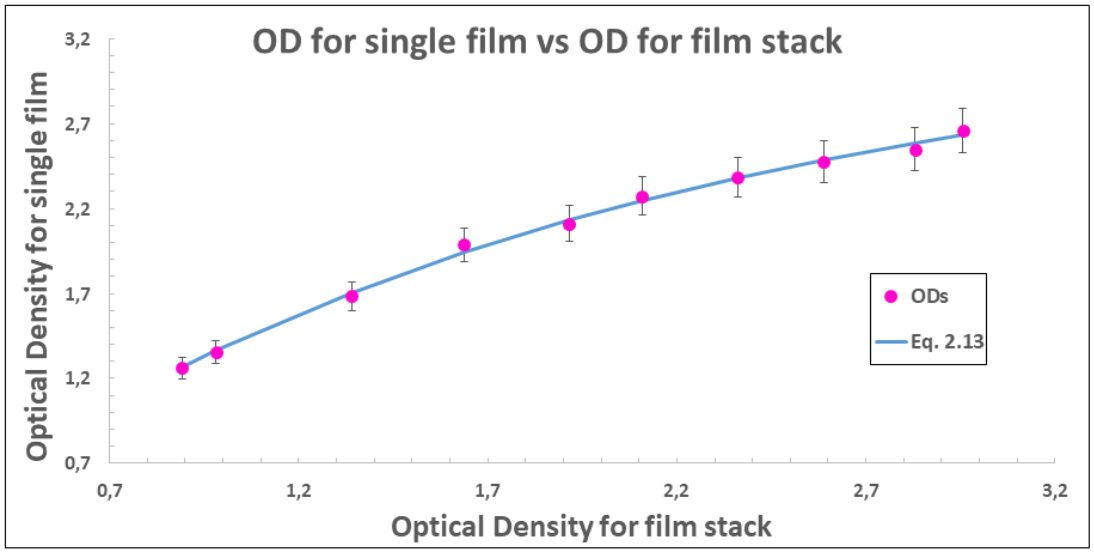

Figure 2.9: OD for single film vs OD for film stack for Cs-137.

In figure 2.9, it can be seen that when using a film stack approach the value for a single film could be determined from the calibration curve (Eq. 2.13) obtained.

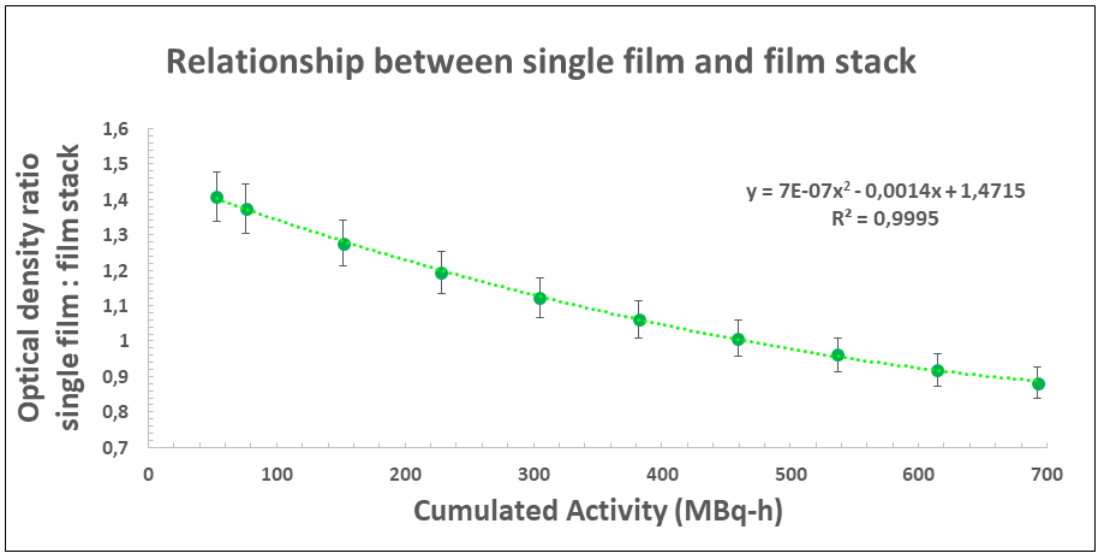

Figure 2.10: Relationship between neutron depletion theoretical model (Eq. 2.13) of the film stack and single film test for Cs-137.

The correction factors to relate the staked film data to the single film data is shown in figure 2.10, which can be represented by a second-order polynomial obtained by the ratio of the single film

measurement to the stack film measurement. The staked film approach has significant time saving advantage compared to the single film approach. This method also enables the user to obtain cumulative doses at multiple time points.

2.3.5. Energy dependence

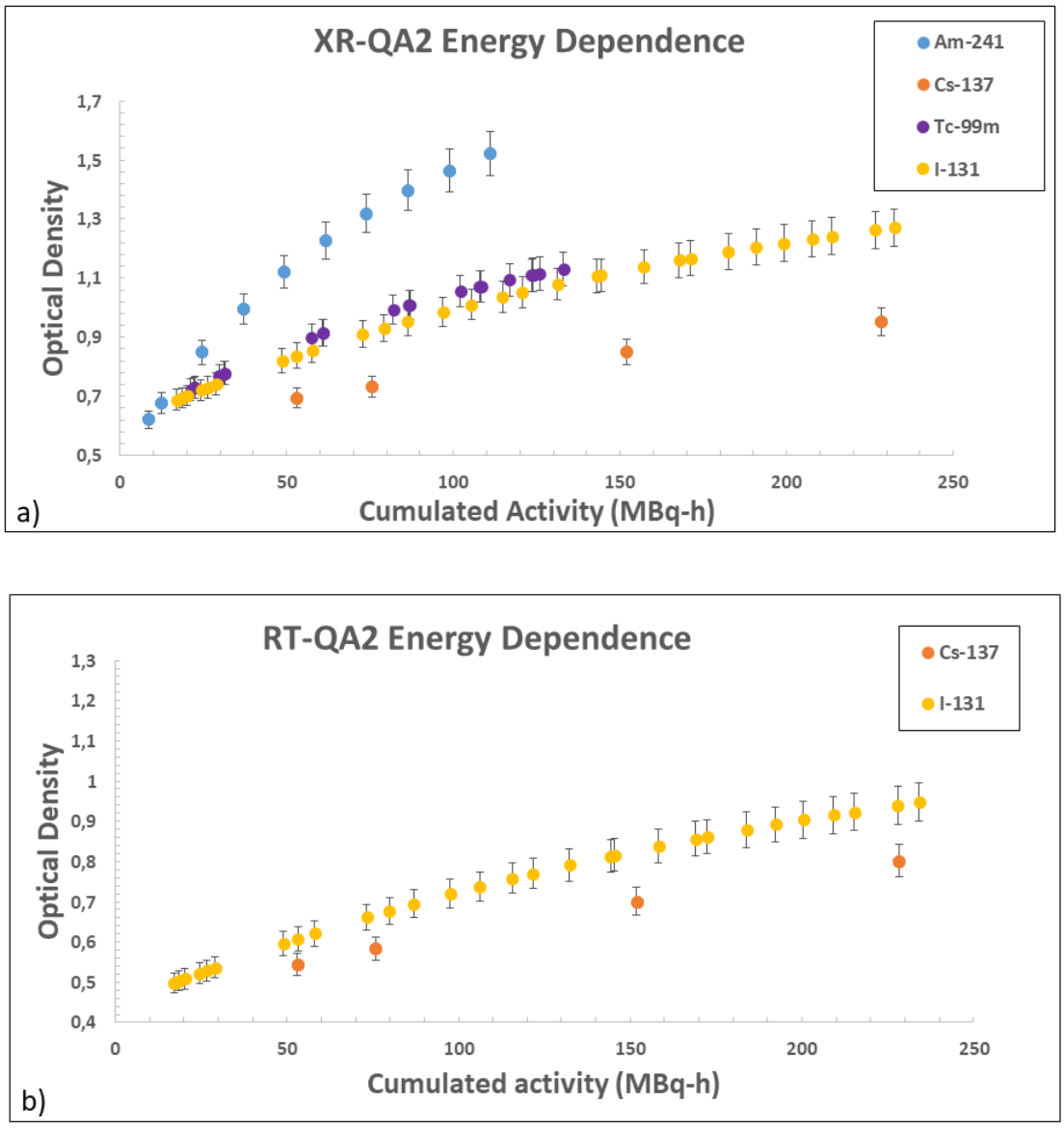

Figure 2.11: Film energy dependence for (a) Gafchromic™ XR-QA2 film and (b) Gafchromic™ RT-QA2 film.

To do the energy dependence comparison test, only gamma energies were considered. Therefore, beta particles were eliminated by using appropriate shielding without compromising the gamma emission, as mentioned above.

From figure 2.11 (a) it is clear that the Gafchromic™ XR-QA2 film is more sensitive for low energy gamma rays. The Gafchromic™ RT-QA2 film's low sensitivity only showed an OD change when using the Cs-137 and I-131 source. The Gafchromic™ XR-QA2 film has a small amount of Bismuth which raises its effective atomic number from 22 to 29 when compared to the Gafchromic™ RT-QA2 film. This will enhance the photoelectric interaction component and can be observed by the energy dependence seen from the lowest energies (Am-241) to the highest energies (Cs-137) of the gamma rays. The Gafchromic™ RT-QA2 film is less sensitive and therefore only responds to higher exposures. We can also observe that the response difference of the Gafchromic™ RT-QA2 film is less pronounced between Cs-137 and I-131 when compared to their counterparts for Gafchromic™ XR-QA2 in figure 2.11 (a).

The same amount of activity for Tc-99m and I-131 was used in this study; however, it should be noted that I-131 and Tc-99m have gamma energies of 364.49kev and 140.51kev, respectively. Thus, the Gafchromic™ RT-QA2 film had a response to the I-131 but not to the Tc-99m due to the higher exposure.

Energy dependence graphs for Am-241 and Tc-99m with Gafchromic™ RT-AQ2 film is not showed since the graphs gave erratic results because there was no change in optical density on the film.

2.4. DISCUSSION

In this study, two Gafchromic™ film types were evaluated as potential radiation detectors for a range of different radionuclides. The relationship between *OD* and cumulated activity could be fitted well with the neutron depletion theoretical calibration curve based on a neutron depletion model and the Beer-Lambert absorption law. In modern nuclear medicine, radiopharmaceuticals are used to diagnose and treat certain diseases. Accurate dosimetry is important to enhance therapy and limit organ-at-risk complications. It is of interest to determine with precision and

accuracy the amount of activity being administered to a patient. The rule of ALARA should always be followed, which keeps radiation doses as Low As Reasonably Achievable. The dose given should also be justified, limited and optimized to give the lowest dose necessary, which will give a good image and still keep the patient safe (5).

By using accurate predetermined calibration curves, we can enhance the accuracy of radiation dose measurements (4). Thus, by using the neutron depletion theoretical model from the theory section in this article, which is based on first principles, we can ensure more accurate results.

When using high activities, it is more convenient to use Gafchromic™ RT-QA2 film; this typically would be to determine therapy dosages. For low diagnostic activities, it is advised to use the Gafchromic™ XR-QA2 film. When there is an uncertainty of energy levels, a combination of films can be used as a multilayer to determine high or low energy. If the energy is very low, multiple layers of Gafchromic™ XR-QA2 film can be used to increase the signal strength.

The Gafchromic™ XR-QA2 film also decreases the statistical variance of data because of its sensitivity to radiation due to the high atomic elements included in its active layer. The statistical variance can also be decreased more when irradiation time is increased.

From the backscatter mediums test, we can see that lead increases the scatter at higher energies and perspex at lower energies. It is thus important to use a backscatter material closest to air, such as CFC, to decrease scatter influences in measurements.

The uncertainty for OD vs Cumulated Activity measurement is in the order of 6 % for most cases presented in this study. The results in this study show the Gafchromic™ film's potential as a radionuclide dosimeter.

2.5. CONCLUSION

From this study, it can be concluded that the neutron depletion theoretical model relating OD to cumulative activity as discussed in the theory section of this article can be constructed and is better to use because it only has three variables and needs fewer data points for fitting of the

data. For nuclear medicine, Gafchromic™ XR-QA2 film will be better to use for dosimetry methods because it has a higher sensitivity to lower cumulated activities and accurate response to high cumulated activities. It also shows more sensitivity to energy. Whereas the RT-QA2 Gafchromic™ film is not sensitive to pick up low cumulated activities and thus only gives results for radionuclides with high cumulated activities. Multiple layers can also be used to increase the film sensitivity. A stacked film approach can be used to set up an OD *vs* time-activity curve, but a correction function must be used to correct for attenuation and backscattering effects.

ACKNOWLEDGMENT

This research and the publication thereof is the result of funding provided by the Medical Research Council of South Africa in terms of the MRC's Flagships Awards Project SAMRC-RFA-UFSP-01-2013/ HARD

REFERENCES

1. Alnawaf H, Butson MJ, Cheung T, Yu PKN. Scanning orientation and polarization effects for XRQA radiochromic film. Phys Medica. 2010;26(4):216–9.
2. McCabe BP, Speidel MA, Pike TL, Van Lysel MS. Calibration of GafChromic XR-RV3 radiochromic film for skin dose measurement using standardized x-ray spectra and a commercial flatbed scanner. Med Phys. 2011;38(4):1919–30.
3. Niroomand-Rad A, Blackwell CR, Coursey BM, Gall KP, Galvin JM, McLaughlin WL, et al. Radiochromic film dosimetry: recommendations of AAPM Radiation Therapy Committee Task Group 55. American Association of Physicists in Medicine. Med Phys. 1998;25:2093–115.
4. Giaddui T, Cui Y, Galvin J, Chen W, Yu Y, Xiao Y. Characteristics of Gafchromic XRQA2 films for kV image dose measurement. Med Phys. 2012;39(2):842–50.
5. Oliveira PA, Santos JAM. Innovative methodology for intercomparison of radionuclide calibrators using short half-life in situ prepared radioactive sources. Med Phys. 2014;41(7).
6. Ahn BC. Personalized Medicine Based on Theranostic Radioiodine Molecular Imaging for Differentiated Thyroid Cancer. Biomed Res Int. 2016;2016.
7. Kelkar SS, Reineke TM. Theranostics: Combining imaging and therapy. Bioconjug Chem. 2011;22(10):1879–903.

8. Hosono M. Perspectives for Concepts of Individualized Radionuclide Therapy, Molecular Radiotherapy, and Theranostic Approaches. Vol. 53, Nuclear Medicine and Molecular Imaging. 2019. p. 167–71.

9. Aldelaijan S, Tomic N, Papaconstadopoulos P, Schneider J, Seuntjens J, Shih S, et al. Technical Note: Response time evolution of XR-QA2 GafChromic™ film models. Med Phys. 2018;45(1):488–92.

10. Cheung T, Butson MJ, Yu PKN. Experimental energy response verification of XR type T radiochromic film. Phys Med Biol. 2004;49(21):N371–N376.

11. Ashland. Gafchromic™ RTQA2 film [Internet]. [cited 2019 Oct 30]. Available from: http://www.gafchromic.com/documents/PC-11804_Gafchromic_RTQA2.pdf

12. Ashland. Gafchromic™ XR film State-of-the-art [Internet]. [cited 2019 Oct 30]. Available from: http://www.gafchromic.com/documents/PC-11805_Gafchromic_XR.pdf

13. Callens MB, Crijns W, Depuydt T, Haustermans K, Maes F, D'Agostino E, et al. Modeling the dose dependence of the vis-absorption spectrum of EBT3 GafChromic™ films. Med Phys [Internet]. 2017 Jun [cited 2019 Dec 2];44(6):2532–43. Available from: http://doi.wiley.com/10.1002/mp.12246

14. Butson MJ, Cheung T, Yu PKN. Measuring energy response for RTQA radiochromic film to improve quality assurance procedures. Australas Phys Eng Sci Med. 2008;31(3):203–6.

15. Butson E, Alnawaf H, Yu PKN, Butson M. Scanner uniformity improvements for radiochromic film analysis with matt reflectance backing. Australas Phys Eng Sci Med. 2011;34:401–7.

16. Devic S, Tomic N, Lewis D. Reference radiochromic film dosimetry: Review of technical aspects. Phys Medica. 2016;32(4):541–56.

17. Das IJ, editor. Radiochromic film: Role and applications in radiation dosimetry. Boca Raton: CRC Press; 2018. 1–387 p.

18. Chu SYF, Ekström LP, Firestone RB. The Lund/LBNL Nuclear Data Search [Internet]. 1999 [cited 2020 Nov 3]. Available from: http://nucleardata.nuclear.lu.se/toi/

19. Bushberg JT, Seibert JA, Leidholdt Jr EM, Boone JM. The Essential Physics of Medical Imaging. 2nd ed. Mitchell CW, editor. Philadelphia: LIPPINCOTT WILLIAMS & WILKINS, a WOLTERS KLUWER business; 2002. 1–933 p.

20. Radionuclide Information Booklet - Canadian Nuclear Safety Commission [Internet]. 2018 [cited 2019 Dec 2]. p. 1–42. Available from: http://www.nuclearsafety.gc.ca/pubs_catalogue/uploads/Radionuclide-Information-Booklet-2018-eng.pdf

21. Butson MJ, Yu PKN, Metcalfe PE. Effects of read-out light sources and ambient light on

radiochromic film. Phys Med Biol. 1998;43(8):2407–12.

22. Rasband WS. ImageJ [Internet]. U.S. National Institutes of Health, Bethesda, Maryland, USA. [cited 2019 Dec 2]. Available from: https://imagej.nih.gov/ij/

23. Alsadig AA, Abbas S, Kandaiya S, Ashikin NARNN, Qaeed MA. Differential dose absorptions for various biological tissue equivalent materials using Gafchromic XR-QA2 film in diagnostic radiology. Appl Radiat Isot. 2017;129:130–4.

24. Cheung T, Butson MJ, Yu PKN. Use of multiple layers of Gafchromic film to increase sensitivity. Phys Med Biol. 2001;46(10).

25. Ören Ü, Rääf CL, Mattsson S. Gafchromic film as a fast visual indicator of radiation exposure of first responders. Radiat Prot Dosimetry. 2012;150(1):119–23.

Chapter 3: The relation between XR-QA2 and RT-QA2 Gafchromic™ film optical density and absorbed dose in water produced by radionuclides.

Maria. M. Joubert, Deté van Eeden, Freek. C. P. du Plessis
Department of Medical Physics, University of the Free State, Bloemfontein 9301

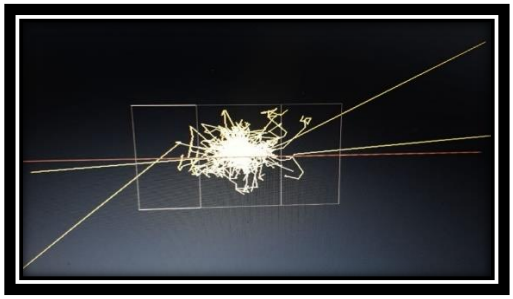

TABLE OF CONTENTS

ABSTRACT

Purpose: In this study, Monte Carlo (MC) simulations were done to relate the dose response of the film to that in water. The effect of backscattering materials (PMMA, lead, polystyrene, and air) were investigated on its influence on film density for radionuclides including Am-241, Tc-99m, I-131, Cs-137.

Methods: A BEAMnrc MC simulation was designed to score a phase space file (PSF) below the container of the radionuclide under consideration to use as an input file for the subsequent DOSXYZnrc MC simulation. The geometry of the container holding the radionuclide was built using the component modules available in BEAMnrc. BEAMDP was used to investigate the container effect on the radionuclide spectrum as well as the fluence. The DOSXYZnrc simulation produced the absorbed dose in XR-QA2 and RT-QA2 Gafchromic™ films. The DOSXYZnrc simulation was repeated for the Gafchromic™ film now replaced with water to get the absorbed dose in water. From these results, conversion factors for the dose in water to the film dose for the different radionuclides, Am-241, Tc-99m, I-131, and Cs-137 were obtained. The actual film dose was calculated using the specific gamma exposure constant (Γ) at a distance of 50 cm for a point source approximation. From the BEAMnrc simulations, the particle fluence was extracted from PSFs at the location on the origin respectively to correct for the fluence at 0.1 cm below the sources from the fluence 50 cm away since the inverse square law will not apply for finite-size sources.

Results: A fitting function based on the neutron depletion model fits the optical density *vs* absorbed film dose data well and can be used as a calibration tool to obtain the film dose from its optical density. Lead as a backscatter material results in a higher optical density change but lower absorbed dose. The XR-QA2 Gafchromic™ film is more sensitive than the RT-QA2 Gafchromic™ film, showing a more responsive optical density (OD) change in the energy range of radionuclides used in this study. Conversion factors were determined to convert the dose in water to the dose in Gafchromic™ film. The Am-241 and I-131 simulated absorbed dose in film to dose in water does not fluctuate as much as the simulated absorbed dose in film and water when using Tc-99m and Cs-137.

Conclusions: MC BEAMnrc simulations are useful to simulate radionuclides and their containers. BEAMDP extracted energy spectra showed that the radionuclide containers produced a Compton effect on the energy spectra and added filtration on the lower spectral photon components. Extracted fluence ratios from PSFs were used to calculate the absorbed dose value at 0.1cm distance from the source. By using the fit function, the dose in the film can be determined for known optical density values. The effect of the backscatter materials showed that the XR-QA2 Gafchromic™ film results in higher optical density values than the RT-QA2 Gafchromic™ film. The absorbed dose in both the films are similar, but not for a radionuclide such as Am-241 with an activity of 74MBq. The lead backscatter material showed to be the most prominent in optical density enhancement, and the air equivalent material was the least prominent. The XR-QA2 Gafchromic™ film is the most sensitive and will be the best option if working with low energies. The absorbed dose in the XR-QA2 Gafchromic™ film also showed a good comparison to the absorbed dose in water for the Am-241 radionuclide with an activity of 74MBq.

Keywords: Gafchromic™ film, Radionuclides, Monte Carlo, DOSXYZnrc, BEAMnrc, BEAMDP.

3.1. INTRODUCTION

Monte Carlo (MC) simulations are the most accurate method to determine dose due to ionizing radiation and can be referred to as the gold standard for dose calculations (1,2) MC codes such as BEAMnrc and DOSXYZnrc has been widely used in radiotherapy due to the importance of accurate dose delivery.

BEAMnrc is primarily used for radiotherapy source modelling (3). The BEAMnrc code was written to have independent component modules (CMs) which are named mainly after the components they were supposed to model, but they can be applied to many other structures (4). This is an advantage as we are able to construct containers with an activity volume inside by using some of the CMs. CMs such as the FLATFILT are designed to handle complex beam flattening filters and have an altering shape which is ideal to model radionuclide container geometries despite being used for radiation machine modelling (4). BEAMDP can be used to analyze the Phase-Space File (PSF) obtained in BEAMnrc.

In order to use the MC codes to calculate the dose, there is a requirement of good distribution estimates of charge, energy, position and direction of particles from the source (5). This information is included in the PSF, which can be collected by using the BEAMnrc code.

When selecting the Energy Spectrum from a PSF in BEAMDP, it will be able to generate an energy spectrum. BEAMDP can then be used to determine the influences of the containers modelled in BEAMnrc on the energy spectra of the activity inside as the original decay particles traverse through the materials. The inverse square law also has an effect on measurements and can be determined by using BEAMDP to investigate PSF at various distances from the radionuclide.

Radionuclide activity and film response can be related to absorbed dose by using MC simulations (6). This enables characterizing the film such that its response is linked to absorbed dose in the film. If the simulations are carried out in water, then it is possible in principle to relate the absorbed dose in the film to the absorbed dose in water by using suitable conversion factors.

Dosimetry uses radiation dosimeters for the quantitative determination of absorbed dose, which is one of the physical procedures used to improve the accuracy of radiation dose delivery (7). Over the years, radiochromic film (RCF) has been used in clinical and research dosimetry applications because it offers high spatial resolution and near tissue-equivalence, making it suitable for dose distribution measurements (8). RCFs are self-developing; thus, there is no need for dark rooms or chemical processing. These films undergo a polymerization process to indicate a colour change once they are exposed to ionizing radiation. These are some of the reasons that RCF is the replacement dosimeter of choice in a growing amount of clinical centres (8).

The energy dependence has been investigated for various types of RCFs, including the XR-QA2 Gafchromic^{TM} film (9–11). RCFs have a lower energy dependence than radiographic films. The manufacturer of the Gafchromic^{TM} films (Ashland Inc, Wayne, N) made films used for dosimetry at low energies more sensitive by adding high Z components to the sensitive layer of the film such as XR-QA2 Gafchromic^{TM} film (11,12). It was found that the XR-QA2 Gafchromic^{TM} film has a pronounced energy dependent response for beam qualities used for x-ray based diagnostic imaging purposes (11). The energy dependence on the RT-QA2 Gafchromic^{TM} film has not been studied yet as far as we know. It has been found that the RT-QA2 film can be used as an alternative

to EBT2 film and that the film depends on the energy of the incident photon and the depth of measurement (13).

Any radioactive point source will emit radiation which spreads its fluence equally in all directions, meaning isotropically. The inverse square law means that as the distance from the point source increases the flux of radiation will decrease with the inverse square of the distance (14). Various experiments have been done to investigate the inverse-square law but none with a distance of 1mm as far as we know due to the difficulties of designing sensitive short-range experiments (15).

When calculating the exposure rate of a radionuclide source at a distance, the air kerma rate constant (Γ) is used to relate the activity of the radionuclide to the exposure rate (16). Each radionuclide has a specific Γ value and can be defined as the amount of air kerma due to gamma and beta emissions in mGy per hour at a distance of 1m from an unshielded 1 GBq radionuclide point source (14).

This study aims to perform MC simulations with BEAMnrc and DOSXYZnrc to relate XR-QA2 and RT-QA2 Gafchromic™ film response to absorbed dose in water and to convert it into absorbed dose in film. The effect of different backscattering materials will also be investigated to determine its influence on film dose since this can play a role in experimental setup procedures for radionuclide film dosimetry.

3.2. MATERIALS AND METHODS

For this study, the film density has to be converted into absorbed dose to water. Water is used as a reference dosimetry phantom because it is similar to the radiation absorption and scattering characteristics of muscles and other soft tissues (7,17,18).

XR-QA2 and RT-QA2 Gafchromic™ film pieces were irradiated by radionuclides including Am-241, Cs-137, Tc-99m, and I-131 respectively. The films were scanned with an Epson Perfection V330 Photo flat-bed document scanner in reflection mode. Initial scans were made before exposure and then after 24h for full polymerization to occur and to correct for background density. Scanner settings were set to 48-bit RGB (16 bits per channel) with a 50 dpi resolution (19,20). The films

were saved as tagged-image-file format (TIFF) images. A template was used to keep the film centralised on the scanner (21). Image J version 1.52i software (National Institutes of Health, Bethesda, MD) (22) was used to get the resulting film response by only using the red channel which is the most sensitive (23). At this stage, we could determine the optical density response as a function of cumulative activity in the film from measurement.

Before MC simulation was introduced to determine the dose ratio between the film and water, cross-section data needed to be calculated at first. The atomic composition, as shown in table 3.1, was used. MC simulations were performed for radionuclides with energies ranging from 13.95 keV to 662 keV according to tables of recommended data (24) for the gamma and beta energies of the radionuclides used in this study.

All simulations were done by using the latest versions of BEAMnrc and DOSXYZnrc (3,25). Both radiation transport software packages, DOSXYZnrc and BEAMnrc, used for the simulations are based on the user code EGSnrc (2,26,27)

Table 3.1: Atomic composition of the active layer in Gafchromic™ film (28) to calculate cross-section data for usage in the Monte Carlo codes.

Composition by element and atom (%)										
Film Model	H	Li	C	N	O	Al	S	Ba	Bi	Z_{eff}
XR-QA2	40.6	0.1	39.8	0.2	18.1	0.0	0.5	0.5	0.2	29.98
RTQA2	42.1	0.0	38.2	0.0	18.5	0.1	0.5	0.5		22.71

In the next step, the BEAMnrc and DOSXYZnrc MC codes were used to simulate the dose per history in the XR-QA2 and RT-QA2 Gafchromic™ film. From these simulations the dose ratio between the film and water $\left(\frac{D_f}{D_w}\right)$ could be calculated. This enabled dose conversion from water into dose in film. BEAMnrc was used to set up the geometry of the container holding the radionuclide shown in figure 3.1: (a) – (d).

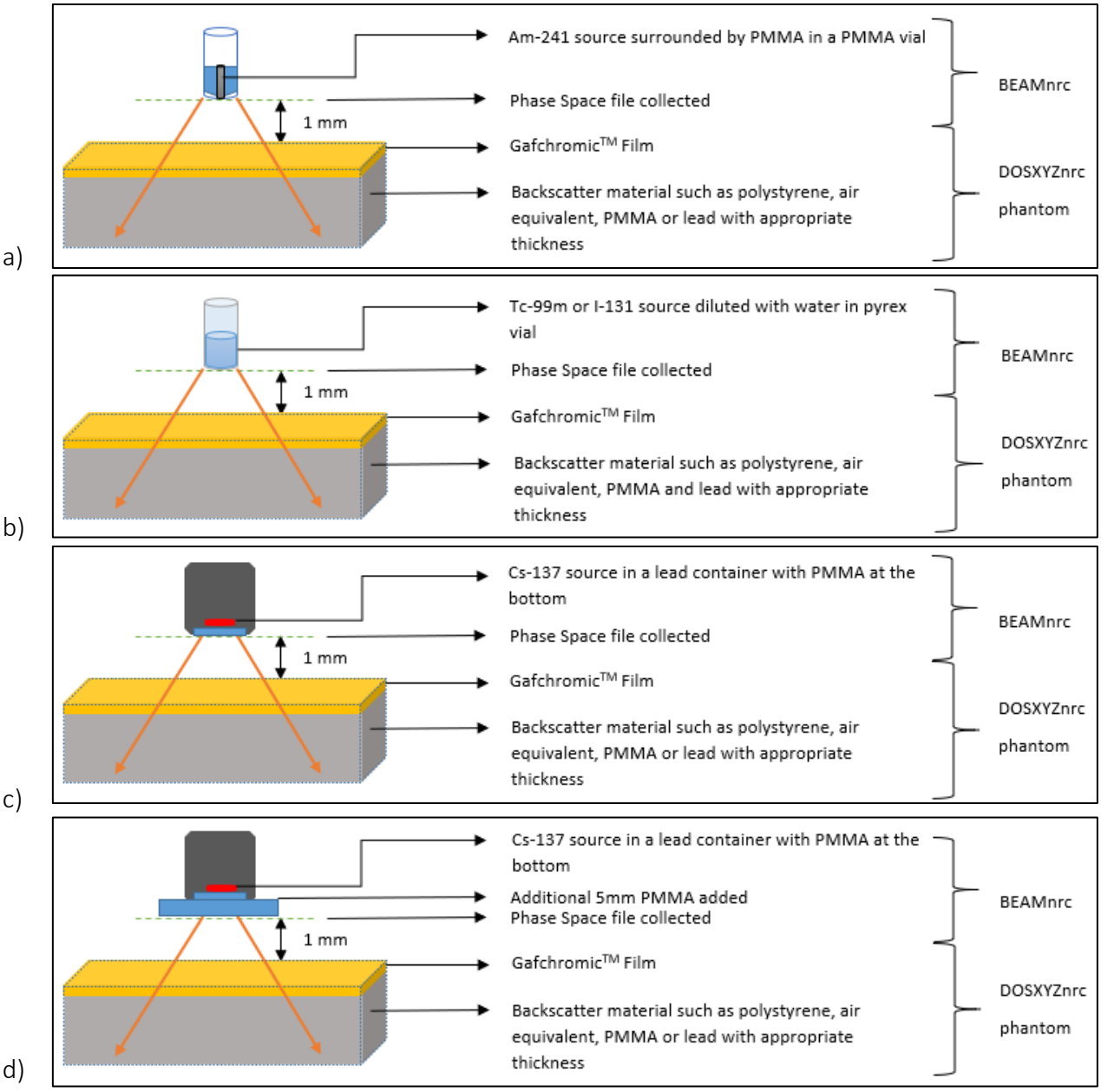

Figure 3.1: Schematic of how the different sources in their containers look like a) Am-241, b) Tc-99m and I-131, c) Cs-137 and d) Cs-137 with an extra layer of PMMA as well as the simulation setup for each. These source geometries were modelled with suitable component modules in BEAMnrc.

First, the transmitted energy spectra of the radionuclides under consideration should be determined to account for scattering in the type of container of the source. Before the radiation reaches the film surface, a BEAMnrc Monte Carlo run simulated the transport of the pure

radionuclide through the container material. A PSF which contains the distribution of charge, energy, position and direction of particles emerging from the radionuclide source was collected just below the container simulated to sample the transmitted energy spectra and scattered photons (2,5). This PSF was in-turn used as the radiation source model to determine the absorbed dose in the film or water in DOSXYZnrc respectively. Figure 3.1 shows the schematic of each source and the simulation setup used. Different backscatter materials were used in the DOSXYZnrc phantom to determine their effects on the dose. They are shown in figure 3.2.

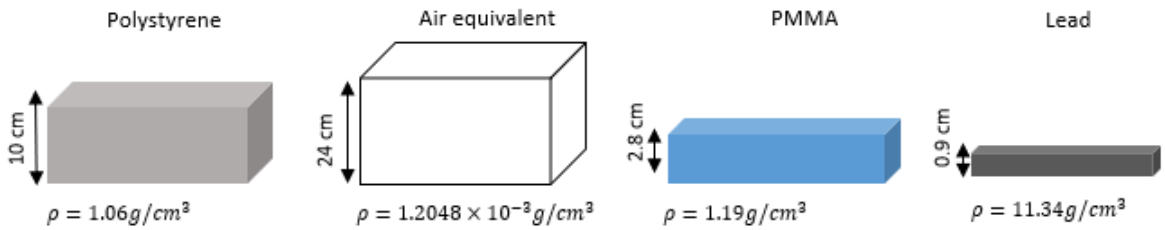

Figure 3.2: The different backscatter materials used with their appropriate thickness and density values (29).

According to the American Association of Physicists in Medicine TG-105, MC simulations should be implemented under the same conditions as the measurements (30). Thus, all simulations and measurements were implemented using the same geometric setup used during the measurements, as shown in figure 3.1.

The DOSXYZnrc Monte Carlo code was used to accurately determine the dose per history in the film layer as exposed under the same conditions as the measurements (5,25). Afterwards, conversion factors were determined to relate the dose per history in film to water by repeating the simulations under the same conditions but with water equivalent film. For the MC simulations, $1x10^8$ histories were simulated to reduce the variance to less than one percent.

EGS Input parameters for MC simulations

The choices of settings are set out in this section as it has a noticeable effect on the simulation results. The selections shown in figure 3.3 are made by using the BEAMnrc and DOSXYZnrc manuals for default and low energy settings (3,25).

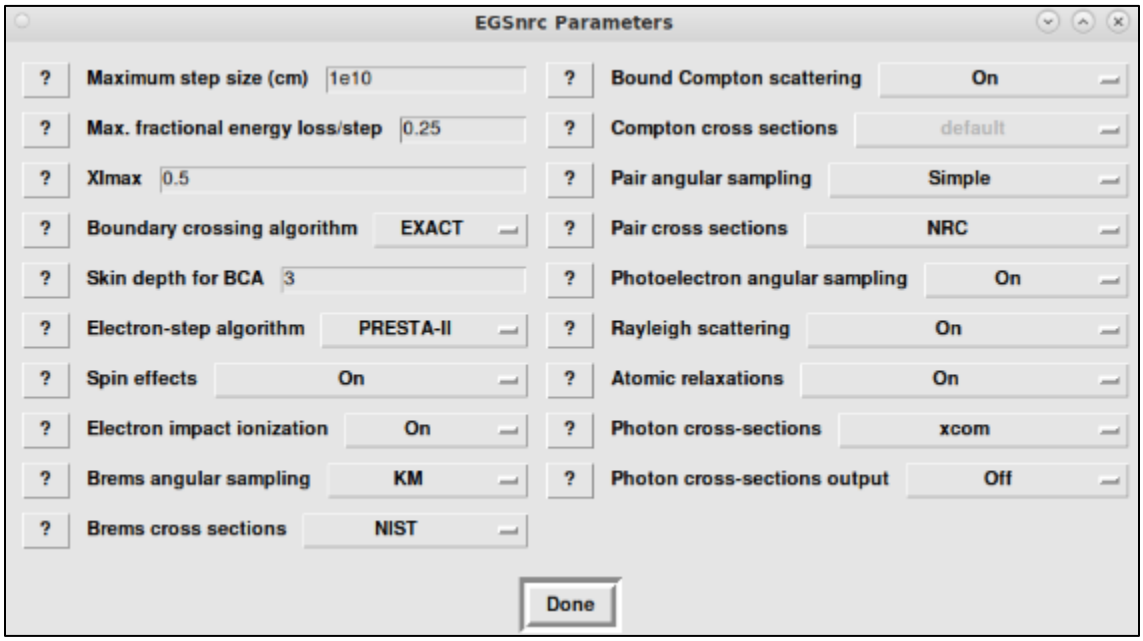

Figure 3.3: EGSnrc parameters used in Simulations for BEAMnrc and DOSXYZnrc

Global ECUT – This defines the global electron cut-off energy in MeV and is set as 0.512 MeV. When an electron's energy falls below this, its kinetic energy will be deposited in the current voxel. This means that an electron with 1 keV energy above the electron rest energy (0.511MeV) will deposit its energy locally (3,25).

Global PCUT – This defines the global photon cut-off energy (PCUT) in MeV and is suggested that 0.01 MeV should generally be used. When a photon's energy falls below 0.01 MeV, its energy will be deposited in the current voxel (3,25).

Boundary crossing algorithm- The EXACT boundary crossing algorithm which is used to transport electrons across boundaries was used because the dose voxels are much smaller than the voxels making up the rest of the phantom in this study (3,25).

Electron-step algorithm – PRESTA-II is the default algorithm used for electron transport corrections due to elastic scattering because most of the radionuclides used in this study have low kilovoltage energies (3,25).

Spin effects– The default setting of 'ON' is used because it is more accurate and also necessary to use for backscatter calculations (3,25).

Electron impact ionization – This was set to 'ON' as this setting is relevant at keV X-ray energy range (3,25).

Brems angular sampling – The KM setting is recommended at low energies which use the entire modified equation 2BS of Koch and Motz (KM) (3,25).

Brems cross-sections -The NIST option was chosen as the cross-sections from the NIST (National Institute of Standards and Technology) bremsstrahlung cross-section database, is the basis for radiative stopping powers recommended by the ICRU (International Commission on Radiation Units and Measurements) (3,25).

Bound Compton scattering – This is set as 'ON' because it is recommended if the energy being simulated is below 1 MeV and if Rayleigh scattering is being simulated (3,25).

Pair cross-sections – This is set to NRC (Nuclear Regulatory Commission) as it is of interest for low energies which are used in this study (3,25).

Rayleigh scattering– Is set to 'ON' as it is recommended for low energy > 1 MeV simulations (3,25).

Atomic Relaxations – The 'ON' option is chosen, which defaults to eadl. The eadl option uses a detailed relaxation scheme based on the EADL (Evaluated Atomic Data Library) transition probabilities (3,25).

Photon cross sections– This is set to 'xcom' which is the default but also of interest for low energies (3,25).

Compton cross-sections, *Pair angular sampling*, *Photoelectron angular sampling* and *Photon cross sections output* - These settings are kept on the default setting as stated in the BEAMnrc User Manual (3).

3.2.1. BEAMnrc and DOSXYZnrc simulations

MC simulations used global cut-off energies including: electron cut-off energy (ECUT) = 0.512 MeV and photon cut-off energy (PCUT) = 0.01 MeV. The boundary crossing algorithm was set at 'EXACT' and the electron-step algorithm to 'PRESTA II". Spin effects, bound Compton scattering, photoelectron angular sampling, Rayleigh scattering and, atomic relaxations were all switched on for the simulations as it is recommended for low energy (<1 MeV) (7). Each simulation used different random number seeds.

A PEGS4 file was generated for input data shown in table 3.1 for energies between 0.001MeV to 2MeV and for XR-QA2 and RT-QA2 Gafchromic^{TM} film. The backscatter materials were also included (Figure 3.2) in the PEGS file to recalculate cross-section data over the energy range above.

The input energy spectrum source file was created from tables of recommended data for each radionuclide found on the Laboratoire National Henri Becquerel webpage (24). This is known as the pure spectrum. The transmitted spectrum was obtained from analysis of PSFs using BEAMDP to determine the effect of the source container on the pure radionuclide spectrum inside the container.

BEAMDP was also used to ensure that the geometry in the x-y scatter plot is correct, as seen in figure 3.4 (31). Since the source geometry is not a point source, BEAMDP was used to investigate the variation of the particle fluence for PSFs located at different distances from the source.

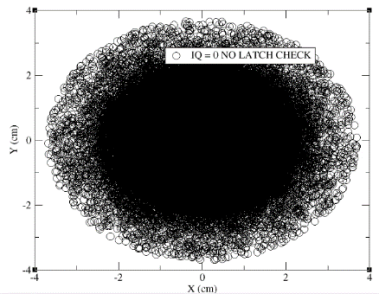

Figure 3.4: The X-Y scatter plot of particles from Cs-137 phase space data which is located in the plane of the film.

For BEAMnrc, the FLATFILT and SLABS CMs were used to compile the source container to replicate the measurement geometry, as seen in Appendix A. The PSF data collected from below the radionuclide container from BEAMnrc was used as a source for DOSXYZnrc that preformed dose calculations in the film, as seen in figure 3.1.

The isource2-option was selected in DOSXYZnrc, which is the phase-space source incident from any direction (25). From the DOSXYZnrc 3ddose files the relevant dose values were extracted as scored in the Gafchromic™ film and water respectively.

EGS_Windows V4.0 was used to make sure the geometry in BEAMnrc, as well as DOSXYZnrc, was correct, and MCSHOW was used to display the dose distribution in the DOSXYZnrc egs4phant phantom file (26).

As stated previously, the MC simulations were performed to calculate $\left(\frac{D_f}{D_w}\right)$ and to analyse particle fluence *vs* PSF position to account for distance correction of calculated dose.

For the $\left(\frac{D_f}{D_w}\right)$ calculation, DOSXYZnrc MC simulations were done to get the dose per history in the films for different backscatter materials. The film material was replaced with water in the DOSXYZnrc simulations to obtain the dose per history in water. This enabled us to have a conversion factor to use to obtain the dose in the film, D_f, by using the following equation.

$$\left(\frac{D_f}{D_w}\right) = \frac{dose/history\ in\ film}{dose/history\ in\ water} \tag{3.1}$$

The dose per history obtained was corrected for each radionuclide as each radionuclide has a certain percentage of gamma and beta decay, as shown in table 3.2.

Table 3.2: Air kerma rate constant ($\boldsymbol{\Gamma}$) and decay percentage for radionuclides used in this study (16,24,32).

Radionuclide	$\boldsymbol{\Gamma}$ (μGy·m^2/GBq·h)	Gamma-decay %	Beta-decay %
Am-241	3.97	84.6	N/A
Tc-99m	14.10	87.87	N/A
I-131	52.20	10	90
Cs-137	82.10	94.4	5.6

For the fluence *vs* distance correction, BEAMnrc simulations were done to collect PSF files at distances: 0.1, 0.5, 1.0, 5.0, 10.0, 30.0 and 50.0 cm from the sources to determine how the fluence is affected as a function of source distance. The fluence ratio between 0.1 cm and 50 cm, $\left(\frac{\Phi_{0.1}}{\Phi_{50}}\right)$ was used to determine the absorbed dose in the film D_f at 0.1 cm below the source.

3.2.2. Dose calculation in water and conversion into film dose

To calculate D_f the specific gamma-ray exposure constant (Table 3.2) for each radionuclide was used to calculate the absorbed dose in water, D_w, using the following formulas:

$$D_{air} = \Gamma \mathrm{At} \ . \left(\frac{\Phi_{0.1}}{\Phi_{50}}\right) \tag{3.2}$$

$$D_w = D_{air} \left(\frac{\Psi_w}{\Psi_{air}}\right) \left(\frac{\mu_{en}}{\rho}\right)_{air}^{w} \tag{3.3}$$

D_{air} is the absorbed dose in air. Γ is the air kerma rate constant which is specific for each radionuclide. At is the calculated activity-time. $\Phi_{0.1}$ is the fluence obtained at 0.1 cm from the radionuclide and Φ_{50} is the fluence obtained at 50 cm from the radionuclide. Ψ_w is the energy fluence in water and Ψ_{air} is the energy fluence in air which are equal in this study. $\left(\frac{\mu_{en}}{\rho}\right)_{air}^{w}$ is the mass energy-absorption coefficient. $\Psi\left(\frac{\mu_{en}}{\rho}\right)$ represents the collision kerma.

The fluence obtained was corrected for each radionuclide as each radionuclide has a certain percentage of gamma and beta decay, as shown in table 3.2.

Since the radionuclide source can be approximated as a point source at 50 cm, it is possible to calculate the dose at 0.1 cm below the finite source from knowledge of $\left(\frac{\Phi_{0.1}}{\Phi_{50}}\right)$. This enabled converting time-activity values from film data into absorbed dose in water. The conversion factors Eq. 3.1 between the dose in water and film were applied to convert the calculated dose in water to the dose in film.

The optical density (OD) *vs* film dose were fitted to Eq. 3.4.

$$OD = \beta(1 - e^{-\alpha t}) + \gamma \tag{3.4}$$

With (t) being different time periods and (γ) represents the film background which is present irrespective of irradiating the film. The curve fitting of OD vs irradiation time will yield the constants α and β.

3.2.3. Effect of different backscatter materials on film dose

By using different backscatter materials such as those shown in figure 3.2, we can determine if they have an effect on the dose absorbed in the Gafchromic™ film as well as water and whether the dose conversion between film and water is affected. From the data obtained, it can be determined which film is the most sensitive and which film results reflect the results in water best. Only figure 3.1: (a)–(c) setup was used during this investigation. The simulation geometries are shown in figure 3.1: (a)–(d). This is a replication of the measurement setup to determine the OD *vs* film dose. Table 3.3 lists the effective atomic number for the backscattering materials used.

Table 3.3: Effective atomic number (Z_{eff}) for backscatter materials used as well as water (29,33).

Material	Z_{eff}
Air equivalent	7.68
Polystyrene	5.74
Lead	82
Water	7.51

3.2.4. Energy dependence of films

Graphs can be obtained to compare the data of all the different radionuclides illustrated in figure 3.1: (a) – (d), for OD *vs* film dose for each radionuclide as measured in XR-QA2- and RT-QA2 Gafchromic™ films respectively. In the simulation, we also included an extra 5mm PMMA layer between the Cs-137 source and the Gafchromic™ film to absorb the beta rays from the Cs-137 source before it reaches the film as shown in figure 3.1(d). For the energy dependence, we only considered the gamma energies. Thus, by using appropriate shielding, such as the inclusion of the extra 5mm PMMA for Cs-137, the beta particles could be eliminated without compromising the gamma emissions.

The Am-241 and the Tc-99m radionuclides emit only gamma energies. The Cs-137 radionuclide emits a beta particle with a maximum energy of 513.97 keV (94.4% abundance) and has a beta range of about 3.8 mm in plastic (34). I-131 has a beta particle with a maximum energy of 606.31 keV and a range of 0.9 mm in glass which is attenuated by the glass vial container which has a thickness of 1mm (34).

3.3. RESULTS

3.3.1. The influence of the radionuclide container on the transmitted energy spectra

The study of radionuclide dose production on film focuses on the lower energy spectra of photon sources, namely between 13.95 keV to 661.657 keV. For most of the radionuclides used in this study, it would be of interest to see if the container of the sources would alter the transmitted energy spectra of the gamma rays of the radionuclide and to what extend it is manifested. To quantify this, the pure radionuclide spectra (without attenuation and container filtering) was compared to the transmitted spectra through BEAMDP analysis of the resulting PSFs of BEAMnrc simulations.

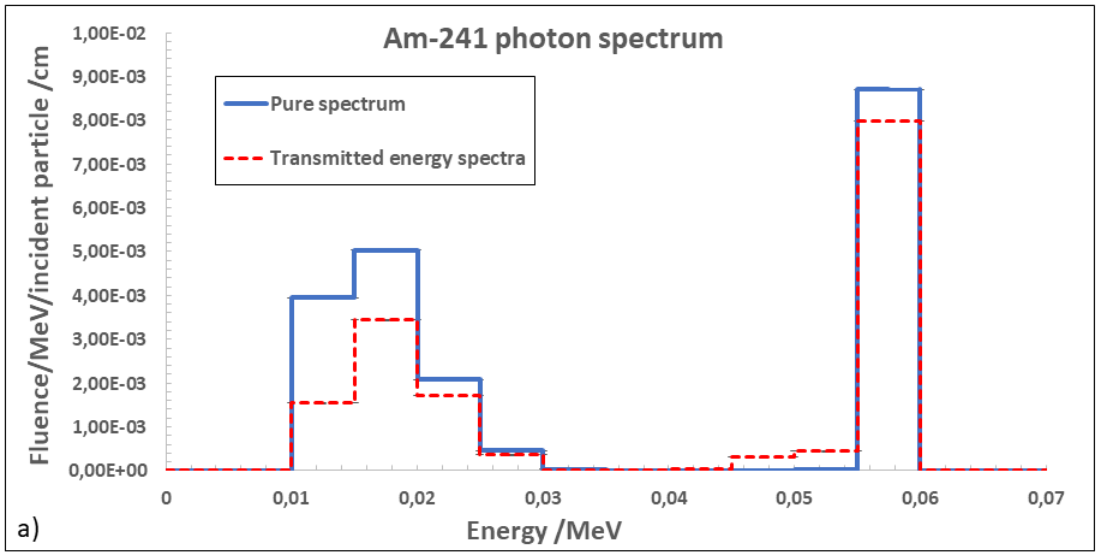
Am-241 photon spectrum
Pure spectrum
Transmitted energy spectra
Fluence/MeV/incident particle /cm
1,00E-02
9,00E-03
8,00E-03
7,00E-03
6,00E-03
5,00E-03
4,00E-03
3,00E-03
2,00E-03
1,00E-03
0,00E+00
0
0,01
0,02
0,03
0,04
0,05
0,06
0,07
Energy /MeV
a)

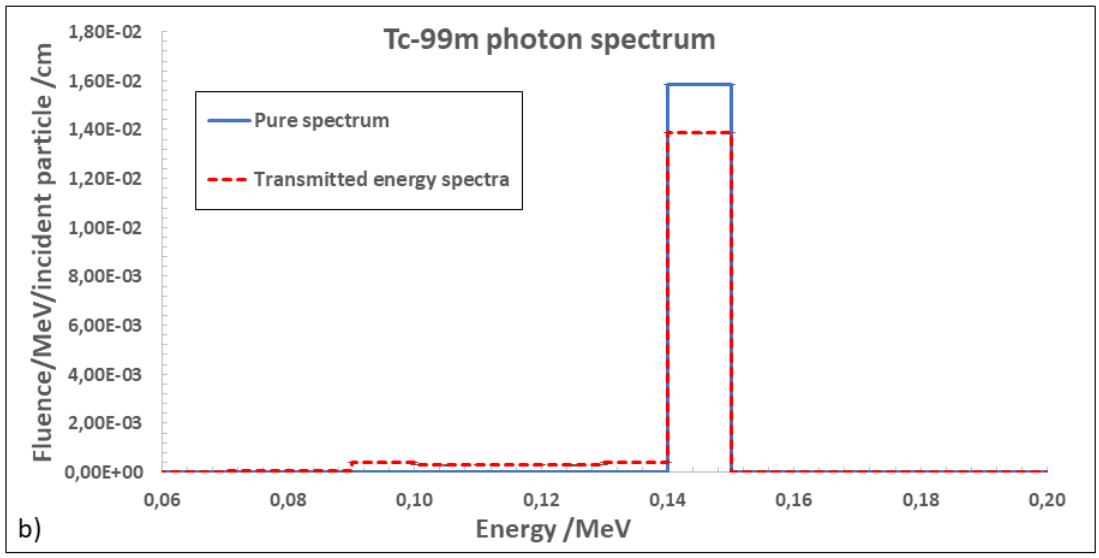
Tc-99m photon spectrum
Pure spectrum
Transmitted energy spectra
Fluence/MeV/incident particle /cm
1,80E-02
1,60E-02
1,40E-02
1,20E-02
1,00E-02
8,00E-03
6,00E-03
4,00E-03
2,00E-03
0,00E+00
0,06
0,08
0,10
0,12
0,14
0,16
0,18
0,20
Energy /MeV
b)

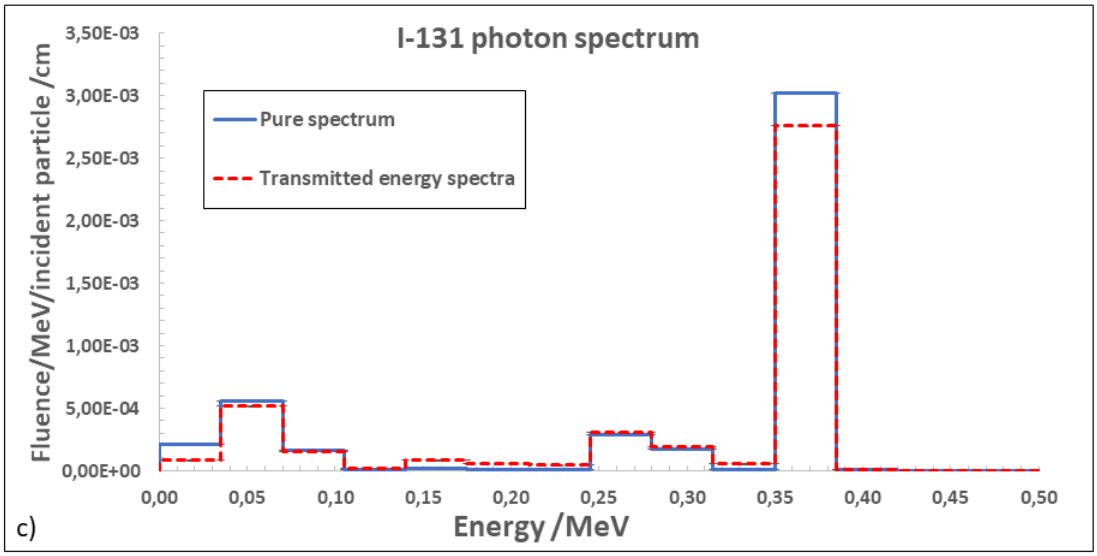
I-131 photon spectrum
Pure spectrum
Transmitted energy spectra
Fluence/MeV/incident particle /cm
3,50E-03
3,00E-03
2,50E-03
2,00E-03
1,50E-03
1,00E-03
5,00E-04
0,00E+00
0,00
0,05
0,10
0,15
0,20
0,25
0,30
0,35
0,40
0,45
0,50
Energy /MeV

c)

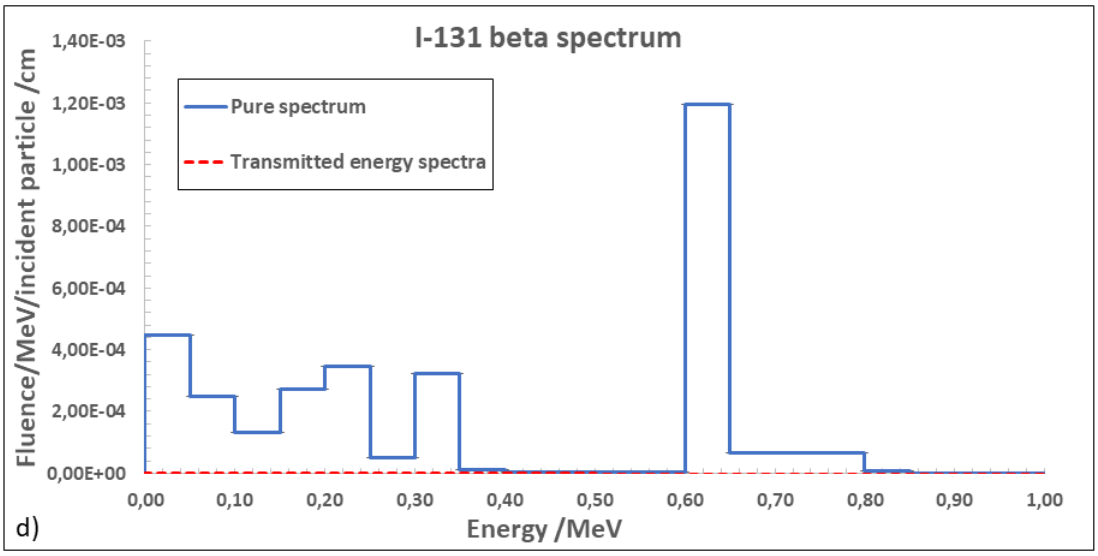
I-131 beta spectrum
Pure spectrum
Transmitted energy spectra
Fluence/MeV/incident particle /cm
1,40E-03
1,20E-03
1,00E-03
8,00E-04
6,00E-04
4,00E-04
2,00E-04
0,00E+00
0,00
0,10
0,20
0,30
0,40
0,50
0,60
0,70
0,80
0,90
1,00
Energy /MeV

d)

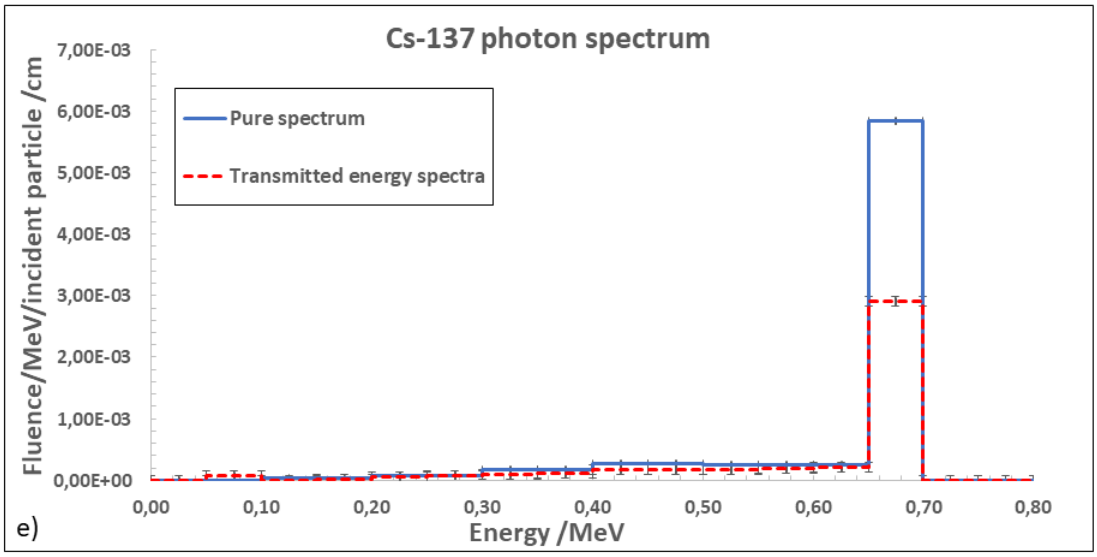
Cs-137 photon spectrum
Fluence/MeV/incident particle /cm
7,00E-03
6,00E-03
5,00E-03
4,00E-03
3,00E-03
2,00E-03
1,00E-03
0,00E+00
Pure spectrum
Transmitted energy spectra
0,00
0,10
0,20
0,30
0,40
0,50
0,60
0,70
0,80
Energy /MeV

e)

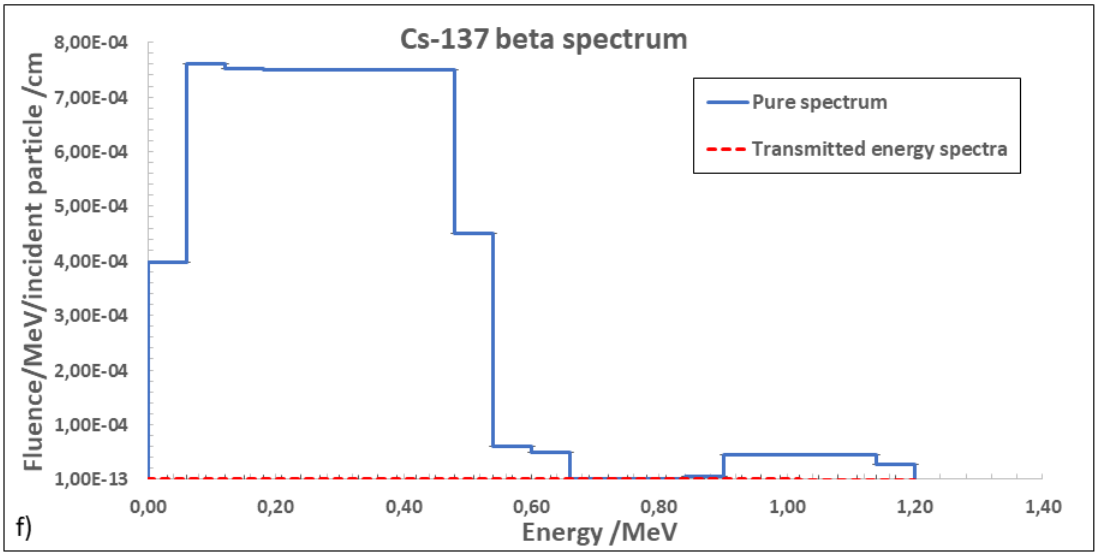
Cs-137 beta spectrum
Fluence/MeV/incident particle /cm
8,00E-04
7,00E-04
6,00E-04
5,00E-04
4,00E-04
3,00E-04
2,00E-04
1,00E-04
1,00E-13
Pure spectrum
Transmitted energy spectra
0,00
0,20
0,40
0,60
0,80
1,00
1,20
1,40
Energy /MeV

f)

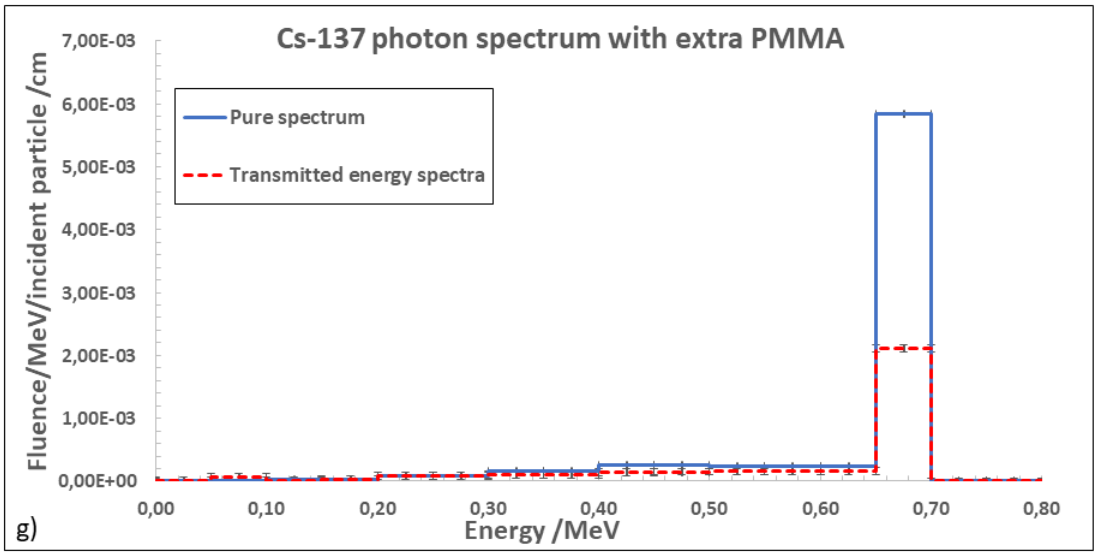

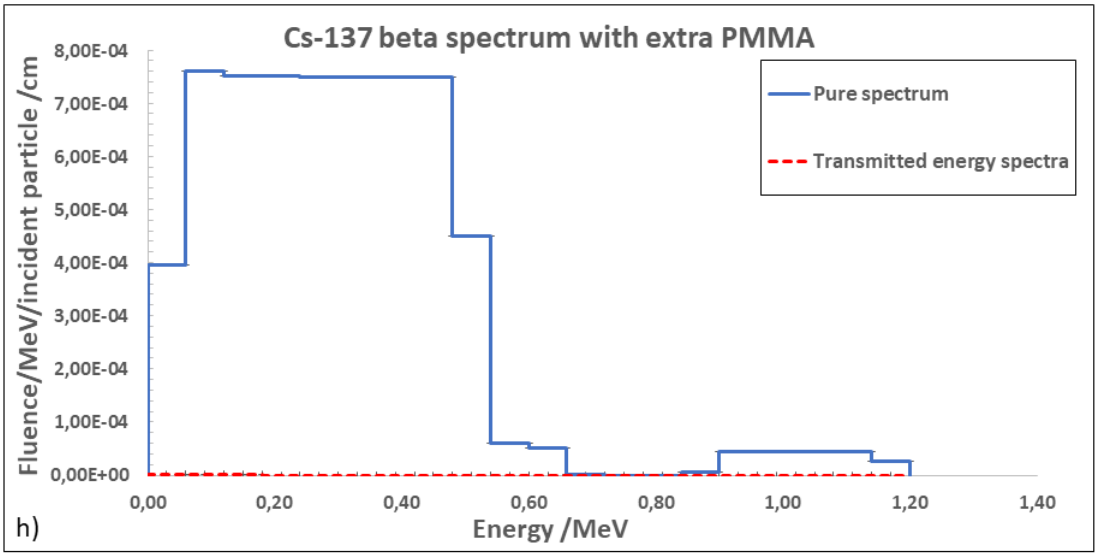

Figure 3.5: (a)-(h): The spectrum differences between the pure radionuclide spectrum and radionuclides in their containers representing the transmitted energy spectra.

Figure 3.5(a) shows the pure Am-241 photon spectrum below the PMMA vial at 0.1 cm distance. It can be seen that the energy peak at 59 keV has decreased due to attenuation in the vial. Also, note that just below the 59 keV energy peak, additional photons are present due to Compton scattering events in the vial. These photons are in the energy range between 45 – 55 keV. Close inspection also shows that the lower photons energies in the pure Am-241 were attenuated mostly

by photo-electric events in the container, e.g. there is a filtering effect at these lower energies between 10 and 30 keV.

Figure 3.5(b) shows similar results as figure 3.5(a), but now the pure radionuclide and transmitted photon spectra are for Tc-99m. The energy peak at 140 keV shows a decrease due to absorption in the glass wall of the vial. Compton events cause additional scattered photons just below the energy peak of Tc-99m for the transmitted energy spectra at the expense of less photons at the primary peak (140 keV) compared to Tc-99m without a container. Compton photons are now appearing at energies below 140 keV down to about 80 keV for the transmitted spectra, which is expected.

Figure 3.5(c) shows the pure radionuclide photon spectrum of I-131 and the spectrum below the glass vial containing I-131. The energy peak at 364 keV shows a decrease due to the glass vial and mainly Compton events that produce additional scattered lower energy photons.

Figure 3.5(d) shows the pure radionuclide beta spectrum of I-131 and the spectrum below the glass vial. It can be noticed that most of the electrons are stopped by the glass vial reducing the exit fluence to very low values when comparing the intensities of the beta spectra without and with the glass vial.

Figure 3.5(e) is the pure radionuclide photon spectrum of Cs-137 and the spectrum below its lead container. The energy peak at 662 keV shows a decrease due to the PMMA window attenuation in the lead container.

Figure 3.5(f) is the pure radionuclide beta spectrum of Cs-137 and the transmitted spectrum below the PMMA window. Most of the electrons of the Cs-137 radionuclide is stopped by the PMMA opening and suppresses the transmitted beta spectrum (see figure 3.1c).

Figure 3.5(g) shows the transmitted Cs-137 photon spectrum with 5 mm additional PMMA (see figure 3.1(d). The 662 keV photo peak is further attenuated by this PMMA layer. Figure 3.5(h) is the beta spectrum of Cs-137 with the extra 5mm PMMA, as shown in figure 3.1(d). The energy peaks of the electrons have decreased due to the extra 5mm PMMA added.

3.3.2. The influence of the finite source size on the particle fluence at different source distances for each radionuclide.

Fluence emitted from finite-size sources does not follow the inverse-square law close to the source. However, at far enough distances, the point source approximation will be accurate. For this reason, we evaluated the fluence as a function of distance from each source so that we could correct for it at 0.1 cm when the dose is calculated at 50 cm using Eq. 3.2.

The next set of graphs show the fluence, Φ, scored in PSF's from BEAMnrc simulations located at the origin of each PSF.

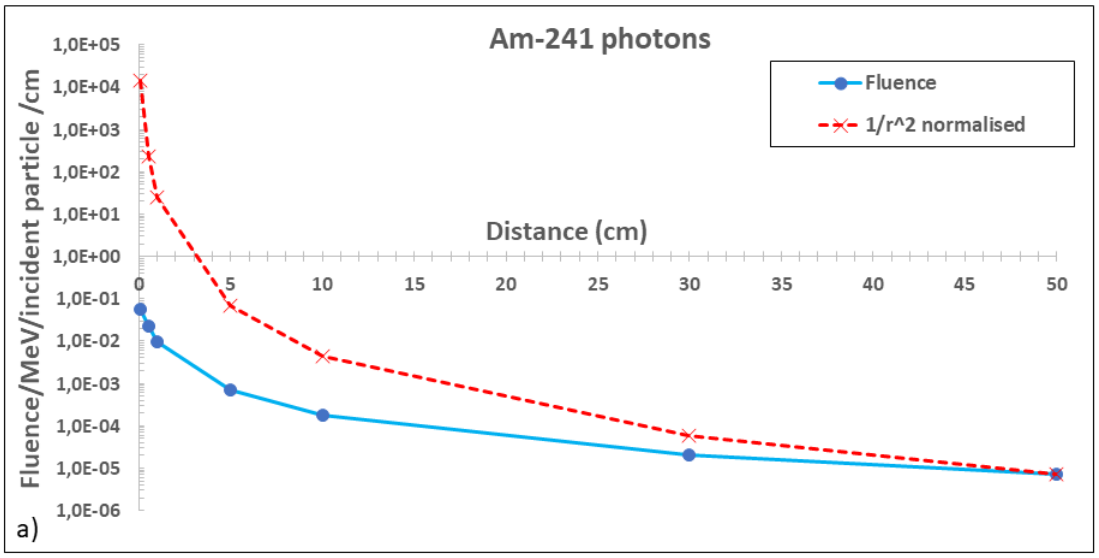

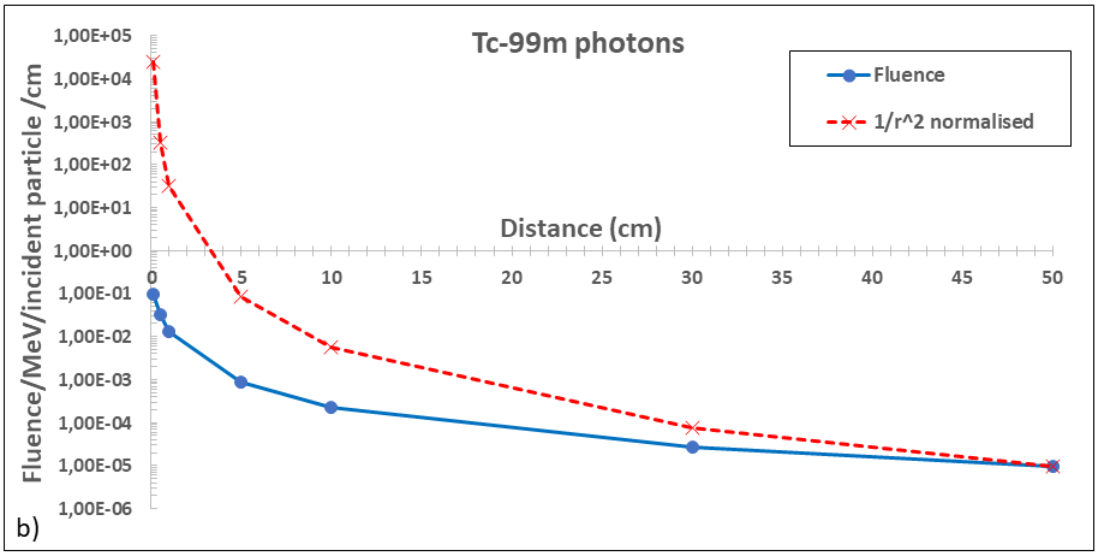
Tc-99m photons
Fluence
1/r^2 normalised
Distance (cm)
Fluence/MeV/incident particle /cm
1,00E+05
1,00E+04
1,00E+03
1,00E+02
1,00E+01
1,00E+00
1,00E-01
1,00E-02
1,00E-03
1,00E-04
1,00E-05
1,00E-06
0
5
10
15
20
25
30
35
40
45
50
b)

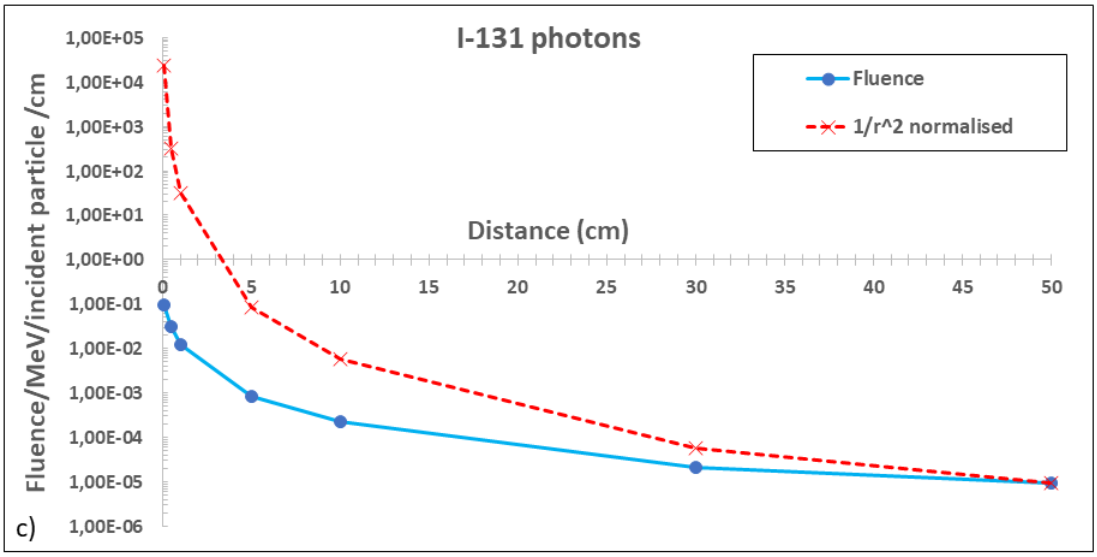
I-131 photons
Fluence
1/r^2 normalised
Distance (cm)
Fluence/MeV/incident particle /cm
1,00E+05
1,00E+04
1,00E+03
1,00E+02
1,00E+01
1,00E+00
1,00E-01
1,00E-02
1,00E-03
1,00E-04
1,00E-05
1,00E-06
0
5
10
15
20
25
30
35
40
45
50
c)

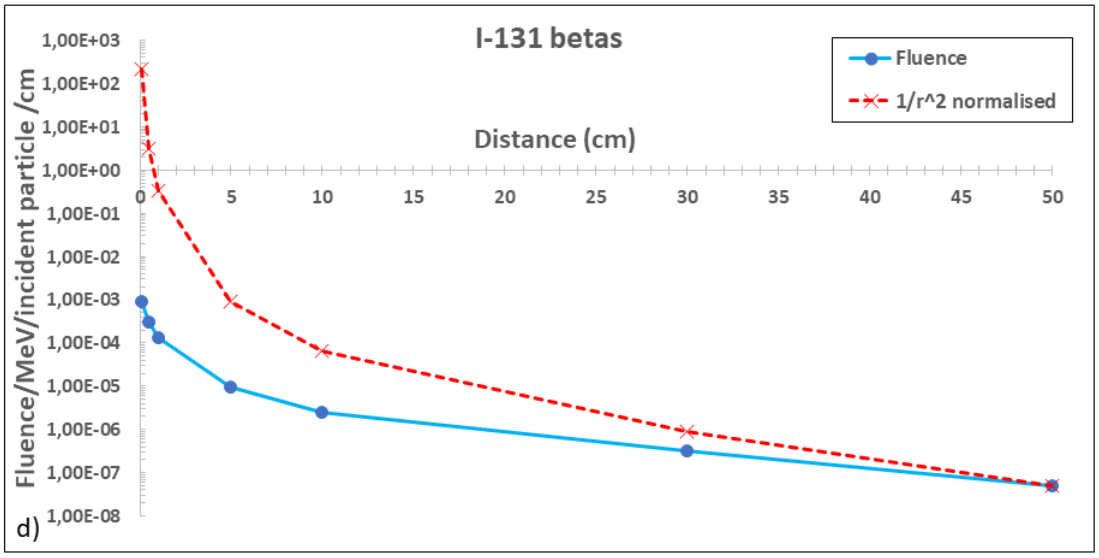
I-131 betas
Fluence
1/r^2 normalised
Distance (cm)
Fluence/MeV/incident particle /cm
1,00E+03
1,00E+02
1,00E+01
1,00E+00
1,00E-01
1,00E-02
1,00E-03
1,00E-04
1,00E-05
1,00E-06
1,00E-07
1,00E-08
0
5
10
15
20
25
30
35
40
45
50
d)

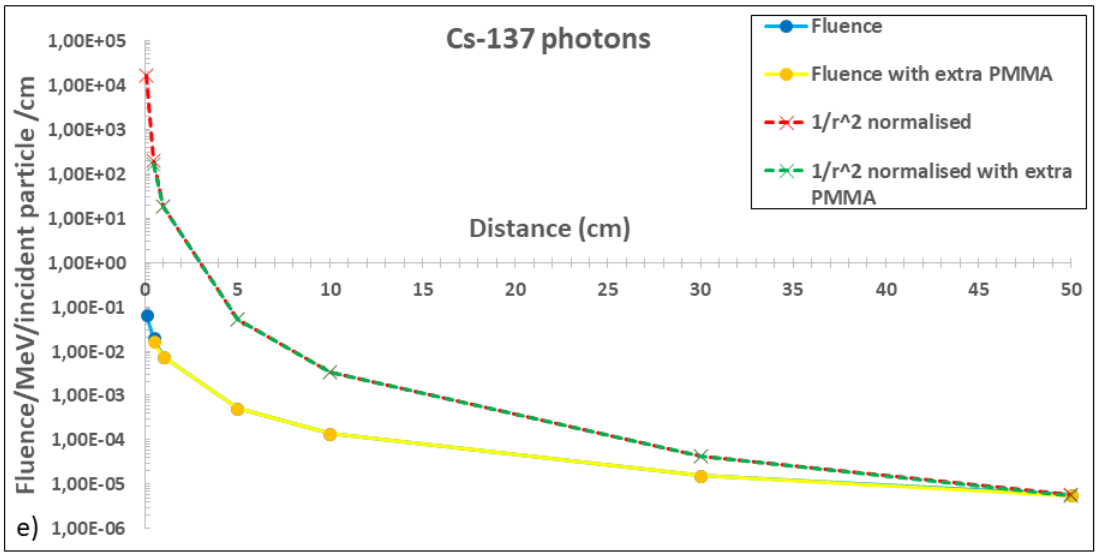
Cs-137 photons
Fluence
Fluence with extra PMMA
1/r^2 normalised
1/r^2 normalised with extra PMMA
Distance (cm)
Fluence/MeV/incident particle /cm
1,00E+05
1,00E+04
1,00E+03
1,00E+02
1,00E+01
1,00E+00
1,00E-01
1,00E-02
1,00E-03
1,00E-04
1,00E-05
1,00E-06
0
5
10
15
20
25
30
35
40
45
50
e)

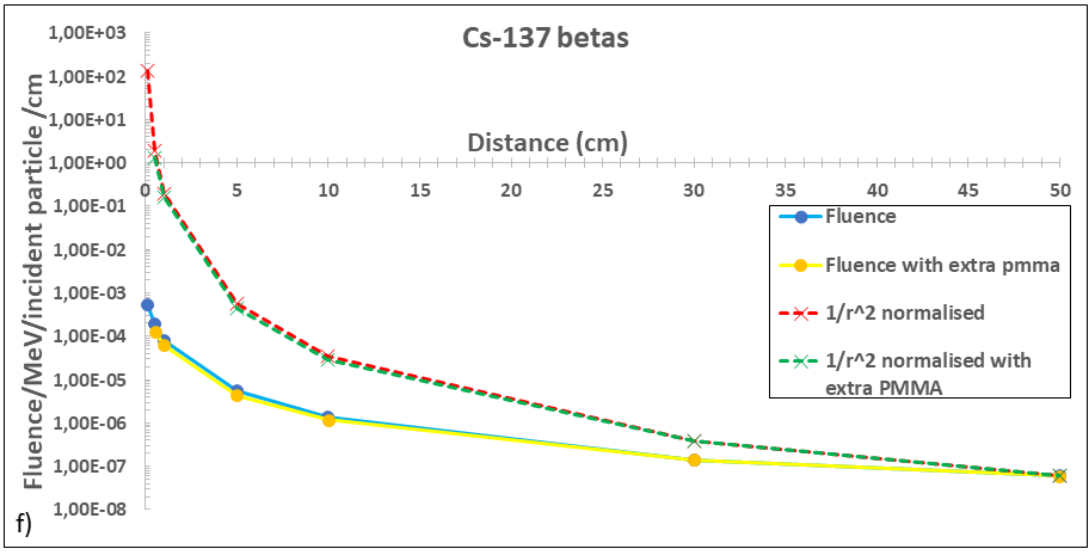

Figure 3.6: Particle fluence from PSF analysis for a) Am-241, b) Tc99-m, c) I-131 photons, d) I-131 betas, e) Cs-137 photons with and without the extra PMMA and f) Cs-137 betas with and without additional PMMA.

From figure 3.6, we can see that the fluence decreases with distance as we would expect due to the diverging nature of emitted photons from these finite sized sources. The resulting fluence from the simulations does not follow the inverse-square law at small distances. At 0.1 cm there is a difference of about 1.4-1.5 x 10^4 between the fluence simulated and the inverse square law.

Table 3.4: Fluence ratios $\left(\frac{\Phi_{0.1}}{\Phi_{50}}\right)$ obtained at 0.1 cm and 50 cm distance to correct for absorbed dose in water at 0.1 cm when calculated at 50 cm (point source approximation) using Eq. 3.2 and mass energy-absorption coefficient ratios $\left(\frac{\mu_{en}}{\rho}\right)^{w}_{air}$ for each radionuclide calculated using Eq. 3.3.

Radionuclide	Fluence Ratio $\left(\frac{\Phi_{0.1}}{\Phi_{50}}\right)$	Mass Energy-Absorption Coefficient Ratios $\left(\frac{\mu_{en}}{\rho}\right)^{w}_{air}$
Am -241	7.71E+03	1.02
Tc-99m	9.83E+03	1.1
I-131	1.70E+04	1.1
Cs-137	1.13E+04	1.1
Cs-137 with extra PMMA	1.13E+04	1.1

From table 3.4 we have the calculated mass-energy absorption coefficient ratios used to convert D_{air} into D_w which are in the range of 1 for all the radionuclides.

3.3.3. MC simulation dose in film and water

Table 3.5: Simulated dose per history obtained from different backscatter media for the XR-QA2-, RT-QA2 Gafchromic™ film and water.

Radionuclide	Backscatter material	Dose/history in XR-QA2	Dose/history in RT-QA2	Dose/history in Water
Am-241	Polystyrene	9.76E-14	7.93E-14	9.96E-14
	Air Equivalent	9.24E-14	7.51E-14	9.43E-14
	PMMA	9.73E-14	7.90E-14	9.90E-14
	Lead	1.17E-13	9.92E-14	1.32E-13
Tc-99m	Polystyrene	1.32E-13	1.25E-13	9.10E-14
	Air Equivalent	1.28E-13	9.97E-14	8.82E-14
	PMMA	1.33E-13	1.25E-13	9.17E-14
	Lead	2.22E-13	2.13E-13	2.18E-13
I-131	Polystyrene	5.50E-14	5.45E-14	4.76E-14
	Air Equivalent	5.40E-14	5.37E-14	4.67E-14
	PMMA	5.51E-14	5.46E-14	4.77E-14
	Lead	6.88E-14	6.84E-14	6.77E-14
Cs-137	Polystyrene	4.88E-13	4.91E-13	3.86E-13
	Air Equivalent	4.65E-13	4.67E-13	3.58E-13
	PMMA	4.87E-13	4.91E-13	3.87E-13
	Lead	6.89E-13	6.59E-13	5.93E-13
Cs-137 with extra 5mm PMMA	Polystyrene	1.77E-13	1.62E-13	1.38E-13
	Air Equivalent	1.71E-13	1.56E-13	1.30E-13
	PMMA	1.78E-13	1.62E-13	1.40E-13
	Lead	2.44E-13	2.22E-13	2.20E-13

From table 3.5, the dose per history in the XR-QA2 Gafchromic™ film is higher for all the radionuclides. This is due to the high Z materials added to the XR-QA2 Gafchromic™ film (see table 3.1) sensitive layer. The RT-QA2 Gafchromic™ film is more sensitive to high energies such as Cs-137. The dose per history in water compares best to XR-QA2 Gafchromic™ film when using low energies such as Am-241.

By using the above data from table 3.5 conversion factors $\left(\frac{D_f}{D_w}\right)$ can be determined to convert the absorbed dose in water to the absorbed dose in the film. The ratio of the film dose to water is per definition $\left(\frac{D_f}{D_w}\right)$ stated in Eq. 3.1 and are shown in table 3.6.

Table 3.6: Conversion factors $\left(\frac{\boldsymbol{D_f}}{\boldsymbol{D_w}}\right)$ to convert dose in water to dose in film evaluated for different backscattering materials.

XR-QA2 film		Polystyrene	Air equivalent	PMMA	Lead
	Am -241	0.98	0.98	0.98	0.88
	Tc-99m	1.45	1.45	1.45	1.02
	I-131	0.99	0.99	0.99	0.88
	Cs-137	1.33	1.31	1.26	1.10
RT-QA2 film	Am -241	0.80	0.80	0.80	0.75
	Tc-99m	1.37	1.37	1.37	0.98
	I-131	0.98	0.98	0.98	0.88
	Cs-137	1.34	1.31	1.27	1.11

From table 3.6, it is noticeable that the conversion factors stay constant when using other backscatter materials except for lead in which it changes. For Cs-137, the conversion factors change because of the different backscatter materials used.

3.3.4. Comparison of absorbed dose in film and water

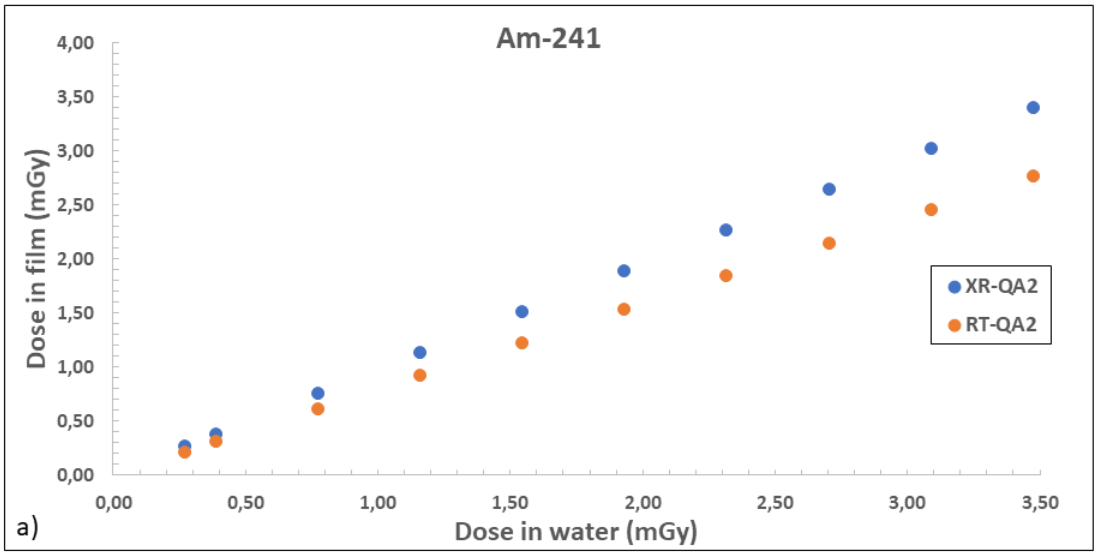

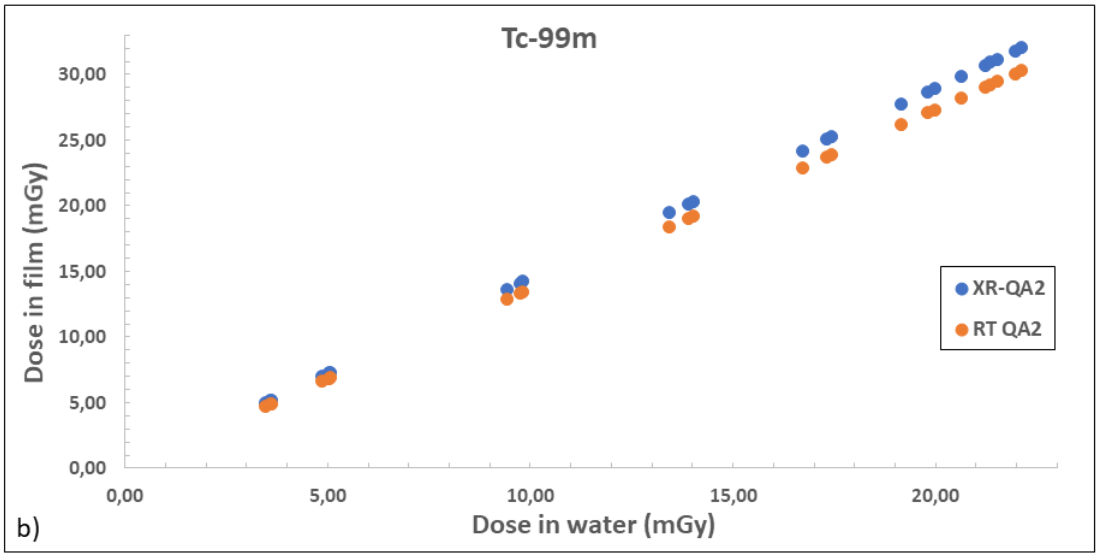

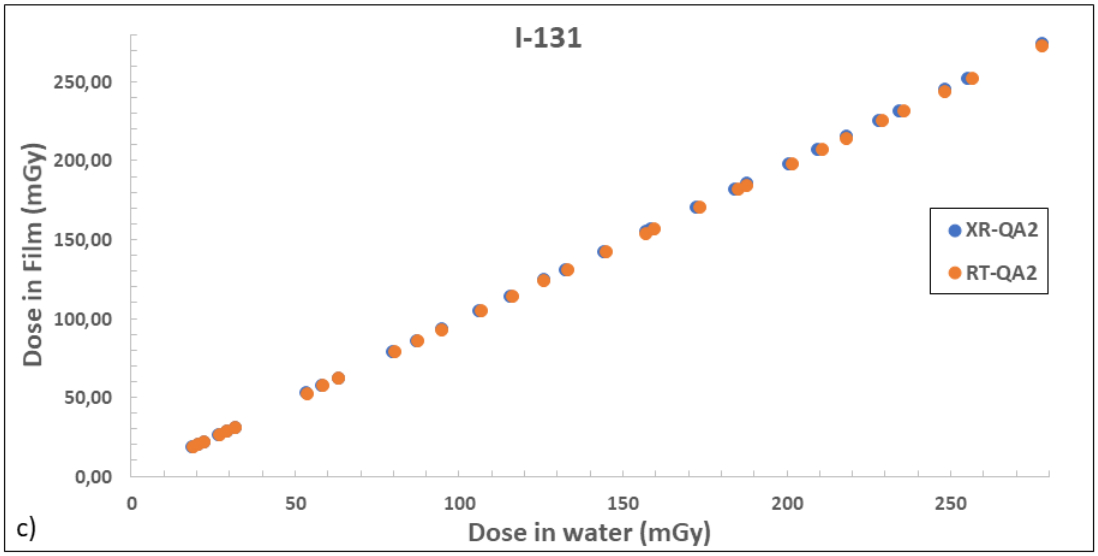

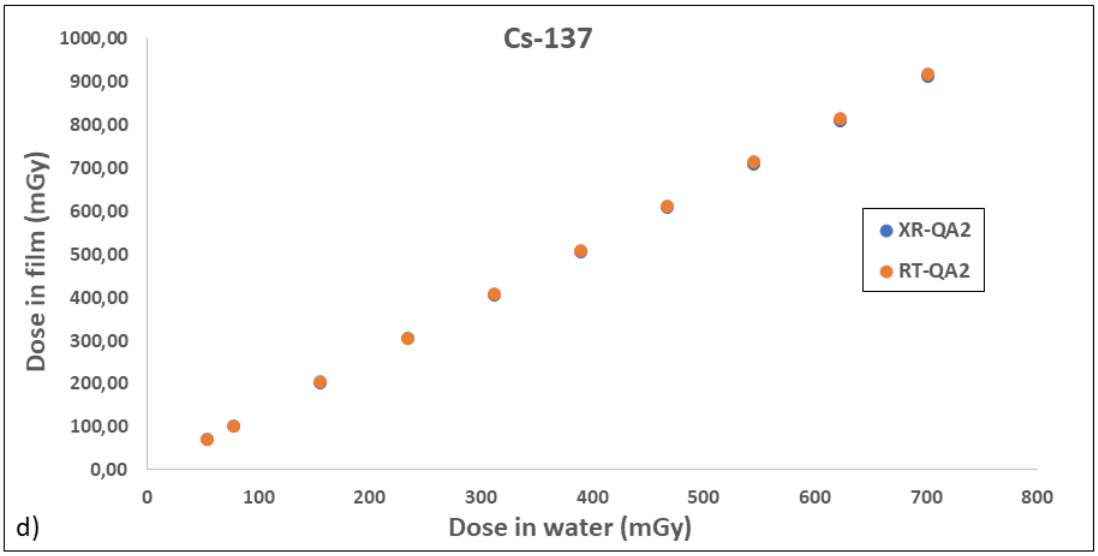

Figure 3.7: (a)-(d): Comparison between dose in XR-QA2 and RT-QA2 Gafchromic™ film with dose in water.

In figure 3.7(a) and 3.7(b) we can see that the XR-QA2 Gafchromic™ film is more sensitive for lower energy isotopes such as Am-241 and Tc-99m which is due to its higher effective atomic number of 29.98 *vs* 22.71 for RT-QA2 Gafchromic™ film. For isotopes with higher photon energies such as in figure 3.7(c) and 3.7(d), for I-131 and Cs-137 respectively, we can see that the response to both films are the same since the predominant interactions in the films will be Compton

scattering. When using Tc-99m, the XR-QA2 Gafchromic™ film would be more sensitive to use in dosimetry applications.

3.3.5. Effect of different backscatter materials on film dose

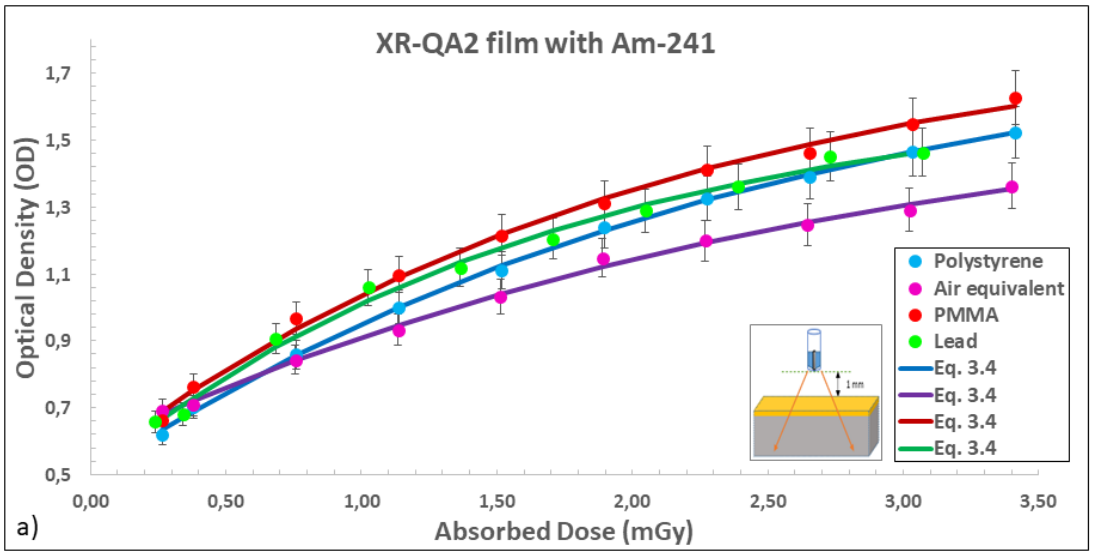

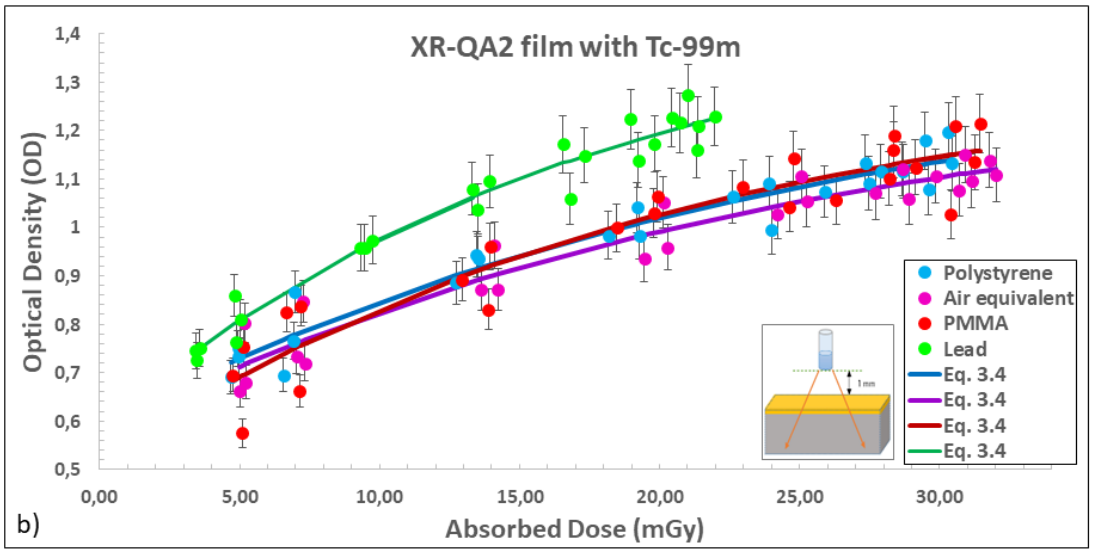

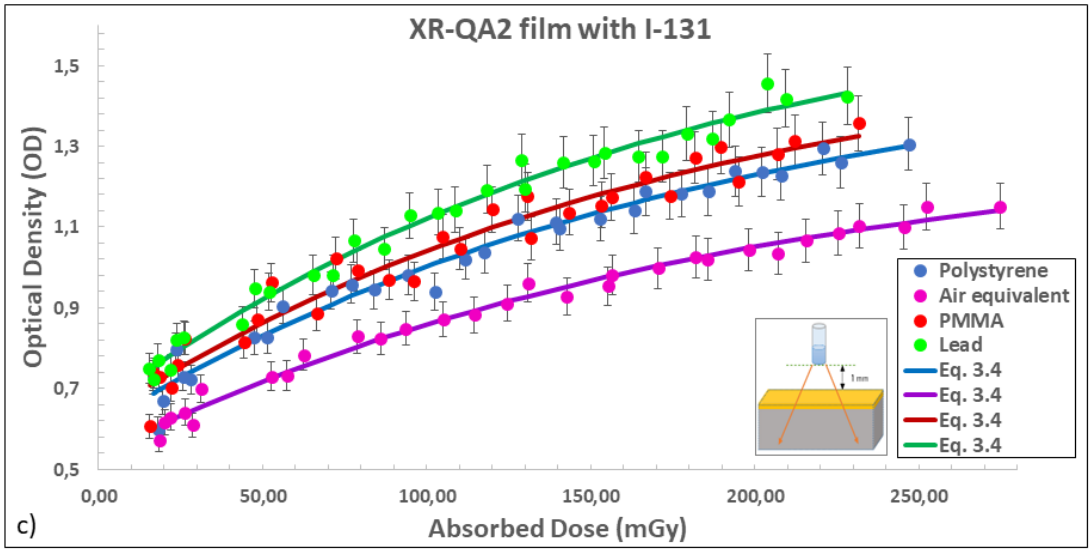

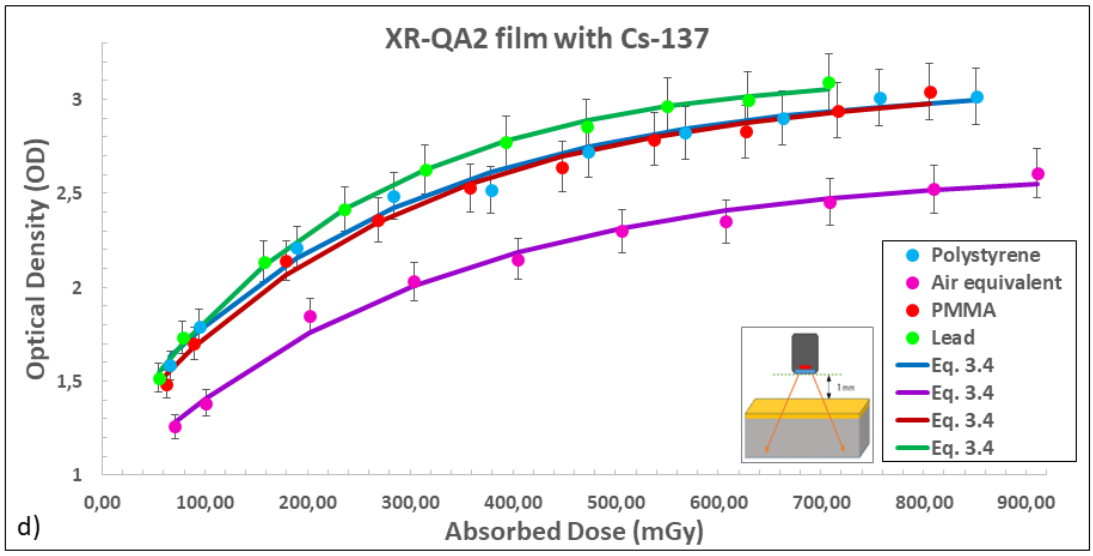

Figure 3.8: Effects of backscatter materials on dose with XR-QA2 Gafchromic™ film a) Am-241 b) Tc-99m c) I-131 and d) Cs-137.

Figure 3.8: (a)-(d) show the effect of different backscatter materials for Am-241, Tc-99m, I-131, and Cs-137 using XR-QA2 Gafchromic™ film. Except for the Am-241 case, lead displays the strongest enhancer for increase in density when acting as a backscattering material. In all cases above air displays the weakest enhancer for film density when it acts as a backscattering material, which is expected due to its small volumetric electron density. On the other hand, lead will have the largest volumetric electron density that can invoke more Compton backscattering onto the

film. Polystyrene and PMMA show similar density enhancement in the XR-QA2 Gafchromic™ film for all cases above except Am-241.

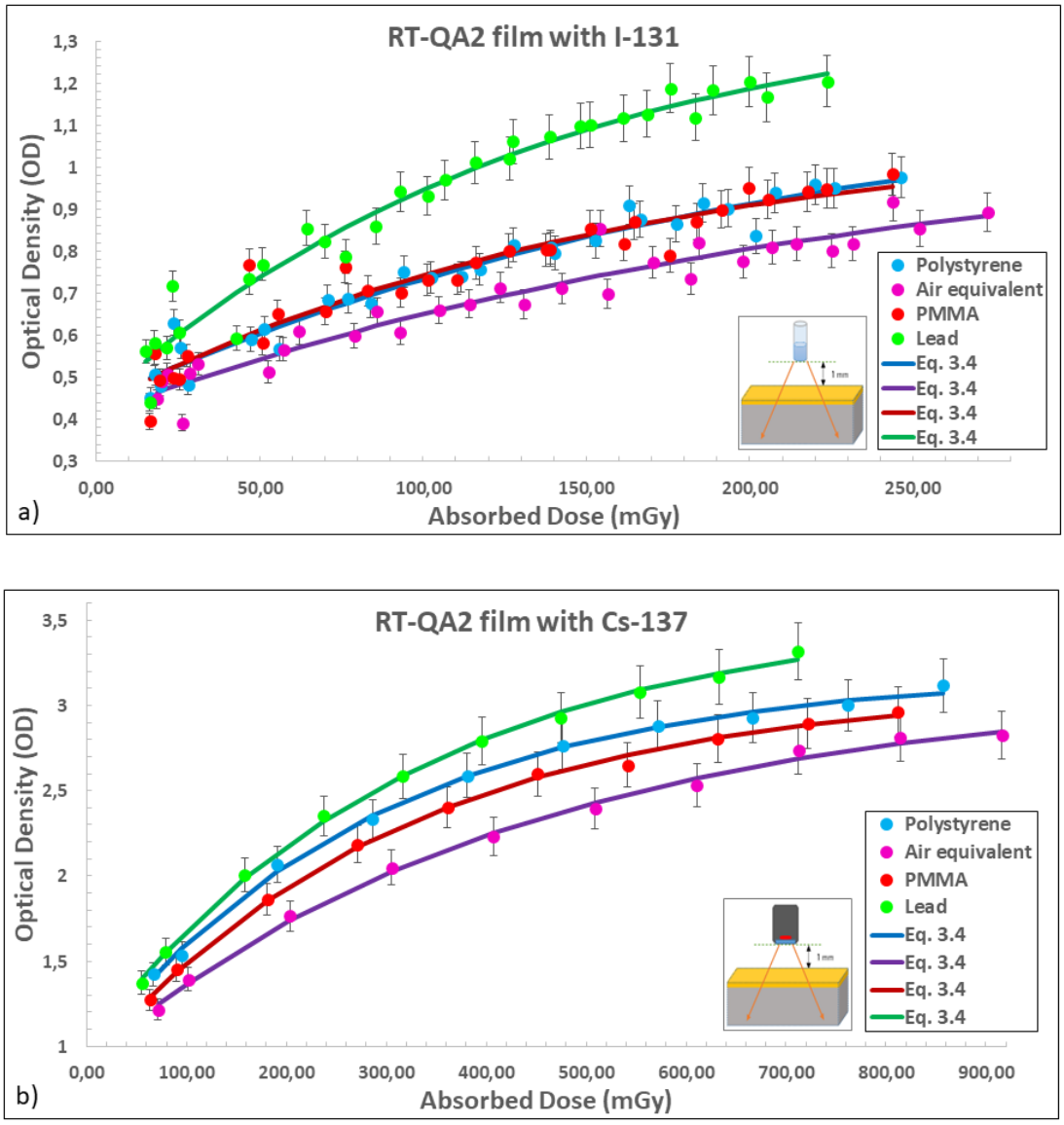

Figure 3.9: Effects of backscatter materials on dose with RT-QA2 Gafchromic™ film a) I-131 and b) Cs-137.

Figure 3.9(a) and 3.9(b) shows the effect of different backscatter materials when using I-131 and Cs-137 with RT-QA2 Gafchromic™ film. The air equivalent material results in the least optical density enhancement due to its lower electron density (as in the case for XR-QA2 Gafchromic™

film). As for the XR-QA2 Gafchromic™ case, lead will cause the most density enhancement due to more particle backscattering into the RT-QA2 Gafchromic™ film.

It is important to note that the OD enhancement in figure 3.8 and 3.9 is due to dose enhancement to the XR-QA2 and RT-QA2 Gafchromic™ film. The dose noted on the graph axes are the calculated dose in film using Eq.'s (3.1), (3.2) and (3.3).

3.3.6. Energy dependence

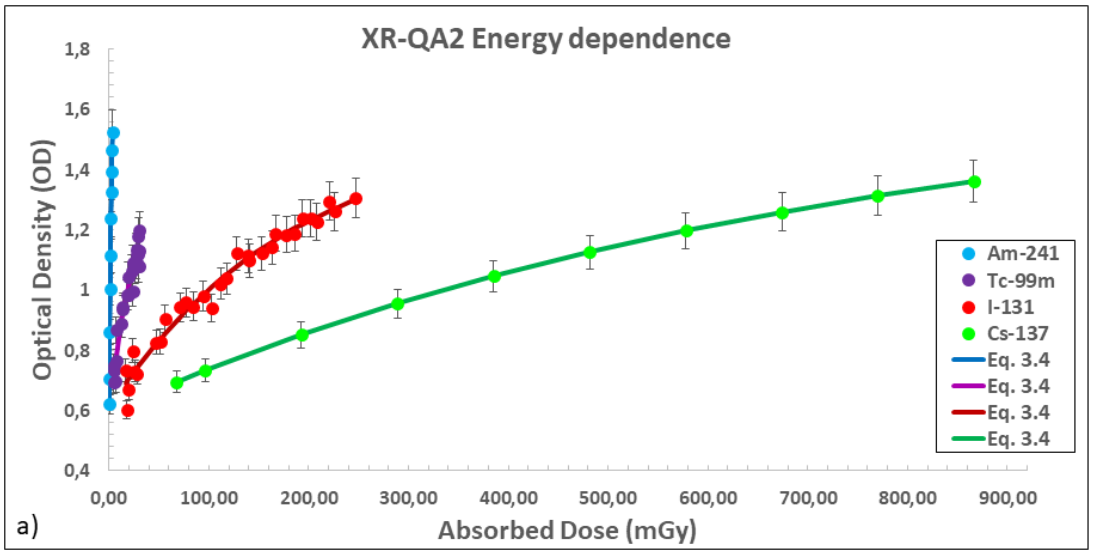

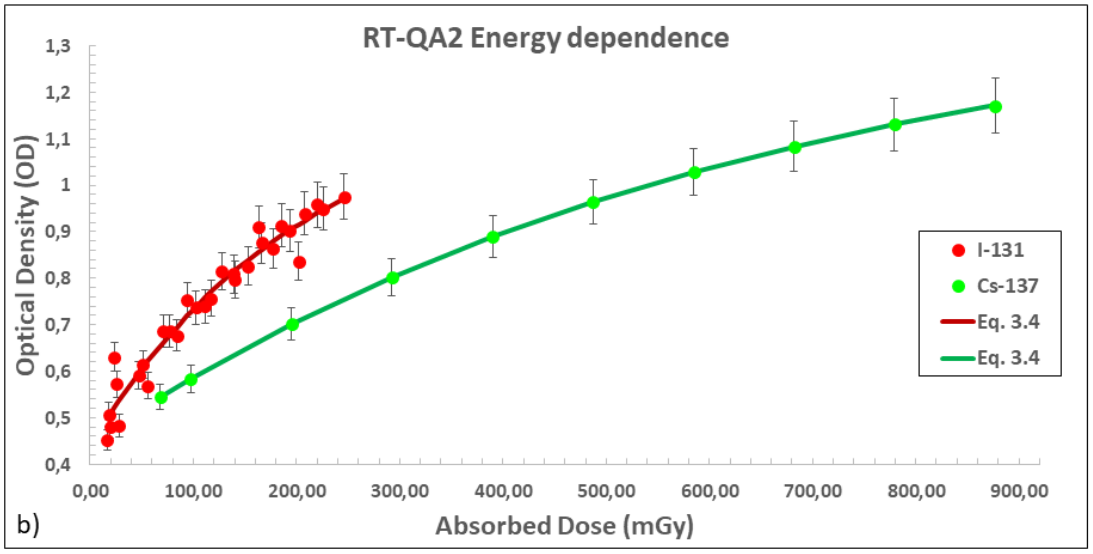

Figure 3.10: (a) – (b): Energy dependence, OD vs dose for XR-QA2 and RT-QA2 Gafchromic™ film for different radionuclides

From figure 3.10(a) it can be seen that the XR-QA2 Gafchromic™ film is sensitive for Am-241 up to Cs-137. The Am-241 energy response is enhanced due to the high Z materials added in the film's sensitive layer giving it an effective atomic number of 29.98 in table 3.1. Due to the limited dose given to the film from Am-241, its dose range is much less (0-3.41 mGy) than Cs-137 (0-911 mGy).

From figure 3.10(b) it is evident that the RT-QA2 Gafchromic™ film only detects high energies. The physical experiment did not result in an OD change when working with Am-241 and Tc-99m, but it did give OD value changes with I-131 and Cs-137. The simulations, however, did result in a dose per history for all the radionuclides.

The OD values for I-131 and Cs-137 is higher for the XR-QA2 Gafchromic™ film than for the RT-QA2 Gafchromic™ film. This is because the XR-QA2 Gafchromic™ film has a higher effective atomic number than the Gafchromic™ film RT-QA2 film.

3.4. DISCUSSION

In this study, two main questions were addressed. The first was how the optical density due to radionuclide exposure could be related to the dose in film. As a benchmark, measurements were done previously to obtain the optical density (OD) in film as a function of activity-time. These results were not shown explicitly in this study. The conversion of time activity into absorbed dose in film were addressed by using at first the specific gamma constant Γ to calculate the dose to water at 50 cm distance from the source. This was to ensure that a point source approximation would be valid. In the next step, BEAMnrc MC simulations were used to construct the geometry of the radionuclide sources used in this study. A set of PSFs was scored at different distances from the source, and out of this information, the ratio of the fluence at 0.1 cm to the value at 50 cm could be calculated. This acted as the fluence correction to account for the finite size of the source. A mass energy-absorption coefficient ratio was used, as well. This enabled calculation of the dose in water at the plane of the film located 0.1 cm below the source. Next up DOSXYZnrc dose

calculations were done to get the dose ratio $\left(\frac{D_f}{D_w}\right)$ between film and water for XR-QA2 and RT-QA2 Gafchromic™ film. This allowed for dose conversion from water into film, which led to the answer of the second question, how can the absorbed dose in water be related to the absorbed dose in the film.

The BEAMDP analysis of the PSF's showed how the original pure energy spectra of the radionuclides changed due to transport through the source container material. Lower intensities for photons were observed as well as increasing Compton components in the transmitted spectra. Electron transmission was also reduced to a high degree.

The fluence scored on the source axis as a function of distance was shown in figure 3.6:(a)–(f). The inverse square function was included to show its relation and the influence of the finite sized sources, which resulted in a difference of 1.4-2.5 x 10^4 due to the distance being 0.1 mm. When the fluence is measured at close distances such as 0.1 mm from the source, the inverse square law is not followed.

The dose conversion factors were nearly constant between air equivalent, PMMA and polystyrene for a given isotope and film type. In all cases, lead showed significantly lower conversion values relating the dose in water to film.

When comparing the dose in film to the dose in water, we see that both film types have the same response for I-131 and Cs-137 in figure 3.7(c) and 3.7(d). For Am-241 and Tc-99m the dose response deviated between the two films with the Am-241 case showing the largest deviation. XR-QA2 Gafchromic™ film has a larger effective atomic number 29.98 compared to RT-QA2 Gafchromic™ film with 22.71. Thus photoelectric events will be more predominant at Am-241 energies in XR-QA2 Gafchromic™ film compared to RT-QA2 Gafchromic™ film.

In figures 3.8: (a)-(d) and figure 3.9: (a)-(b) the OD *vs* dose measurement phantom will play a role in the OD density response of both films. Thus, for calibration purposes, care should be taken with the backscattering material, and correction should be made to convert the dose into water. Lead is the strongest OD enhancer with air the least. More water equivalent materials such as PMMA and polystyrene shows similar results in all cases except for the Am-241 case in figure 3.8(a).

In figure 3.10(a) the XR-QA2 Gafchromic™ film energy dependence shows a sharp rise for the Am-241 case getting progressively less as the radionuclide photon energy increases. A similar trend is observed for the RT-QA2 case when I-131 is compared to Cs-137 in figure 3.10(b).

In figures 3.8, 3.9 and 3.10, the OD *vs* dose data were fitted with Eq. 3.4 and shown as solid lines. This indicates the usefulness of using this equation to account for the OD *vs* dose. It is based on the neutron-depletion model, where the assumption is that the film contains a finite amount of activation centres that is depleted as it is exposed to radiation.

3.5. CONCLUSION

This study shows that the neutron depletion model fits the data fairly well. If the OD of the Gafchromic ™ film such as XR-QA2 and RT-QA2 is known the dose in the film can be determined by using the model. The XR-QA2 Gafchromic™ film shows to be more sensitive to lower energies and the RT-QA2 Gafchromic™ film more sensitive to higher energies which is confirmed by the theory and the energy dependence results. It is also emphasized that the type of container the radionuclide is in, will have an effect on the absorbed dose as well as how far the film is from the radionuclide where the introduced fluence corrections were made as seen in figure 3.6: (a) – (f). The backscatter material that showed the most OD enhancement effect for a given dose is caused by lead.

Lead as a backscatter material decreases the dose in the film as well as in the water due to the absorption effect it has because the absorbed dose increases in the lead as the lead has a high density and atomic number (20). Conversion factors were determined to use the dose in water and convert it to the dose in film.

ACKNOWLEDGMENT

This research and the publication thereof is the result of funding provided by the Medical Research Council of South Africa in terms of the MRC's Flagships Awards Project SAMRC-RFA-UFSP-01-2013/ HARD

REFERENCES

1. Van Eeden D, Du Plessis FCP. Hybrid Monte Carlo source model: Advantages and deficiencies. Polish J Med Phys Eng. 2018 Jun 1;24(2):65–74.

2. Kawrakow I, Walters BRB. Efficient photon beam dose calculations using DOSXYZnrc with BEAMnrc. Med Phys [Internet]. 2006 Jul 28 [cited 2020 Jan 7];33(8):3046–56. Available from: http://doi.wiley.com/10.1118/1.2219778

3. Rogers DWO, Walters B, Kawrakow I. BEAMnrc Users Manual. National Research Council of Canada Report PIRS-0509(A) revL [Internet]. Ottawa; 2020 [cited 2020 May 20]. Available from: https://nrc-cnrc.github.io/EGSnrc/doc/pirs509a-beamnrc.pdf

4. Rogers DWO, Faddegon BA, Ding GX, Ma C-M, We J. BEAM:A Monte Carlo code to simulate radiotherapy treatment units. Med Phys [Internet]. 1995 [cited 2020 Jul 9];22(5):503–24. Available from: https://people.physics.carleton.ca/~drogers/pubs/papers/Ro95.pdf

5. Jabbari K, Anvar H, Tavakoli M, Amouheidari A. Monte carlo simulation of siemens oncor linear accelerator with beamnrc and dosxyznrc code. J Med Signals Sens. 2013 Jul 1;3(3):172–9.

6. Tomic N, Devic S, Deblois F, Seuntjens J. Reference radiochromic film dosimetry in kilovoltage photon beams during CBCT image acquisition. Med Phys. 2010;37(3):1083–92.

7. Ade N, van Eeden D, du Plessis FCP. Characterization of Nylon-12 as a water-equivalent solid phantom material for dosimetric measurements in therapeutic photon and electron beams. Appl Radiat Isot. 2020 Jan 1;155.

8. Devic S, Tomic N, Lewis D. Reference radiochromic film dosimetry: Review of technical aspects. Phys Medica. 2016;32(4):541–56.

9. Chiu-Tsao ST, Ho Y, Shankar R, Wang L, Harrison LB. Energy dependence of response of new high sensitivity radiochromic films for megavoltage and kilovoltage radiation energies. Med Phys [Internet]. 2005 Nov 1 [cited 2020 Jul 2];32(11):3350–4. Available from: https://aapm.onlinelibrary.wiley.com/doi/full/10.1118/1.2065467

10. Lindsay P, Rink A, Ruschin M, Jaffray D. Investigation of energy dependence of EBT and EBT-2 Gafchromic film. Med Phys [Internet]. 2010 Jan 13 [cited 2020 Jul 2];37(2):571–6. Available from: http://doi.wiley.com/10.1118/1.3291622

11. Tomic N, Quintero C, Whiting BR, Aldelaijan S, Bekerat H, Liang L, et al. Characterization of calibration curves and energy dependence GafChromic ^{TM} XR-QA2 model based radiochromic film dosimetry system. Med Phys [Internet]. 2014 May 29 [cited 2020 Jul 2];41(6Part1):062105. Available from: http://doi.wiley.com/10.1118/1.4876295

12. Ashland | always solving [Internet]. [cited 2020 Jul 30]. Available from: https://www.ashland.com/

13. Jagtap AS, Mora G. Investigation of absorbed-dose energy dependence of RTQA2 film over EBT2 film using Monte Carlo simulation [Internet]. 2019 [cited 2020 Jul 2]. p. 1. Available from: https://www.postersessiononline.eu/173580348_eu/congresos/ICCR-MCMA2019/aula/-P_119_ICCR-MCMA2019.pdf

14. Cherry SR, Sorenson JA, Phelps ME. Physics in Nuclear Medicine. 4th ed. Philadelphia: Saunders Elsevier; 2012. 1–523 p.

15. Gräfe J, Poirier Y, Jacso F, Khan R, Liu H, Eduardo Villarreal-Barajas J. Assessing the deviation from the inverse square law for orthovoltage beams with closed-ended applicators. J Appl Clin Med Phys [Internet]. 2014 Jul 8 [cited 2020 Oct 22];15(4):356–66. Available from: https://onlinelibrary.wiley.com/doi/abs/10.1120/jacmp.v15i4.4893

16. Ninkovic MM, Adrovic F. Air Kerma Rate Constants for Nuclides Important to Gamma Ray Dosimetry and Practical Application. In: Gamma Radiation [Internet]. Croatia: IntechOpen; 2012 [cited 2020 Jul 22]. p. 1–16. Available from: https://www.intechopen.com/books/gamma-radiation/air-kerma-rate-constants-for-nuclides-important-to-gamma-ray-dosimetry-and-practical-application-

17. Khan FM. The Physics of Radiation Therapy. 3rd ed. Lippincott & Wilkins; 2003. 1–560 p.

18. Absorbed Dose Determination in External Beam Radiotherapy An International Code of Practice for Dosimetry Based on Standards of Absorbed Dose to Water [Internet]. 2000 [cited 2020 Apr 9]. Available from: https://www-pub.iaea.org/MTCD/publications/PDF/TRS398_scr.pdf

19. Devic S, Seuntjens J, Hegyi G, Podgorsak EB, Soares CG, Kirov AS, et al. Dosimetric properties of improved GafChromic films for seven different digitizers. Med Phys. 2004;31(9):2392–401.

20. Alsadig AA, Abbas S, Kandaiya S, Ashikin NARNN, Qaeed MA. Differential dose absorptions for various biological tissue equivalent materials using Gafchromic XR-QA2 film in diagnostic radiology. Appl Radiat Isot. 2017;129:130–4.

21. Butson MJ, Cheung T, Yu PKN. Evaluation of the magnitude of EBT Gafchromic film polarization effects. Australas Phys Eng Sci Med. 2009 Mar;32(1):21–5.

22. Rasband WS. ImageJ, U.S. National Institutes of Health, Bethesda, Maryland, USA. http://imagej.nih.gov/ij/. 2014.

23. Alva H, Mercado-Uribe H, Rodríguez-Villafuerte M, Brandan ME. The use of a reflective scanner to study radiochronic film response. Phys Med Biol. 2002;47(16):2925–33.

24. Nuclear Data – Table – Laboratoire National Henri Becquerel [Internet]. [cited 2020 May 21]. Available from: http://www.lnhb.fr/nuclear-data/nuclear-data-table/

25. Walters B, Kawrakow I, Rogers DWO. DOSXYZnrc Users Manual. National Research Council of Canada Report PIRS-794 revB [Internet]. 2020 [cited 2020 May 20]. Available from: https://nrc-cnrc.github.io/EGSnrc/doc/pirs794-dosxyznrc.pdf

26. Kawrakow I, Mainegra-Hing E, Rogers DWO, Tessier F, Walters BRB. The EGSnrc Code System: Monte Carlo Simulation of Electron and Photon Transport. National Research Council of Canada Report PIRS-701 [Internet]. 2020 [cited 2020 May 20]. Available from: https://nrc-cnrc.github.io/EGSnrc/doc/pirs701-egsnrc.pdf

27. EGSnrc [Internet]. [cited 2020 May 20]. Available from: https://nrc-cnrc.github.io/EGSnrc/

28. Das IJ, editor. Radiochromic film: Role and applications in radiation dosimetry. Boca Raton: CRC Press; 2018. 1–387 p.

29. Attix FH. Appendix. In: Introduction to Radiological Physics and Radiation Dosimetry [Internet]. Madison, Wisconsin: WILEY-VCH Verlag GmbH & Co. KGaA; 2004 [cited 2020 Jul 24]. p. 525–98. Available from: https://onlinelibrary.wiley.com/doi/book/10.1002/9783527617135

30. Chetty IJ, Curran B, Cygler JE, DeMarco JJ, Ezzell G, Faddegon BA, et al. Report of the AAPM Task Group No. 105: Issues associated with clinical implementation of Monte Carlo-based photon and electron external beam treatment planning. Vol. 34, Medical Physics. John Wiley and Sons Ltd; 2007. p. 4818–53.

31. Ma C-M, Rogers DWO. BEAMDP as a General-Purpose Utility. National Research Council of Canada Report PIRS-0509(E) revA [Internet]. [cited 2020 Jun 28]. Available from: https://nrc-cnrc.github.io/EGSnrc/doc/pirs509e-beamdp-utility.pdf

32. Bushberg JT, Seibert JA, Leidholdt Jr EM, Boone JM. The Essential Physics of Medical Imaging. 2nd ed. Mitchell CW, editor. Philadelphia: LIPPINCOTT WILLIAMS & WILKINS, a WOLTERS KLUWER business; 2002. 1–933 p.

33. Muhammad D, Kakakhel B, Aslam A, Kakakhel MB, Shahid SA, Younas L, et al. Soft tissue and water substitutes for megavoltage photon beams: An EGSnrc-based evaluation. J Appl Clin Med Phys. 2016;17(1):408–15.

34. Radionuclide Information Booklet - Canadian Nuclear Safety Commission [Internet]. Canadian Nuclear Safety Commission. 2018 [cited 2020 Jul 9]. p. 1–42. Available from: http://www.nuclearsafety.gc.ca/eng/resources/radiation/radionuclide-information.cfm

Chapter 4: Conclusion and future development

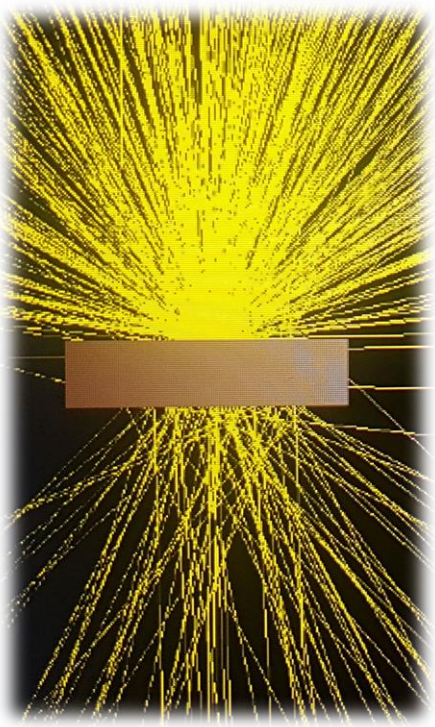

TABLE OF CONTENTS

4.1 Summary

In Chapter 1, it was discussed why RCF is the dosimeter of choice due to all the advantages it offers. This study shows that Gafchromic™ film can detect low amounts of radiation which can be useful in the Nuclear Medicine department for standard source calibration or radionuclide dosimetry studies.

In Chapter 2, OD vs time activity curves were obtained for each radionuclide with the different films. It resulted that the XR-QA2 Gafchromic™ film is the most sensitive for low energy radionuclides and that the RT-QA2 Gafchromic™ film should be used for higher energy radionuclides. The neutron depletion model fits the data extremely well and can be the model of choice due to having only three parameters which increases its accuracy and stability. When comparing the OD values for all the backscatter materials used it showed that when using lead, the OD change is much higher than when using CFC which is an air equivalent material which showed the lowest OD increase. This is due to lead having a significant backscatter effect. The sensitivity of the films can be enhanced by using multiple film layers at once. A new method is also shown that could save time when doing this study. Instead of radiating one piece of film at a time, a stack can be radiated, and one piece of film can be removed after a certain period has passed. The stacked data can then be used to get the single film approach values.

Chapter 3 focused on getting the absorbed dose values in the film from its OD values. This was possible by doing MC simulations and employing the specific gamma exposure factor for each radionuclide. BEAMnrc simulations were used to simulate the radionuclide in their container with success which enabled us to first inspect the influence of the radionuclide containers by using BEAMDP. This showed that the containers used, do have an effect on the radionuclide spectrum and thus should be carefully chosen when used in studies. This chapter also shows that the XR-QA2 Gafchromic™ film is the most sensitive at lower energies. BEAMDP was also used to get the fluence at 0.1 cm and 50 cm. At distances as small as 0.1 cm, the inverse-square law is not followed, and thus conversion factors had to be used to obtain accurate data at 0.1 cm from the source. DOSXYZnrc was used to obtain conversion factors to relate absorbed dose in water to

absorbed dose in film. These results showed that 0.9 cm thickness of lead as a backscatter material has a greater change in OD but also shows lower absorbed dose values where the air equivalent material shows higher absorbed dose values.

From the results obtained it can be concluded that the XR-QA2 Gafchromic™ film can be used in nuclear medicine departments as it is appropriate for the low energy radionuclides and that the neutron depletion based theoretical model fits the data extremely well. This study also shows that we are able to get the absorbed dose in film from OD or activity-time values by using the neutron depletion theoretical model and MC simulations.

4.2 Future work

During the measurements and simulations, a distance of 0.1 mm was used between the film and the radionuclide. For future studies, this distance can be increased and avoid having to use fluence conversion factors. This study used two types of films. The XR-QA2 Gafchromic™ film which is used for diagnostic QA and the RT-QA2 Gafchromic™ film which is used for radiation treatment QA. The RT-QA2 Gafchromic™ film can be replaced with a different diagnostic QA film which is as sensitive as the XR-QA2 Gafchromic™ film, and the results can be compared. It can also be investigated when lead will have a bigger contribution to scatter or absorption by using different thicknesses as backscatter material. The possibility of using the film for clinical dosimetry and standard source calibration can also be included as future studies.

APPENDICES

A. Input File for the BEAMnrc simulations

Input file of the 'FLATFILT' and 'SLABS' CM that contains the materials and dimensions for Cs-137 with the extra 5mm PMMA.

FLATFILT CM #1		
OUTER RADIAL BOUNDARY FOR CM (CM)		3.7
DISTANCE OF FRONT OF MATERIAL IN CM TO REFERENCE PLANE (CM)		0
NUMBER OF LAYERS		4
LAYER DIMENSIONS		
LAYER 1	Layer thickness (cm)	1
	Number of conical sections	1
LAYER 2	Layer thickness (cm)	4.9
	Number of conical sections	1
LAYER 3	Layer thickness (cm)	1.4
	Number of conical sections	1
LAYER 4	Layer thickness (cm)	0.1
	Number of conical sections	2
LAYER 1 PROPERTIES		
CONE #	1	Outer region
ECUTIN (MEV)	0.512	0.512
PCUTIN (MEV)	0.01	0.01
DOSE ZONE	0	0
ASSOCIATE WITH LATCH BIT	0	0
MATERIAL	Pb	Air
TOP RADIUS	2.7	3.7
BOTTOM RADIUS	3.7	3.7
LAYER 2 PROPERTIES		
CONE #	1	Outer region
ECUTIN (MEV)	0.512	0.512
PCUTIN (MEV)	0.01	0.01
DOSE ZONE	0	0
ASSOCIATE WITH LATCH BIT	0	0
MATERIAL	Pb	Air
TOP RADIUS	3.7	3.7
BOTTOM RADIUS	3.7	3.7
LAYER 3 PROPERTIES		
CONE #	1	Outer region
ECUTIN (MEV)	0.512	0.512
PCUTIN (MEV)	0.01	0.01
DOSE ZONE	0	0
ASSOCIATE WITH LATCH BIT	0	0
MATERIAL	Pb	Air
TOP RADIUS	2.8	3.7
BOTTOM RADIUS	2.8	3.7

LAYER 4 PROPERTIES			
CONE #	1	2	Outer region
ECUTIN (MEV)	0.512	0.512	0.512
PCUTIN (MEV)	0.01	0.01	0.01
DOSE ZONE	0	0	0
ASSOCIATE WITH LATCH BIT	0	0	0
MATERIAL	PMMA	Pb	Air
TOP RADIUS	1.5	2.8	3.7
BOTTOM RADIUS	1.5	2.7	3.7

SLABS CM #2	
HALF-WIDTH OF OUTER SQUARE BOUNDARY (CM)	3.7
DISTANCE OF FRONT OF MATERIAL IN CM TO REFERENCE PLANE (CM)	7.5
NUMBER OF SLABS	1

SLAB DIMENSIONS AND PROPERTIES	
SLAB THICKNESS (CM)	0.5
ECUTIN (MEV)	0.512
PCUTIN (MEV)	0.01
DOSE ZONE	0
ASSOCIATE WITH LATCH BIT	0
ESAVE FOR THIS REGION	0
MATERIAL	PMMA

B. Ethical clearance

Research approval from the University of the Free State Health Sciences Research Ethics Committee. Ethics clearance number: UFS-HSD2019/1505/0110

UNIVERSITY OF THE FREE STATE
UNIVERSITEIT VAN DIE VRYSTAAT
YUNIVESITHI YA FREISTATA

UFS·UV
HEALTH SCIENCES
GESONDHEIDSWETENSKAPPE

Health Sciences Research Ethics Committee

26-Aug-2019

Dear **Ms Maria Joubert**

Ethics Clearance: **Comparison between measured and simulated activity using gafchromic film with radionuclides.**
Principal Investigator: **Ms Maria Joubert**
Department: **Medical Physics Department (Bloemfontein Campus)**
APPLICATION APPROVED

Please ensure that you read the whole document

With reference to your application for ethical clearance with the Faculty of Health Sciences, I am pleased to inform you on behalf of the Health Sciences Research Ethics Committee that you have been granted ethical clearance for your project.

Your ethical clearance number, to be used in all correspondence is:**UFS-HSD2019/1505/0110**

The ethical clearance number is valid for research conducted for one year from issuance. Should you require more time to complete this research, please apply for an extension.

We request that any changes that may take place during the course of your research project be submitted to the HSREC for approval to ensure we are kept up to date with your progress and any ethical implications that may arise. This includes any serious adverse events and/or termination of the study.

A progress report should be submitted within one year of approval, and annually for long term studies. A final report should be submitted at the completion of the study.

The HSREC functions in compliance with, but not limited to, the following documents and guidelines: The SA National Health Act. No. 61 of 2003; Ethics in Health Research: Principles, Structures and Processes (2015); SA GCP(2006); Declaration of Helsinki; The Belmont Report; The US Office of Human Research Protections 45 CFR 461 (for non-exempt research with human participants conducted or supported by the US Department of Health and Human Services- (HHS), 21 CFR 50, 21 CFR 56; CIOMS; ICH-GCP-E6 Sections 1-4; The International Conference on Harmonization and Technical Requirements for Registration of Pharmaceuticals for Human Use (ICH Tripartite), Guidelines of the SA Medicines Control Council as well as Laws and Regulations with regard to the Control of Medicines, Constitution of the HSREC of the Faculty of Health Sciences.

For any questions or concerns, please feel free to contact HSREC Administration: 051-4017794/5 or email EthicsFHS@ufs.ac.za.

Thank you for submitting this proposal for ethical clearance and we wish you every success with your research.

Yours Sincerely

Dr. SM Le Grange
Chair : Health Sciences Research Ethics Committee

Health Sciences Research Ethics Committee
Office of the Dean: Health Sciences
T: +27 (0)51 401 7795/7794 | E: ethicsfhs@ufs.ac.za
IRB 00006240; REC 230408-011; IORG0005187; FWA00012784
Block D, Dean's Division, Room D104 | P.O. Box/Posbus 339 (Internal Post Box G40) | Bloemfontein 9300 | South Africa
www.ufs.ac.za